# THE CATALYTIC ROLE OF BIRNESSITE IN THE MAILLARD REACTION AND THE ABIOTIC FORMATION OF HUMIC SUBSTANCES

A Thesis submitted to the College of Graduate Studies and Research
in Partial Fulfilment of the Requirements for

**the Degree of Doctor of Philosophy**

in the Department of Soil Science
University of Saskatchewan
Saskatoon

**By**
**Aleksander Jokic**
**Fall 2000**

## PERMISSION TO USE

In presenting this thesis in partial fulfilment of the requirements for a Postgraduate degree from the University of Saskatchewan, I agree that the Libraries of the University may make it freely available for inspection. I further agree that permission for copying of this thesis in any manner, in whole or in part, for scholarly purposes may be granted by the professor or professors who supervise my thesis work or, in their absence, by the Head of the Department or the Dean of the College in which my thesis work was done. It is understood that any copying or publication or use of this thesis or parts thereof for financial gain shall not be allowed without my written permission. It is also understood that due recognition shall be given to me and to the University of Saskatchewan in any scholarly use which may be made of any material in my thesis.

Requests for permission to copy or to make other use of material in this thesis in whole or in part should be addressed to:

Head of the Department of Soil Science
University of Saskatchewan
51 Campus Drive
Saskatoon, Saskatchewan S7N 5A8

**Dedicated to my parents and to Ruzica**

# ABSTRACT

Humic substances are ubiquitous in soils and sediments. Because of their agricultural and environmental importance humic substances have been the subject of much research. One of the most crucial components of this research has been the investigation of their formation pathways in nature. The Maillard (browning) reaction involving the polycondensation of carbohydrates and amino acids has been postulated as being an important abiotic pathway for humic substance formation. However, there are significant gaps in knowledge. The catalytic role of minerals common in soils and sediments in the Maillard reaction and the resultant formation of humic substances in nature is little understood and the effect of light is unknown.

In the present dissertation it is shown that birnessite, a tetravalent manganese oxide common in soil and sediment environments, exerted a pronounced catalytic effect on the Maillard reaction between glucose and glycine both at room temperature (25°C) and particularly at 45°C, a surficial soil temperature frequently encountered in tropical and subtropical regions, and even in temperate regions during the summer months.

Light, even of moderate intensity, exerted a significant promoting effect on browning in the glucose-glycine-birnessite system. The catalytic effect of birnessite on the Maillard reaction was still evident even under conditions of complete darkness and therefore may occur at any depth in soil and related environments.

Molecular topological shape analysis was applied to investigate the initial reaction between glucose and glycine to form the Amadori compound fructosylglycine which is an intermediate product in the Maillard reaction. Molecular Iso-Density

Contours (MIDCO's), electron density contour faces of constant electron density, were constructed for glucose, glycine and fructosylglycine. The structure of the Amadori compound was optimized at a quantum mechanical level and its ground state electron energy calculated. The calculations indicate that the Amadori compound and water on one hand and the separate entities glucose and glycine on the other hand are very close to each other in terms of their ground state energy. Therefore the reaction between glucose and glycine to form the Amadori compound is slow.

Polyphenols in terrestrial and aquatic environments are regarded as important precursors in the formation of humic substances. In the presence of catechol, the accelerating effect of birnessite on the polymerization and polycondensation in the glucose-glycine-catechol ternary system was even more dramatic compared with the catalytic effect on the Maillard reaction alone. This points to a linking of the polyphenol and Maillard reaction pathways into an integrated pathway – a significant advancement in the understanding of natural humification processes.

# ACKNOWLEDGEMENTS

I wish to thank my supervisor, Dr. P.M. Huang for his encouragement and guidance during the years of my research.

I wish to express my appreciation to the members of my Advisory Committee Drs. D. Anderson, A. Baranski, E. de Jong, and J. Germida for constructive suggestions and criticisms. I thank Dr. M. Schnitzer, the external examiner of my thesis defence, for his comments and suggestions.

I would like to acknowledge the assistance and very useful suggestions of Drs. P. Mezey and Z. Zimpel of the Mathematical Chemistry Research Unit, Department of Chemistry concerning molecular topological analysis. Thanks are due to Drs. J.-L. Du and J. Weil, of the Department of Chemistry for EPR analyses.

I wish to express my gratitude to S. Blechinger, Dr. R. de Freitas, and A. Seib of the Soil Microbiology section, Department of Soil Science for assistance. Thanks also go to B. Goetz, Land Resource Unit, Agriculture and Agri-Food Canada for assistance in AA spectroscopy. I thank B. Chatson of the Plant Biotechnology Institute-National Research Council, Saskatoon, for useful suggestions concerning NMR analysis.

I express my gratitude to Drs. A. Frenkel, Materials Research Laboratory, University of Illinois at Urbana-Champaign and M. Vairavamurthy, Brookhaven National Laboratory, Upton, New York for the XANES analyses.

I thank Dr. M.C. Wang, Department of Soil Environmental Science, National Chung Hsing University, Taiwan for assistance in isolation of humic substances and $^{14}C$ tracer experiments.

I sincerely thank all members of Dr. P.M. Huang's research group for assistance and friendship.

Financial support from the Canadian Wheat Board, the College of Graduate Studies and Research and the Natural Sciences and Engineering Research Council of Canada (NSERC) is gratefully acknowledged.

## TABLE OF CONTENTS

# LIST OF TABLES

# LIST OF FIGURES

# 1. INTRODUCTION

Humic substances have been a field of study for centuries, and may be defined based on today's knowledge as "a general category of naturally occurring, heterogeneous organic substances that can generally be characterized as being yellow to black in colour, of high molecular weight and refractory" (Aiken et al., 1985). They are ubiquitous and can be found wherever organic matter is decomposing or has been transposed as is the case in sediments (Hayes et al., 1989).

The relative importance of abiotic and biotic processes in humification in soils and sediments still remains obscure even though much research has been devoted to them (Huang, 1990). Abiotic transformations of organic material in soil have often been ignored in the past because of the experimental difficulty of distinguishing abiotic processes from microbiological ones (McBride, 1994) especially since they often occur together. For example the oxidative polymerization of phenols, which is an important precursor reaction in the formation of humic substances, is catalysed both by enzymes and abiotic (inorganic) catalysts (Dec and Bollag, 1990; Huang, 1990; Bollag, 1992; Shindo and Huang, 1992; Pal et al., 1994; Bollag et al., 1995; Wang and Huang, 1997). Nevertheless, over the last four decades, many soil scientists have derived from experimental results a common theory that humic substances are also formed by heterogeneous catalytic effect of inorganic components of soils (Wang et al. 1986; Huang 1990). Presently, the oxidative polymerization of polyphenols in soils is thought to be one of the major processes of formation of humic substances (Wang et al. 1986).

Many soil inorganic components including oxides, hydroxides, oxyhydroxides, short-range ordered (SRO) minerals, clay-size layer silicates, primary minerals and natural soils have been shown to possess the ability to abiotically transform natural and anthropogenic organic compounds in soils.

The Maillard reaction was initially proposed by Maillard (1912, 1913) who investigated the formation of yellow-brown to dark-brown "pigments" or melanoidins upon refluxing solutions of glucose and lysine together. Since then, evidence has accumulated which suggests that natural humic substances may be produced by condensation reactions between sugars and amino acids (Hodge, 1953; Ikan et al., 1996).

Of the short-range ordered metal oxides, manganese oxides have by far the strongest catalytic effect (Shindo and Huang, 1982, 1984a; Huang 2000). Indeed, Mn oxides are considered the most important abiotic redox active minerals found in many soils and sediments (Risser and Bailey, 1992). The ability of Mn oxides to coat other mineral surfaces, thereby imparting increased reactivity allows them to exert a catalytic effect that is much greater than their actual abundance (Bartlett, 1986).

Although the Maillard reaction is perceived to be an important pathway in humification processes, it is slow under ambient conditions (Hedges, 1978). Since birnessite is a very reactive Mn oxide common in soils and sediments, it is hypothesized in the present dissertation that it could catalyze the Maillard reaction and the resultant formation of humic substances in nature. Birnessite may also protect the substrates against microbial decomposition by absorbing them into micropores and internal surfaces which are too small to permit the entry of hydrolytic enzymes produced by the microorganisms. Moreover, polyphenols that have been shown to be important precursors

in the abiotic formation of humic substances (Shindo and Huang, 1982) could also interact with the Maillard reaction resulting in the formation of humic polycondensates.

The objectives of the present research were: (1) to investigate birnessite catalysis of the Maillard reaction between glucose and glycine and the resultant formation of humic substances; (2) to investigate the influence of light on birnessite catalysis of the Maillard reaction; (3) to attempt to model the formation of a Maillard reaction intermediate using *ab initio* computation techniques and (4) to investigate the catalytic role of birnessite in polycondensation of glycine and glucose as influenced by catechol.

The evidence that birnessite exerts a catalytic role in the Maillard reaction and the resultant formation of humic substances would advance the frontiers of knowledge on the mechanisms of humification. Further, the integration of the polyphenol and Maillard reaction pathways would be a significant advancement in the understanding of natural humification processes.

# 2. LITERATURE REVIEW

## 2.1 The Nature of Soil Organic Matter

One of the most important processes in the carbon cycle is that of humification, the process whereby various organic molecules found in biomass consisting of dead and decaying plant and animal remains are converted into soil organic matter or humus (Wershaw, 1994). The dead biomass can be mineralized or transformed by enzymatic or non-enzymatic degradation reactions into a series of complex organic compounds (Bollag et al., 1998). This process occurs in two stages (Hayes, 1991). The initial step involves a series of degradative processes leading to the formation of substrates. Not all organic residues are completely converted and a substantial portion such as the more refractory lignin subunits are little changed (Kögel-Knaber, 1993). This is followed by further transformation of the substrates and refractory components via a series of complex synthetic processes which result in the formation of humus.

### 2.1.1 Chemical Composition

The chemical composition of soil organic matter is estimated to consist of: carbohydrates, 10% ; N-components (including proteins, peptides, amino acids, purines, pyrimidines, and heterocyclics), 10%; lipids (alkanes, alkenes, fatty acids and esters), 10% and humic substances approximately 70% (Schnitzer, 1991). These are average values for agricultural soils and may vary in specific environments. Soil studies on carbohydrates, N-containing compounds and lipids, have benefited from advances by organic chemists and biochemists specializing in these domains. However advances in

humic substance chemistry have come about largely as the result of research by soil chemists and, to a considerably lesser extent, coal chemists (Schnitzer and Schulten, 1998).

### 2.1.2 Occurrence and Distribution

The major groups of naturally occurring polymers are: i) cellulose; ii) hemicelluloses; iii) lignin; iv) non-lignin aromatic compounds such as tannins, flavonoids, various phenols and aromatic acids; v) lipids; vi) cutin and suberin; vii) nitrogenous compounds; and viii) humic substances. The first three are the major components of vascular plant cell walls whereas phenols and aromatic acids can also be formed by the degradation of lignin. Cellulose, hemicelluloses and proteins are rapidly degraded while lignin and lipids are much more refractory in nature (Allison, 1973). These naturally occurring polymers are described below.

1) Cellulose: The cell walls of the majority of vascular plants consist primarily of cellulose a homopolymer of β-D-glucose. The glucose units are linked via 1,4-glucosidic bonds into relatively long and straight chains which are bound in parallel by hydrogen bonding and form groups called fibrils (Wershaw, 1994). The fibrils can range in diameter from 2.5 to 20 nm depending on plant tissue type (Harada and Côté, 1985).

2) Hemicelluloses: Hemicelluloses are polysaccharides which as a group constitute about one-third of the dry weight of most higher land plants (Wilkie, 1983). They are abundant in lignified cells and within plant cell walls form an aqueous gel containing bundles of cellulose microfibrils embedded in regular or irregular orientations. Unlike cellulose, they are readily hydrolyzed by acid forming sugars such as L-arabinose, D-

xylose, D-mannose, D-glucose, L-rhamnose, D-glucuronic acid, 4-O-methyl-D-glucuronic acid, and D-galactouronic acid (Wilkie, 1983).

3) Lignin: Lignin is one of the three major constituents (together with cellulose and hemicelluloses) of plant cell walls. Whereas cellulose and hemicelluloses are polysaccharides that form chain-like polymers, lignin consists of aromatic polymers which are composed of three phenyl propane monomers, i.e., coniferyl alcohol, sinapyl alcohol and *p*-hydroxycinnamyl alcohol (Figure 2.1). The proportions of each monomer vary with plant type (Wershaw, 1994).

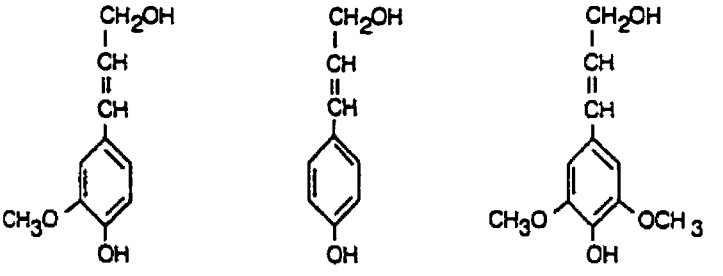


**Figure 2.1** Chemical structure of the lignin monomeric units coniferyl, *p*-hydroxycinnamyl, and sinapyl alcohols (Stevenson, 1994).

Some lignin found in wood is present in the form of lignin-carbohydrate complexes with the phenylpropane groups attached to hemicellulosic chains by benzyl ether linkages (Koshijima et al., 1989).The molecular weights of the complexes range from 600 to 800 Daltons. The carbohydrate portions are hydrophilic in nature while the lignin portions are generally more hydrophobic. The mineralization of lignin in soil is not well understood but the degradation is an extremely important process because of the

formation of phenolic compounds, such as catechol, pyrogallol, orcinol, syringic acid and ferulic acid, which are vital in humification mechanisms (Bollag et al., 1998).

4) Non-lignin aromatic compounds: Many non-lignin aromatic compounds also occur in nature such as the tannins, flavonoids, various phenols and aromatic acids. Tannins are non-lignin derived aromatic compounds found in plants. They are found in considerably lower quantities than lignin in plants and probably make a correspondingly lesser contribution to humic substance structure.

5) Lipids: Lipids are water-insoluble compounds that are extracted from plant or animal cells by nonpolar organic solvents. Commonly used terms for lipids include fats, oils and waxes. The triglycerides are the most abundant lipids; two other important categories are the phospholipids and the steroids (Wershaw, 1994).

6) Cutin and suberin: Cutin, the polymeric material that coats epidermal cells of leaves, functions as a barrier to water loss from plant tissue. Chemically it is a polyester composed of hydroxy and hydroxy-epoxy fatty acids (Kolattukudy and Espelie, 1985). Suberin is the polymeric coating on cork cells located between the inner and outer bark layers, but its composition is still not fully understood (Kolattukudy and Espelie, 1985).

7) Nitrogen compounds: Nitrogen-containing compounds are relatively abundant in soil organic matter (Wershaw, 1994). Amino sugars are present in microbial cell walls and extracellular polysaccharide secretions (Joergensen and Meyer, 1990). Various studies have demonstrated that a significant proportion of the nitrogenous compounds in soil humic substances consist of proteins or amino acids and amino sugars. Proteinaceous material in soil originates from animals, plants, and microorganisms; proteins and peptides of plant tissues are rich in alanine, glycine and lysine (McKeague et al., 1986).

8) Humic substances: Because of their importance, humic substances are treated in a separate section below.

### 2.1.3. Humic substances

The terminology of humic chemistry has a long history dating from the early work of Achard (1786) who extracted a dark precipitate from peat using dilute aqueous NaOH that we now call "humic substances." Humic substances are a whole group of organic compounds formed in soil and aquatic environments which, because of their complex nature, are typically defined as including all of the soil, water or sediment organic compounds except the proteins, polysaccharides and lipids (Buffle, 1990).

They comprise the bulk (circa 70%) of the organic constituents of most soil and sediment environments. Because living organisms are made up of a very large number of different organic compounds, their degradation and the possible recombination of the resulting products may lead to an almost infinite variety of different organic structures. It is, therefore, not surprising that humic substances exhibit a broad range of properties, even if they behave as a whole at the macroscopic environmental level. This whole group of compounds is operationally divided into the so-called fulvic and humic fractions and humin, for the sake of simplicity. However a close study of any particular property (e.g., molecular weight or functional group content) of the whole group often shows that it follows a wide frequency distribution, without a clear demarcation between fulvic acid and humic acid (Buffle, 1990).

Although humic chemistry has evolved through an interesting course over the last 200 years, soil scientists generally agree on four terms (Aiken et al., 1985):

1) **Humic substances:** a general category of naturally occurring, biogenic, heterogeneous organic substances from soil or sediment that can be characterised as being yellow to black in colour, of high molecular weight and refractory in nature.

2) **Humic acids:** Humic acids consist of the fraction of humic substances that is precipitated from aqueous solutions when the pH is decreased below 2 (Aiken et al., 1985). Hence humic acids may well be present in solution in natural waters. Soil scientists generally consider humic acids to be that fraction of organic matter which is precipitated at pH 1 from the aqueous alkaline extracts of soil (Hayes et al., 1989).

3) **Fulvic acids:** A fraction of humic substances that is soluble under all conditions of pH.

4) **Humin:** A fraction of humic substances that is so intimately bound with soil minerals that it is not soluble in water at any pH value.

One of the most definitive characteristics of humic substances is that these acidic organic molecules are large, with molecular weights ranging from ≅500 to >100 000 Daltons (Hedges, 1988), and as a result are incredibly complicated in structure (Bollag et al., 1998). Fulvic acids represent the low-molecular weight fraction of the humic substances group. Their molecular weights range from a few hundred to a few thousand Daltons, whereas those of the humic acids range from thousands to hundreds of thousands (Buffle, 1990). Since most common biochemical structure units such as simple sugars, amino acids, fatty acids, and cinnamyl alcohols (the building blocks of lignins) have molecular weights less than 500 Daltons, it can be inferred that humic substances must ultimately result from abiotic and biotic polymerisation and polycondensation reactions involving such small precursors.

Another important characteristic of humic substances in terms of their formation mechanisms is that only a fraction of the polymers (up to 20%) can typically be accounted for as recognisable biochemicals, with the remainder present in a wide and complex variety of polycondensation products (Thurman, 1985).

A third universal property of humic substances is that they contain significant amounts of nitrogen (Hedges, 1988). Amino acids, the most common nitrogenous substances in living organisms, however, exhibit little tendency to spontaneously combine with each other under most "natural" conditions (Hedges, 1978) and are themselves usually a minor component of humic polymers (Thurman, 1985). Therefore, the presence of nitrogen in humic substances has been taken as evidence for polycondensation reactions which involve nitrogenous precursors. Schnitzer (1985) noted that approximately 30 % of the nitrogen in fulvic and humic acids extracted from temperate soils originates from amino acids. This rises to 50 % for tropical soils. The respective contents of amino sugars for temperate soils are 1 to 2 % for humic acid nitrogen and between 4 and 5 % for fulvic acid nitrogen. For tropical soils this rises to 3 to 5 % for humic acids and 8 to 9 % for fulvic acids. Both Schnitzer (1985) and Stevenson (1986) note that 30 to 50 % of the nitrogen in soil humic substances is of unknown chemical origin. This unknown nitrogen can be divided into hydrolyzable unknown nitrogen and insoluble nitrogen species (Wershaw, 1994). Such unidentified nitrogenous compounds could include Schiff bases formed by the reaction of amino groups in proteins and/or amino acids with carboyxl groups from lignin degradation products, and melanoidin polymers formed by Maillard reaction polycondensations between amino acids and reducing sugars.

Humic substances are typically yellow to brown-black in colour and acidic in nature. Thus humic molecules must contain, in addition to acidic functional groups, conjugating systems of resonating electrons capable of absorbing blue light. Although the acidity of humic substances can be assumed to be largely due to the presence of carboxylic and phenolic functionalities, the range of possible chromophores is broad and includes both benzene and furan ring systems. Incorporated into the humic polymers are various phenols, quinones, heterocyclics, and benzoic acids containing reactive carboxyl, hydroxyl, carbonyl, and thiol groups that can bind with carbohydrates and amino acids (Bollag et al., 1998).

Fulvic and humic acids originating from soil include a larger proportion of aromatic compounds (in particular benzene carboxylic and phenolic compounds) whereas the fulvic and humic acids from sediments and aquatic sources (i.e., those formed in lakes, rivers and oceans) are much more aliphatic (Buffle, 1990). The fraction of carbon that is aromatic in nature in humic extracts can vary from 10 to 74% (Sihombing et al., 1991). All humic substances are fairly resistant to biological degradation, i.e., refractory; their mean residence times are often in the range of centuries to millennia (Buffle, 1990).

Humic substances occur ubiquitously in terrestrial and aquatic environments, indicating that many precursors and several formation pathways exist. Distinguishing among these pathways has been difficult because individual scientists have tended to concentrate their efforts on specific types of samples (e.g., soil, sediment or water) for which different isolation or fractionation methods are often used (Thurman, 1985).

**2.1.3.1 Structure**

The macromolecules of humic substances, formed from a wide variety of precursors and in a range of conditions, present highly complex mixtures of molecules. These substances have defied all attempts at separation into pure, or reasonably pure fractions, and thus the investigator has no choice but to work with mixtures. Therein lies the greatest difficulty in studies of humic structures. Despite the remarkable advances that have been made in chemistry, it is important to realise that in order to make progress in studies of structures of macromolecules, there is a need to work with pure or reasonably pure substances. There is often a tendency to assume that the investigative tools of the chemist are more powerful than their performance would imply. All investigative tools, be they chemical or physical, may of course be applied to any sample, regardless of its simplicity or complexity, and data will be obtained. However interpretations of these samples will be severely restricted when mixtures are considered. Such difficulties are extreme in the cases of humic substances, which represent the epitome of molecular heterogeneity and complexity.

The search for structure in humic substances can be said to have undergone several phases which may be appropriately designated as the following (Ziechmann, 1988):

1) Introduction of concepts and an extensive nomenclature (1780-1850);

2) Presentation of the first detailed structural formulae (1920-1970);

3) Comparable endeavours to (2) above to derive models without chemical details (1950 onwards);

4) Application of modern physical techniques for an improvement of structural understanding (1950 onwards);

5) Elucidation of the genesis of humic substances as a contribution to their structural investigation.

The start of this development may be seen in the first attempts of classical chemistry to treat and characterise humic substances by the creation of nomenclature such as humic acids, fulvic acids, hymatomelanic acids, and even crenic or apocrenic acids. These attempts were connected with such names as Berzelius (1839) and Hoppe-Seyler (1889) and others. The next point in this direction was the assignment of a structural formula to humic substances.

Dragunov et al. (1948) proposed a model with aromatic and quinonoid rings connected by several bridges (Figure 2.2).

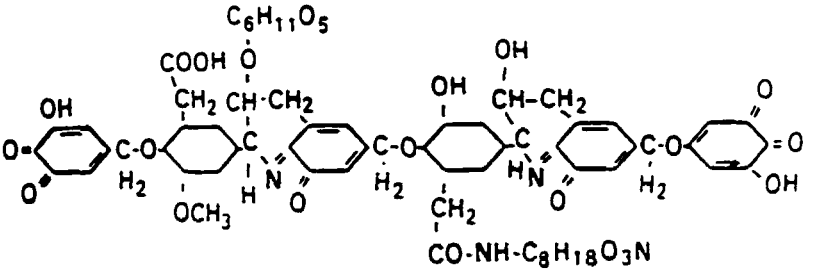


**Figure 2.2** Dragunov et al's (1948) structure of a humic acid molecule.

The observed functional groups of humic acids are like non-humic substances (e.g., carbohydrates, peptides). Kleinhempel's model (1970) is only slightly altered but offers more details (Figure 2.3).

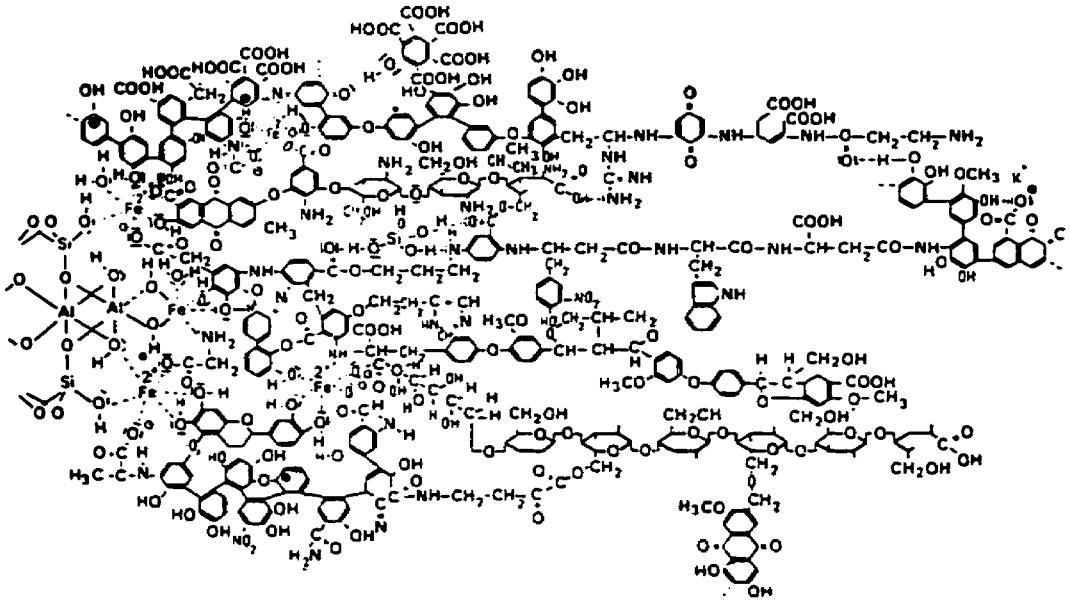

**Figure 2.3**. Linking of structural units according to Kleinhempel (1970).

The molecules in Schnitzer's model (1972) (Figure 2.4) are composed of distinct benzene rings, substituted by phenolic and carboxylic acid groups. The interconnection of the so-called "building blocks" is based merely on hydrogen bonds.

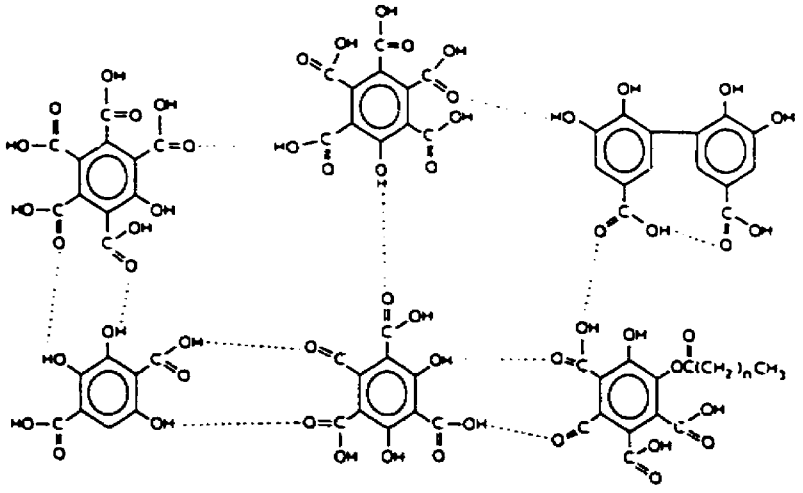

**Figure 2.4** The structure of fulvic acids according to Schnitzer (1972).

In conjunction with this period was the formulation of structural models which lacked distinctive details. This would at first seem to be an apparent regression. Nevertheless, the model could still provide useful information. For example, an attempt in this direction is the formulation of the principle of structure in humic substances by Thiele and Kettner (1953), which involved a coordination with parts of molecules and their structural functions (Figure 2.5).

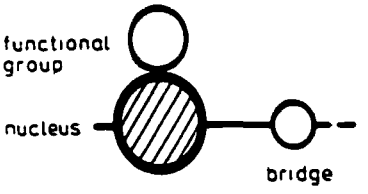


**Figure 2.5** The structural model of humic substances by Thiele and Kettner (1953).

The model was modified by Pauli (1967), who considered the spatial order of magnitude (Figure 2.6). Pauli describes the humic particle as a micelle, from the point of view of colloid chemistry, formed by polyones and mononeS. In this region of the building stones, nuclei, bridges, and functional groups can be observed in more detail and in distinct dimensions.

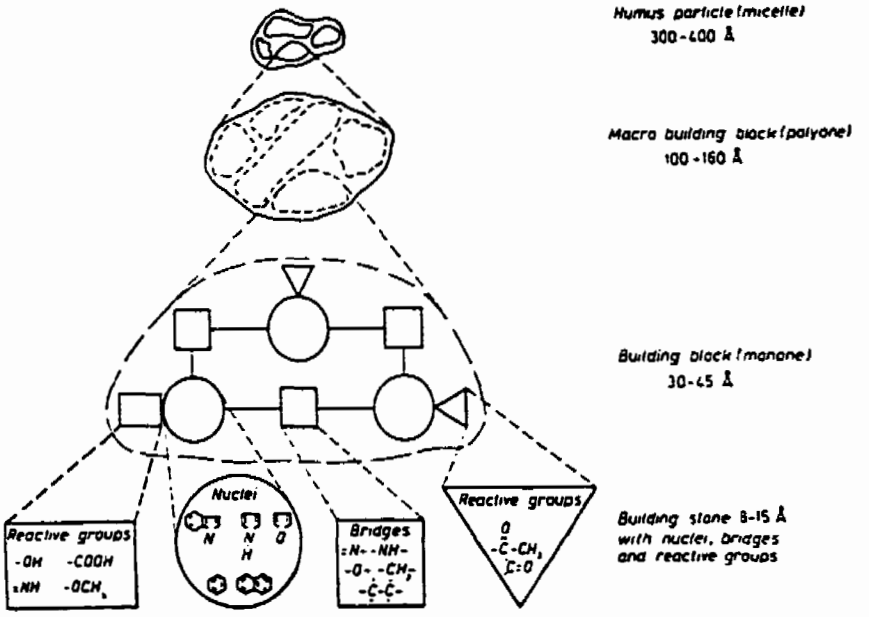


**Figure 2.6** The structure of humus molecules according to Pauli (1967).

Thurman and Malcolm (1983) attempted to consider, using a three step "separate-degrade-identify" approach, the problem of structural analysis of humic substances. The separation methods they applied were gel filtration, adsorption chromatography, pH gradient adsorption chromatography, and anion and cation exchange. Chlorination and methylation with $^{13}C$ were carried out, and identification took place using $^{13}C$ nuclear magnetic resonance (NMR) spectroscopy. Finally numerous data were obtained by elemental analysis and by the determination of the functional groups, the aromatic and aliphatic parts, the amount of amino acids and carbohydrates, and the molecular weight.

Ziechmann (1988) proposed a basic structure for naturally occurring humic substances (Figure 2.7):

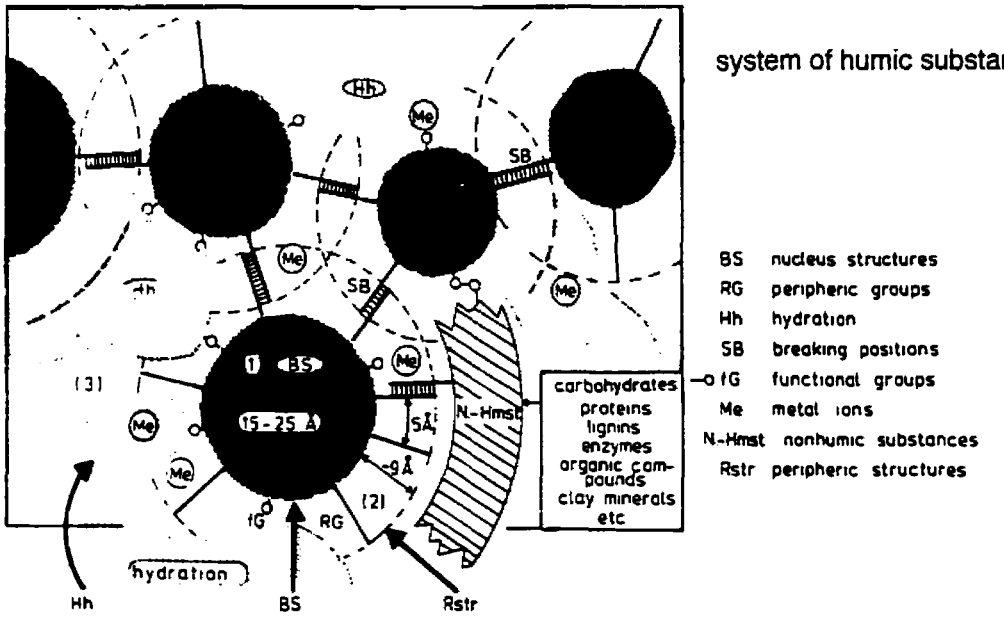


**Figure 2.7** Pattern of the basic structures of humic substances (Ziechmann. 1988).

Further contributions to a chemical structure for humic substances were provided by Schulten and Schnitzer (1991) based on long-term chemical, $^{13}C$ nuclear magnetic resonance spectroscopy, pyrolysis-field ionization mass spectrometry and Curie-point pyrolysis-gas spectrometry of extracted humic acids and whole soils. Their structure for humic acid which is based on alkylbenzenes. alkyl naphthalene and alkylphenanthrenes has a high aliphatic content. Humic acids have been reported to contain up to 10 % of carbohydrates by weight (Lowe. 1978) and a similiar content was reported for nitrogenous material in HA (Khan and Sowden. 1971). Schnitzer and

Schulten (1998) proposed a structure for humic acid of molecular formula $C_{342}H_{388}O_{124}N_{12}$ and molecular weight of 6650.8492 g $mol^{-1}$ (Figure 2.8).

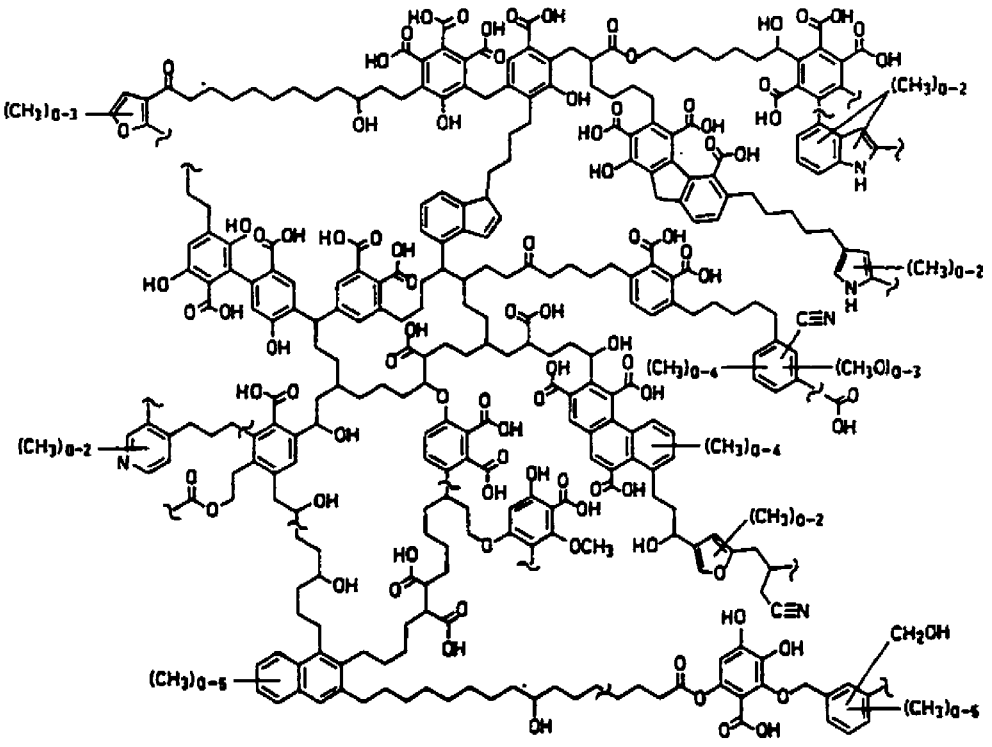

**Figure 2.8** Two-dimensional chemical structure for humic acids (Schulten and Schnitzer, 1993).

Recently Conte and Piccolo (1999) have challenged the traditional assumption that humic substances are large polymers that possess linear or coiled conformations. They consider humic substances in solution to consist of loosely bound, reversible self-associations of relatively small molecules and the dominant binding forces holding them together are intermolecular hydrophobic interactions.

Humic substances by their very complexity pose a challenge in attempts to elucidate their structure. Many spectroscopic methods are of limited use in the information they provide because of the polymeric and polyelectrolytic nature of humic substances (MacCarthy and Rice, 1985). Essentially two different approaches are possible:

1) Chemical or pyrolytic degradative studies using techniques such as pyrolysis-field ionization mass spectrometry (Py-FIMS) and Curie-point pyrolysis-gas chromatographic-mass spectrometry (Py-GC-MS). Developments in these two techniques have allowed the creation of two and three dimensional structural models of humic substances (Schnitzer and Schulten, 1998).

2) Spectroscopic, non-degradative studies such as (a) Ultraviolet-visible absorption spectroscopy, (b) Infrared absorption spectrometry, (c) Nuclear Magnetic Resonance (NMR) spectroscopy - both solid state and liquid, (d) Electron Spin Resonance (ESR) spectroscopy, (e) X-ray photoelectron spectroscopy, (f) Raman spectroscopy, (g) and Fluorescence spectroscopy. Of these methods, NMR has shown the most promise, and gone the furthest in shedding light on humic substance structure. Some of the spectroscopy methods are described below.

**Ultraviolet-visible absorption spectroscopy** - Absorption of radiation in the ultraviolet (UV) and visible regions of the electromagnetic spectrum results from electronic transitions involving bonding electrons (Brown, 1980). The UV-visible region of the spectrum is generally divided into three parts; the vacuum UV (100 to 200 nm), the UV (200 to 400 nm), and the visible (400 to 800 nm). The vacuum UV range, however, is not useful for the study of humic substances, because water and most other solvents used with humic substances absorb strongly in this region (Bloom and Lenheer, 1989).

Strong absorption in the UV region is expected for entities such as humic and fulvic acids which contain aromatic groups. The UV-visible spectra for discrete aromatic compounds substituted with COOH and OH groups show not only that these compounds absorb strongly in the UV region but also that, in general, absorbance increases with decreasing wavelength down to about 210 to 240 nm. The very strong absorbance at very short wavelengths (e.g., 210 nm) can be attributed to the benzenoid bands of carboxyphenols (Baes and Bloom, 1990). In humic substances, heterogeneous substitution results in chromophores with overlapping bands (MacCarthy and Rice, 1985). Also, slight differences in the bonding environment of a macromolecular structure can result in spectral shifts (Brown, 1980).

Non-aromatic chromophores may also contribute to UV absorption in humic substances. These could include α,β-unsaturated ketones and dicarbonyls. An especially active dicarbonyl is *p*-benzoquinone, which absorbs strongly in the UV region and absorbs weakly in the short-wavelength region of the visible spectrum. Solution pH affects the spectra of humic substances by causing a change in the absorption maximum, and absorptivity of the chromophores due to the ionisation or protonation of carboxyl and hydroxyl groups. Also, ionisation or protonation can cause conformational changes in the macromolecular structure that result in greater or lesser exposure of chromophores to the solvent (Brown, 1980; Baes and Bloom, 1990). The absorption spectra of humic substances in the visible region are generally featureless with increasing absorbance at shorter wavelength (Flaig et al., 1975; Hayes and Swift, 1978; Stevenson 1994; Baes and Bloom, 1990). Despite the lack of discrete visible bands, absorption in the UV-visible region has been of great interest to many scientists and the ratio of the absorbance at 465 nm to that at 665 nm ($E_4/E_6$ ratio) is commonly used to characterise

humic substances (Kononova 1966; Flaig et al., 1975; Chen et al., 1977; Ghosh and Schnitzer, 1979; Stevenson, 1994). The $E_4/E_6$ ratios of humic acids are generally less than 5 whereas those for fulvic acids are generally greater than 5. The ratio varies with the source of a humic substance (Kononova, 1966). UV-visible absorption maxima of phenol, salicylic acid and benzoquinone species are shown in Table 2.1 (Scott, 1964).

**Table 2.1** UV visible absorption maxima of phenol, salicylic acid and *p*-benzoquinone species (Scott, 1964)

| Compound | λmax, nm |
|---|---|
| Phenol | 210, 270 |
| Salicylic acid | 204, 236, 307 |
| p-Benzoquinone | 242, 281, 434 |

The absorbance and $E_4/E_6$ ratios of humic or fulvic acids vary with pH (Chen et al., 1977; Ghosh and Schnitzer 1979; Baes and Bloom, 1990). With decreasing pH, the absorbance decreases (Ghosh and Schnitzer, 1979; Tsutsuki and Kuwatsuka, 1979). Salt concentrations can also affect absorbance and $E_4/E_6$ ratios (Ghosh and Schnitzer, 1979) as can the solvent used (Baes and Bloom, 1990).

The source of the weak absorption of visible radiation by humic substances is uncertain (Bloom and Lenheer, 1989). Simple aromatic structures that can be used to account for UV absorption do not absorb in the visible region. Simple quinones absorb visible radiation, but only very weakly at wavelengths greater than 500 nm. Three

explanations have been offered for the observed absorption by humic substances in the visible region:

1. Humic substances contain chromophoric groups that absorb visible radiation; these chromophores would have to possess extended conjugation of unsaturated bonds beyond single aromatic rings (Tsutsuki and Kuwatsuka, 1979), e.g. as shown in Figure 2.9 below;

2. The apparent absorption of visible radiation is, to a large extent, not really true absorption but is the scattering of light (Chen *et al.*, 1977) though it should be noted that Baes and Bloom, (1990) disagree with this contention at least for fulvic acids; and

3. The structure of humic substances contains complexes that have charge-transfer bands in the visible regions (Ziechmann, 1972; Ziechman and Mittel, 1976; Lindqvist, 1972,1973).

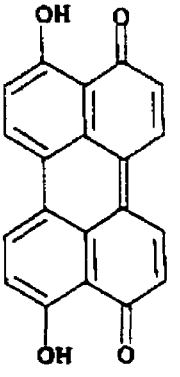


**Figure 2.9** 4,9-dihydroxyperylene-3,10-quinone (Tsutsuki and Kuwatsuka, 1979).

**Infrared spectroscopy** - Infrared spectroscopy has long been used for structural studies of humic substances, and its theory and application with regard to studies of exchangeable protons, metal binding, and hydrogen bonding properties have been reviewed by MacCarthy and Rice (1985).

Infrared spectroscopy is a technique for the study of molecular structures which is based on the absorption of infrared radiation by the vibrational modes of bonded atoms. The frequency of absorption is dependent on the vibrational mode, the strength of the bonds involved, and the masses of the atoms. The intensity of absorption is to a large degree a function of the change in dipole moment involved in the vibration.

Oxygen NMR spectroscopy ($^{17}O$) of humic substances is still very difficult because of the low natural abundance of $^{17}O$ and its poor NMR spectral characteristics. Therefore NMR spectroscopy can only provide such spectral information indirectly through the effect of oxygen on protons, $^{13}C$ or $^{15}N$ nuclei. Infrared absorption spectroscopy is perhaps more suitable than NMR for the study of oxygen in humic substances. Infrared absorption spectroscopy can also be used for determination of "purity" or contaminant assessment. Extraction or derivatization techniques for humic substances often leave inorganic impurities, such as clays, silicic acid, borates, fluoroborates, phosphates, or sulphates, all of which are readily detected by infrared spectroscopy. Non-humic biomolecules, such as proteins and carbohydrates, can also be detected (Bloom and Lenheer, 1989).

Despite infrared spectroscopy's relative usefulness in the study of humic substances, the obtained spectra are essentially featureless, as a result of band broadening, caused by the overlapping of multitude absorption bands from individual constituent structures and also shifting of absorption bands caused by group functionality. Some characteristic bands can be diagnosed however. These are (1) OH stretch at approximately 3400 $cm^{-1}$ (Senesi et al., 1989), (2) asymmetric and symmetric stretching of alkyl $CH_2$ groups at approximately 2910 $cm^{-1}$ (Senesi et al., 1989), (3) C=O

stretching of carbonyl and carboxyl at 1720-1710 $cm^{-1}$ (Senesi et al., 1989; DeKimpe and Schnitzer, 1990), (4) C=C stretch and/or asymmetric $-COO^-$ stretch at approximately 1510 and 1600 – 1650 $cm^{-1}$ (Senesi et al., 1989), (5) OH bend at 1400 $cm^{-1}$ (MacCarthy and Rice, 1985), and (6) C-O stretch and O-H deformation of COOH groups at 1220 $cm^{-1}$ (Senesi *et al.*, 1989).

**Nuclear magnetic resonance spectroscopy** - Although nuclear magnetic resonance (NMR) spectroscopy has been used to investigate the structures of humic substances for over 35 years, it is only in the past two decades, that its full potential has become apparent. The application of NMR spectroscopy to the study of humic substances has fostered a quantum leap in the continued emergence of humic substance chemistry as an increasingly important branch of science. New and powerful NMR techniques are among the most useful tools currently available to humic substance researchers and are providing definitive information that is at the forefront of the field (Xing et al., 1999). NMR spectroscopy has revolutionised some of the basic concepts of humic substances, indicating that these materials are not predominantly aromatic in nature, but are in fact, considerably aliphatic. The NMR data show that humic substances from different environments differ considerably in structure. These unique capabilities of NMR spectroscopy are complemented by the non-destructive nature of the technique, which allows the complete recovery of what are frequently very precious samples of humic substances.

Schnitzer and Barton (1963) were the first to use NMR to study humic substances when they obtained $^{1}H$ NMR spectra of soil organic extracts. The first well-resolved liquid-state $^{13}C$ NMR spectra of humic substances were presented by Gonzalez-

Vila et al. (1976) and Wilson and Goh (1977a,b). Liquid $^{13}C$ NMR spectroscopy has gradually been superceded by solid-state spectroscopy, particularly the CPMAS (cross polarization magic angle spinning) technique and variants thereof.

The first solid-state $^{13}C$ NMR spectra were published by Miknis et al. (1979), Newman et al. (1980), and Hatcher et al. (1980). At static magnetic fields of ≥4.7T, limited magic angle spinning (MAS) speeds due to rotor materials or design result in the observation of significant spinning sideband intensity for many carbon functional groups. In samples with large chemical shift anisotropy, there may be large spinning sidebands which make it difficult to interpret the spectra. The signals will usually be singlets and reliance will have to be put on the chemical shifts for peak assignments. The intensities of the lines are dependent on many factors, including the length of the contact pulse. Since the signal is distributed among centrebands and sidebands, the sensitivity of the experiment is decreased (Axelson, 1987). Samples with several magnetically nonequivalent nuclei may exhibit severe overlap of resonances, thus reducing the ability to perform accurate analyses.

Several options exist for simplifying and quantifying MAS spectra, and these include:

(1) Calculating sideband intensities in simple compounds from a knowledge of the spinning rate and the chemical shift anisotropy to enable corrections to be made. (Herzfeld and Berger, 1980).

(2) Spinning the sample at different rates and estimating the relative sideband intensities,

(3) Using sideband suppression techniques (Dixon, 1981; Dixon et al., 1982; Hemings and Dejaeger, 1983).

(4) Synchronisation of data acquisition with sample spinning (Maricq and Waugh, 1979).

(5) Separation of sidebands and centrebands via a 2-D resolved experiment (Aue et al., 1981).

(6) High spinning speeds of 8 kHz or more in combination with ramp CPMAS (Cook et al., 1996; Cook and Langford, 1999).

(7) Direct polarization magic angle spinning (DPMAS) combined with $T_1^C$ correction obtained from CP/T1-TOSS spectra (Xing et al., 1999).

The last two procedures seem to offer quantitation or near quantitation in solid state $^{13}C$ NMR studies of purified soil humic extracts.

The most important functional groups in humic substances that have been identified with the aid of NMR spectroscopy are shown in Table 2.2.

### 2.1.3.2. Physicochemical Characteristics

In most agricultural soils, humic substances are present in much lower amounts than mineral colloids but contribute approximately one-half of the cation exchange capacity (MacCarthy et al., 1990). Exchange sites on humus adsorb both macronutrients and micronutrients and prevent their rapid leaching from soil (Wershaw, 1994). Humic substances also act as a reservoir for nitrogen, phosphorus and sulphur which are not usually bound by exchange sites, and provide a considerable part of the buffering capacity of soils. Soil water holding capacity and porosity are also determined to a substantial degree by their humic substance content.

**Table 2.2** Chemical shift assignments in the CPMAS $^{13}C$ NMR spectra of fulvic and humic acids (Malcolm, 1989)

| Shift range (ppm) | Possible assignations |
|---|---|
| 0-50 | Unsubstituted saturated aliphatic carbons |
| 10-20 | Terminal methyl groups |
| 15-50 | Methylene groups in alkyl chains |
| 29-33 | Methylene carbon α, β, δ, ε, from terminal methyl group |
| 35-50 | Methylene carbons of branched alkyl chains |
| 41-42 | α-Carbon in aliphatic acids |
| 45-46 | $R_2NCH_3$ |
| 50-95 | Aliphatic carbon singly bonded to one oxygen or nitrogen atom |
| 51-61 | Aliphatic esters and ethers; methoxy and ethoxy groups |
| 57-65 | Carbon in $CH_2OH$ groups; $C_6$ in polysaccharides |
| 65-85 | Carbon in CH(OH) groups; ring carbons of polysaccharides; ether-bonded aliphatic carbon |
| 90-101 | Carbon singly bonded to two oxygen atoms; C, anomeric carbon in polysaccharides; acetal or ketal |
| 110-160 | Aromatic and unsaturated carbon |
| 110-120 | Protonated aromatic carbon |
| 118-122 | Aromatic carbon *ortho* to oxygen-substituted aromatic carbon |
| 120-140 | Unsubstituted and alkyl-substituted aromatic carbon |
| 140-160 | Aromatic carbon substituted by oxygen and nitrogen; aromatic ether, phenol, aromatic amines |
| 160-230 | Carbonyl, carboxyl, amide, ester carbons |
| 160-190 | Largely carboxyl carbons |
| 190-230 | Carbonyl carbons |

Part of the importance of humic substances derives from their interactions with natural environments which include (Hayes and Swift, 1978; Wershaw, 1994):

1. The effect of humic substances on the biological availability of elements and chemical compounds in the aqueous environment.

2. The effect of humic substances on photochemical processes in water.

3. The effect of light on the formation and degradation of humic substances.

4. The formation of chlorinated organic compounds through the chlorination of aquatic humic substances.

5. The nature of humic substance-metal interactions.

6. Humic substance-xenobiotic interactions.

7. The formation and maintenance of good soil structure.

Chen and Aviad (1990) noted that the action of humic substances on plant growth could be divided into direct (i.e., those involving uptake by plant tissue) and indirect effects. The net effect is that humic substances exert a positive effect on plant growth and at the same time reduce the uptake of harmful materials by plants.

Direct effects:

i) Effects on membranes resulting in improved transport of nutritional elements.

ii) Enhanced protein synthesis.

iii) Plant-hormonelike activity.

iv) Enhanced photosynthesis.

v) Effects on enzyme activity.

Indirect effects:

i) Solubilization of microelements (e.g., Fe, Zn, Mn) and some macroelements (e.g., K, Ca, P).

ii) Reduction of active levels of toxic elements.

iii) Enhancement of microbial populations.

## 2.2 Manganese (IV) oxides in Natural Environments

### 2.2.1 Occurrence and distribution

Manganese oxide minerals are ubiquitous in terrestrial and aquatic environments (McKenzie, 1989). Mn oxides in soils are generally amorphous but crystalline forms have also been reported. Manganese oxide minerals are found in the form of manganese nodules in marine environments. They frequently occur in conjunction with Fe oxides (McKeague et al., 1968; Childs, 1975; Sidhu et al., 1977) and can occur as discrete particles or partial coatings or films on soil and sediment particles (Burns and Burns, 1977; Giovanoli and Balmer, 1981; Post et al., 1982; Manceau and Combes, 1988), or as suspended particulates in water columns (Larson and Hufnal, 1980; McKenzie, 1989). Under certain soil conditions rhizosphere bacteria oxidize $Mn^{2+}$ to $Mn^{4+}$ and deposit $MnO_2$ on the outside of plant roots (Paul and Clark, 1989). Birnessite is one of the most common of the Mn oxide minerals (McKenzie, 1989).

### 2.2.2 Structure and Morphology

The Mn oxide minerals range in morphological complexity from the well-ordered crystalline (e.g., pyrolusite) to the more amorphous short-range ordered varieties

(e.g., birnessite). Most of the oxides can be divided into two categories i.e., those possessing tunnel structures and those possessing layer structures.

**Tunnel Structures**

These Mn oxides consist of single, double or multiple chains of $MnO_6$ octahedra linked via shared corners into a framework of enclosed tunnels. The tunnels contain water molecules and cations such as K, Na, Pb etc. Representative oxides with this structure include pyrolusite, ramsdellite, nsutite, hollandite, cryptomelane, coronadite, romanechite and todorokite (McKenzie, 1989).

Pyrolusite – This mineral is also known as $\beta$-$MnO_2$ and has the true composition $MnO_2$. Being the most stable form of $MnO_2$ it consists of single chains of $MnO_6$ octahedra created by edge sharing and has a tetragonal crystal system with rutile structure.

Ramsdellite – It is a rare form of $MnO_2$ and also consists of $MnO_6$ chains but has an orthorhombic crystal form and diaspore type structure.

Nsutite – It is described by Giovanoli (1969) as an intergrowth of pyrolusite and ramsdellite. The term encompasses several oxides considered to be modifications of $\gamma$-$MnO_2$ and $\rho$-$MnO_2$. Nsutite possesses a hexagonal crystal system.

Hollandite, Cryptomelane and Coronadite – These minerals have the tetragonal crystal system and contain foreign cations as part of their structure; Ba is present in hollandite, K in cryptomelane, and Pb in coronadite.

Romanechite – It consists of a framework of double and triple chains of $MnO_6$ octahedra with a monoclinic crystal system. Its tunnels contain K, Ba and other cations.

Todorokite – It is sometimes referred to as "10Å-manganite", it is common in both terrestrial and aquatic environments (McKenzie, 1989). Todorokite has tunnels of

varying widths, and an orthorhombic or monoclinic crystal system of still unknown structure.

**Layer structures**

Mn oxides of layer structure are composed of edge-sharing $MnO_6$ octahedra, and include vernadite, rancieite, lithiophorite, buserite and birnessite.

Vernadite – This mineral is also known as δ-$MnO_2$ and is a poorly crystalline Mn oxide. It is considered to be "random-stacked" birnessite by some, e.g., Giovanoli (1970a) and Giovanoli and Brutsch (1979) while others (e.g., Burns et al., 1974; Chukhrov et al., 1980; Chukhrov and Gorshkov, 1981) considered it as a separate phase. More recently, Manceau et al. (1992a) with the aid of high resolution XANES (X-ray absorption near-edge structure) spectroscopy noted that δ-$MnO_2$ does not possess a layered structure and should not be considered as long-range disordered birnessite. With the aid of EXAFS (extended X-ray absorption fine structure) spectroscopy, Manceau et al. (1992b) found that synthetic vernadite (δ-$MnO_2$) had edge- and corner-sharing $Mn^{4+}$ octahedra and a three dimensional anionic framework.

Rancieite – Although rancieite was regarded by Perseil and Giovanoli (1979) as not being a distinct mineral phase, others such as Bardossy and Brindley (1978), Potter and Rossmann (1979), and Chukhrov et al. (1980) disagreed, arguing that it is similiar to birnessite in structure except for having different interlayer cations.

Buserite –Giovanoli (1970b) considered it to have a layer structure analogous to that of birnessite but with extra hydroxyl and water in the interlayers which cause the $MnO_6$ octahedra to be 1 nm apart. Upon loss of water from the interlayers there is collapse of the 1 nm d value to 0.7 nm and the formation of birnessite. Recently, the conversion of

synthetic Na-rich buserite to hexagonal ($H^+$-exchanged) birnessite at low pH (2-5) was investigated by Silvester et al. (1997), and Drits et al. (1997).

Birnessite – It refers to hydrated manganese oxides with nonstoichiometric formulae consisting of $MnO_6$ octahedral sheets which are 0.7 nm apart. The interlayers are occupied by $H_2O$ and OH. Until recently the structure of birnessite was not known (McKenzie, 1989) but more recent research (Manceau et al., 1992a, 1992b) has provided further information. One in six of the octahedral sites in the $MnO_6$ octahedral sheets is vacant (McKenzie, 1989). Every sixth octahedral site in the $MnO_6$ octahedral layer in hexagonal birnessite (HBi) is unoccupied but synthetic Na-rich birnessite (NaBi) consists of Mn octahedral sheets with very few vacancies (Silvester et al., 1997).

Originally, Manceau et al. (1992a) did not find any compelling evidence for the presence of large amounts of $Mn^{3+}$ and $Mn^{2+}$ in birnessite as was previously thought to be the case (McKenzie, 1989). Based on evidence supplied by EXAFS spectroscopy, Manceau et al. (1992b) concluded that the structure of synthetic NaBi was a monoclinic subcell similiar to that of chalcophanite, but containing no corner sharing $Mn^{4+}$- $Mn^{4+}$ octahedra. Interlayer structure and layer stacking were determined by the nature of the interlayer cation.

More recently, structural models (Figure 2.10) were proposed by Silvester et al. (1997) for synthetic NaBi and its low pH form, HBi on the basis of X-ray and selected-area electron diffraction (SAED) studies which include the presence of $Mn^{2+}$ and $Mn^{3+}$. The idealized structural formula for NaBi varied from $Na_{0.167}(Mn^{4+}_{0.833}Mn^{3+}_{0.167})O_2$ to $Na_{0.333}(Mn^{4+}_{0.722}Mn^{3+}_{0.222}Mn^{2+}_{0.055})O_2$ indicating that a significant amount of $Mn^{3+}$ and even $Mn^{2+}$ was present in the birnessites. The presence of approximately 5% of Mn(II)

and 25% of Mn(III) in synthetic birnessite was confirmed by Nesbitt and Banerjee (1998) using X-ray photoelectron (XPS) spectroscopy).

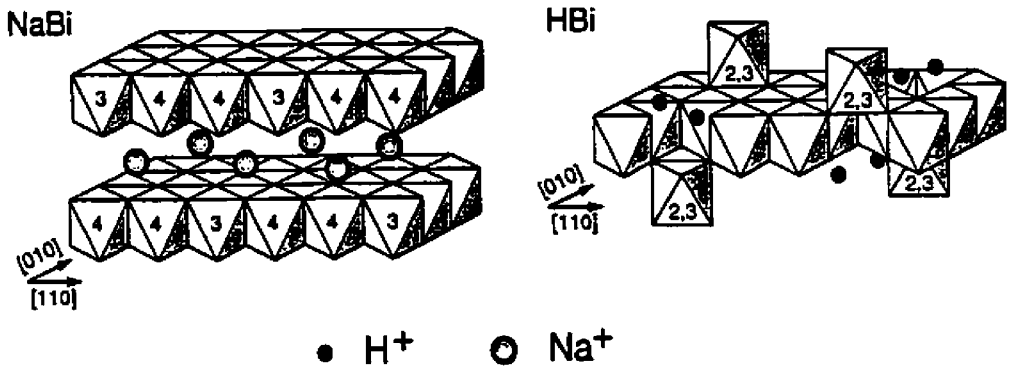


**Figure 2.10** Proposed structural models for NaBi and HBi as determined by chemical studies and EXAFS spectroscopy. The numbers on the faces of the octahedra in the NaBi structure refer to the sequence of Mn valency in the [110] or [10] directions. The numbers on the triple corner sharing octahedra in the HBi structure indicate that a mixture of $Mn^{3+}$ and $Mn^{2+}$ cations occupy these sites (Silvester et al., 1997).

### 2.2.3 Reactivity in natural environments

Of all the short-range ordered metal oxides, manganese oxides demonstrate by far the highest catalytic effect (Shindo and Huang, 1982, 1984a; Huang 1991). Indeed, the effectiveness of Mn oxides as electron acceptors in a very wide range of redox reactions is unique among common soil minerals (McBride, 1989a). Therefore, Mn oxides are considered the most important abiotic redox-active minerals found in many soils and sediments (Risser and Bailey, 1992). The nonstoichiometric nature of Mn oxides means that the Mn has a variable oxidation state between (IV) and (II) depending on its

surrounding environment. This combined with high surface area is the reason for their catalytic activity (McBride, 1989a). The ability of Mn oxides to coat other mineral surfaces, thereby imparting increased reactivity, results in their exerting a catalytic effect that is proportionally much greater than their actual abundance (Bartlett, 1986).

## 2.3 Formation Mechanisms of Humic Substances in Natural Environments

### 2.3.1 Introduction

Several pathways have been proposed for the formation of humic substances and are summarized in Figure 2.11. These pathways involve the formation of humic substances from decomposing plant, animal and microbial remains.

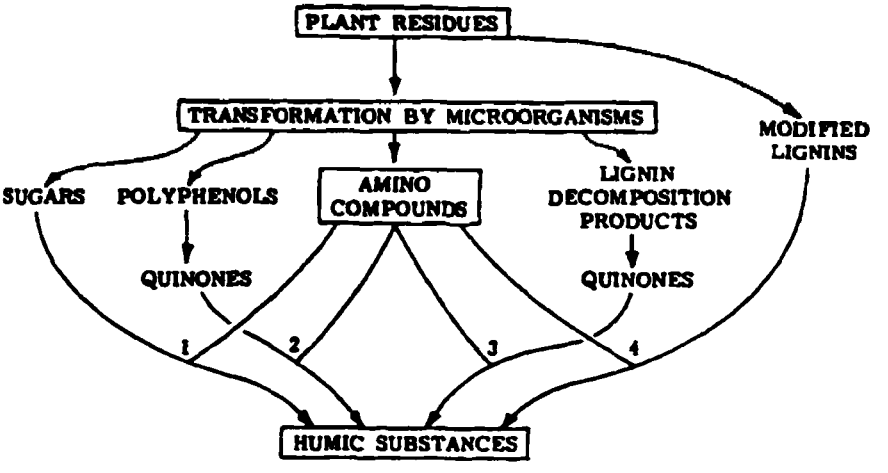


**Figure 2.11** Mechanisms for the formation of soil humic substances. Amino compounds synthesized by microorganisms are seen to react with reducing sugars (pathway 1), quinones (pathways 2 and 3) and modified lignins (pathway 4) to form complex humic substance like polymers (Stevenson, 1994).

Unlike pathways 2 to 4 which can be biotic (enzymatic) or abiotic (nonenzymatic) the Maillard reaction (pathway 1) involves nonenzymatic polycondensation reactions:

1. Pathway 1 is the melanoidin or "browning reaction" model and involves polycondensation reactions between simple reducing sugars and amino acids formed as by-products of microbial metabolism. The carbonyl of the sugar and nitrogen of the amino acid (or ammonia) react together forming a Schiff base. The resulting N-substituted glucosamine undergoes a complex series of dehydration and condensation reactions to produce both simple chemical products and brown nitrogenous polymers (Stevenson, 1994; Wershaw, 1994).
2. Pathway 2 is similar to 3 except that the polyphenols are formed by microbial action from non-lignin sources of carbon such as cellulose, plant waxes etc. The polyphenols then undergo reaction as in pathway 3.
3. In pathway 3 (Figure 2.11) lignin is degraded according to a model proposed by Kononova (1966) and Martin and Haider (1971). This differs from Waksman's lignin model (pathway 4, Figure 2.11) since phenolic aldehydes and acids released from lignin during microbiological attack undergo enzymatic (phenoloxidase) or abiotic (soil mineral catalyzed) conversion to semiquinones or quinones which then undergo humification reactions.
4. The lignin-protein model (pathway 4, Figure 2.11) was first proposed by Waksman in 1932. Lignin is partially degraded microbially and loses methoxyl ($CH_3O$) groups forming o-hydroxyphenols. These undergo a series of complex reactions eventually forming protohumic polymers. This theory has been superseded by the polyphenol pathway of humic substance formation (pathways 2 and 3).

### 2.3.2 Biotic Formation Mechanisms

#### 2.3.2.1 Microorganisms and Enzymes

Pathways 2 and 3 can be mediated either biotically or abiotically. The abiotic formation of humic substances (from either pathway 2 or 3) is considered in section 2.3.3. The Maillard reaction (pathway 1) is considered separately in section 2.3.3.2.

**The Polyphenol Model (Pathways 2 and 3)**

Based on current knowledge, the major plant constituents, such as cellulose and hemicellulose, lignins and proteins are important initial materials for the processes of humification. There exist two major sources of phenolic compounds - one from microbial synthesis using non-lignin sources such as cellulose and hemicellulose and aliphatic algal components (pathway 2, Figure 2.11) and the other from the microbial degradation of lignin (pathway 3, Figure 2.11).

**Microbial degradation of cellulose and hemicellulose (pathway 2)**

Cellulose is a polymer consisting of glucose subunits linked together by 1,4-glucoside bonds. Two different categories of enzymes (the endo-1,4-$\beta$-glucanases and the exo-1,4-$\beta$-glucanases) can hydrolyze cellulose to water-soluble polysaccharide fragments. The cellulose fragments are then hydrolyzed to glucose or oxidized to sugar acids by 1,4-$\beta$-glucosidase. These enzymes are produced by certain fungi and bacteria (Eriksson and Wood, 1985; Wood, 1988, 1989). Hemicellulase enzymes are found in soil bacteria, rot fungi and in marine algae (Dekker, 1985).

Soil fungi can synthesize melanins (non-lignin derived phenolics and quinones) which possess properties similar to those of soil humic acids. *Aspergillus sydowi*, *Epicoccum nigrum*, *Hendersonula toruloidea*, and *Stachybotrys atra* and *chartarum* have been shown to produce fungal melanins (Martin and Haider, 1969; Haider and Martin, 1970; Haider et al. 1972; Haider, 1976). Culturing *Aspergillus sydowi* in a glucose-asparagine medium for several weeks yielded detectable quantities of humic substance precursors such as orsenillic acid, 2,4-dimethylresorcinol, orcinol, p-hydroxybenzoic acid, protocatechuic acid, *p*-hydroxycinnamic acid, and 2,4,6-trihydroxybenzoic acid (Haider and Martin, 1970).

It is interesting that melanins produced by *Epicoccum nigrum* or *Hendersonula toruloidea* have a relatively high content of phenolic and aromatic groups whereas those derived from *Stachybotrys* are more aliphatic in nature. *Stachybotrys* fungi are prominent colonizers of plant residues in composts and in the field. Their melanins are relatively stable to further degradation and are precursors of both the aliphatic and aromatic portions of the humic macromolecule (Haider, 1994). The epiphytic fungi *Phaeosphaeria spartinicola* and *Phaeosphaeria halima* have been experimentally demonstrated to form dark brown substances similar to salt marsh humic substances when grown on substrates enriched with aqueous leaf extract of *Spartina alterniflora* (Loisel) (Filip and Alberts, 1993).

**Microbial degradation of lignin (pathway 3)**

The high molecular weight lignins are degraded by microbial attack and/or free radical mechanisms to smaller molecular fragments which can react with proteins and their degradation products to form nitrogen-containing humic substance like polymers. The enzyme mediated oxidation reactions which cause lignin degradation result in the cleavage of aryl phenol sidechains and ether linkages, and cause demethoxylation, aromatic hydroxylation and carboxylation. These reactions usually occur extracellularly because the lignin polymer is too large to pass through the cell membrane of the microorganisms (Flaig, 1988; Wershaw, 1994).

Fungi are the most important lignin-degrading microorganisms, specifically the white-rot fungi and the related litter-decomposing Basidiomycetes (Kirk and Shimada, 1985). These microorganisms occur in forest soils but are rare in arable ones. Lignin degradation in arable soils is mostly caused by Deuteromycetes, Actinomycetes and Streptomycetes species. They degrade lignin in a synergistic manner since single species are normally not well adapted for complete degradation (Haider, 1994).

Many investigations on lignin degradation have used the white rot fungus *Phaerochaete chrysosporium*. It and related organisms secrete extracellular peroxidase and phenoloxidase enzymes. Hydrogen peroxide ($H_2O_2$) is required by the peroxidase enzymes to degrade lignin and it has been postulated that white-rot fungi also produce aldehyde and acid reductase enzymes to help them in this (Schoemaker et al, 1989). *Phaerochaete chrysosporium* catalyses $C_\alpha$-$C_\beta$ cleavage of the lignin molecule through the action of hydrogen peroxide dependent oxygenase and peroxidase. This is followed by further oxidation (Tien and Kirk, 1984; Kuwahara et al., 1984; Chen and Chang, 1985). The sequence of reactions is shown in Figure 2.12.

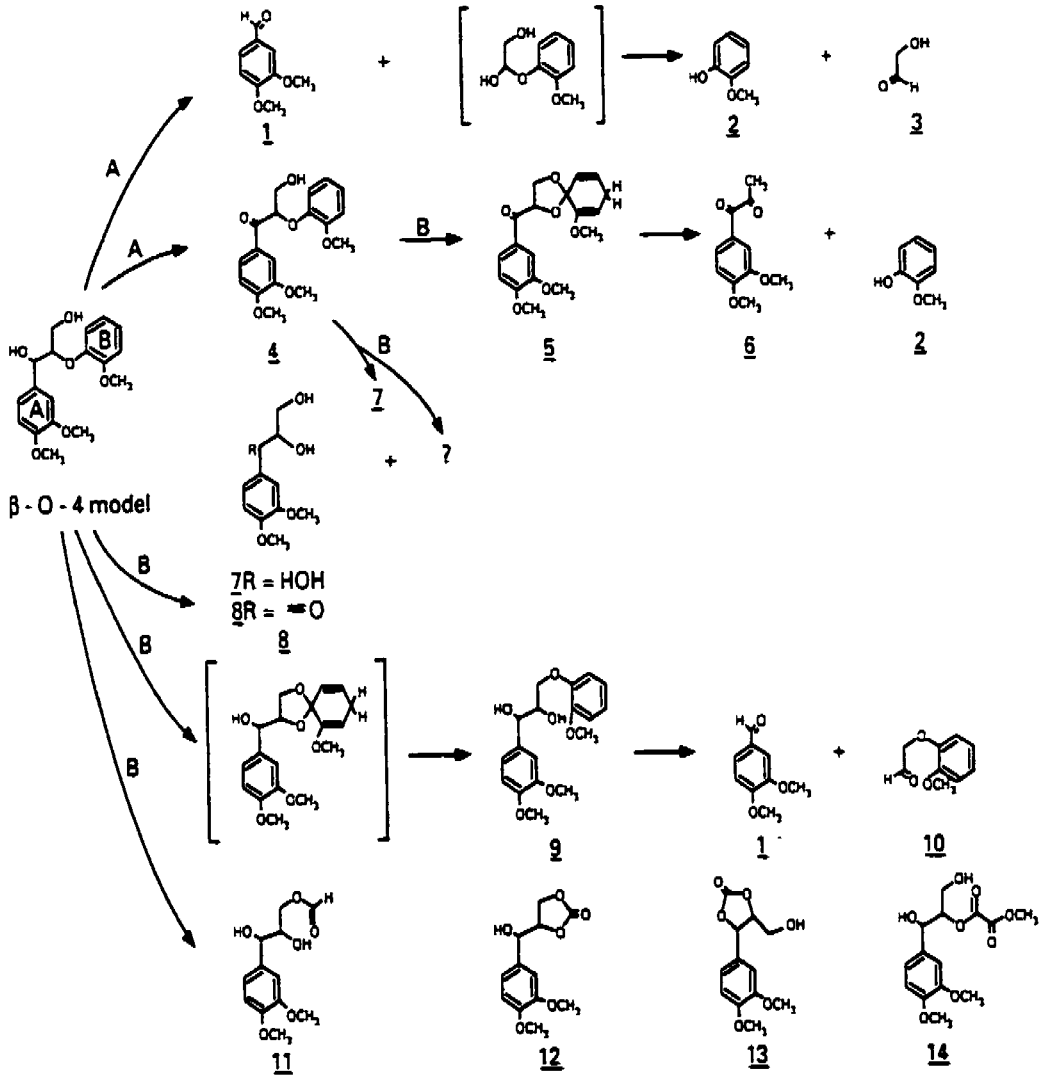


**Figure 2.12** Reaction products of oxidation of *β*-O-4 lignin model compounds by a ligninase-$H_2O_2$ system. Oxidation of either the A or B ring may take place as indicated (Kirk and Farrell, 1987).

Actinomycetes have also been shown to degrade lignocellulose particularly in arable soils. Under laboratory conditions *Streptomyces* sp. EC22, *Streptomyces viridosporus* T7A and *Thermonospora fusca* BD25 were shown to degrade ball-milled

wheat straw with the formation of humic acid-like substances (Trigo and Ball, 1994). These and similar results provide support for the role of actinomycetes in humification processes in soils and sediments.

Deuteromycetes (Fungi Imperfecti) are important microorganisms involved in the synthesis of soil humic substances. Martin and Haider (1971) have shown that fungi such as *Hendersonula toruloidea*, *Epicoccum nigrum*, *Aspergillus sydowi* and *Stachybotrys atra* and *Stachybotrys chartarum* degrade lignin and cellulose. Some of the possible synthesis and transformation pathways of polyphenols (humic substance precursors) by the deuteromycetes *Epicoccum nigrum* are shown in Figure 2.13.

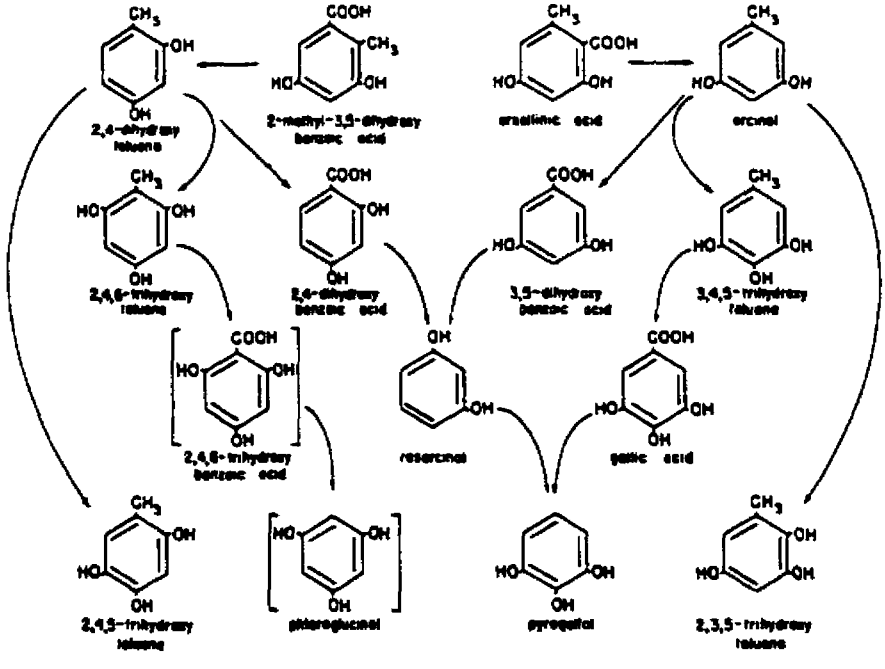

**Figure 2.13** Synthesis and transformations of phenols by *Epicoccum nigrum*. Orsellinic and cresorsellinic (2-methyl-3,5-dihydroxybenzoic) acids are the phenolic compounds that are initially synthesized. The other phenols are formed through introduction of hydroxyl groups, decarboxylation and oxidation of methyl groups (Haider and Martin, 1967).

Kononova (1966) postulated that the stages leading to the formation of humic substances were:

Stage 1: "Fungal attack of simple carbohydrates and parts of the protein and cellulose in the medullary rays, cambrium and cortex of plant residues."

Stage 2: "Xylem cellulose being decomposed by aerobic myxobacteria and in particular by fungi."

Stage 3: "Lignin being decomposed and phenols released during decay serving as source materials for humus synthesis."

**The Lignin-Protein Model (pathway 4)**

According to the model proposed by Waksman (1932), lignin was incompletely degraded by microorganisms with loss of methoxyl groups and the formation of o-hydroxyphenols (Stevenson, 1994). Aliphatic sidechains were oxidized to form carboxyl groups. Waksman's original lignin-protein theory of humification was substantially modified following studies by Flaig (1966). Flaig proposed that lignin underwent oxidative degradation reactions forming simple phenolic monomers. These monomers were then polymerized to produce humic substances (the polyphenol model, see below). Furthermore Martin and Haider (1971) proposed that phenolic compounds produced by microorganisms such as fungi could be incorporated into humic macromolecules. Accordingly the original lignin-protein model (lignin is microbially altered to form humic substances) has been largely superseded by the polyphenol model (microbial degradation of lignin to simple polyphenolic compounds which then undergo oxidative polymerization/polycondensation reactions under abiotic or biotic conditions to form humic substances, pathway 3, Figure 2.11).

### 2.3.3 Abiotic Formation Mechanisms

#### 2.3.3.1 Heterogeneous Catalytic Transformations of Natural Organic Compounds by Soil Minerals

Abiotic processes are extremely significant in soil and related environments. Reactions are catalysed by various crystalline and non-crystalline soil minerals, metal ions and sunlight (photocatalysis) and involve the formation of organo-mineral complexes, and nutrient and toxic substance release and retention (Bartlett, 1986; Wang et al., 1986; McBride, 1994; Huang, 1995; Smolen and Stone, 1998).

The classic definition of catalysts was originally proposed over 160 years ago as:

> Bodies which have the property of exerting on other bodies an action by means of which action they produce decomposition in bodies, and form new compounds into the composition of which they do not enter. This new power, hitherto unknown, is common in both organic and inorganic nature. I shall call it catalytic power. I shall also call catalysis the decomposition of bodies by this force. (Berzelius, 1836).

i.e., a catalyst is a substance that accelerates the rate of a chemical reaction and is unchanged in the process. This definition has been adhered to by one school of thought to the present, e.g., Pizzigallo et al. (1995) state that "by definition, a true catalyst cannot be altered by the reaction it catalyzes." However Bell (1941) noted that "a catalyst is a substance which appears in the rate expression to a power higher than that to which it appears in the stoichiometric equation" and therefore a reactant or product can also act as a catalyst. Many substances that are classified as catalysts can be altered or destroyed during the course of a reaction either through combination with reaction products or as a result of the process that gives them their catalytic activity (Moore and Pearson, 1981). Hence a catalyst can be considered to be a substance that alters the rate of a reaction regardless of its fate. For example, catalysts that are used in industrial engineering

processes undergo change with use (Twigg, 1989). Therefore an important criterion for a catalyst is that it alters the mechanism of the original reaction thereby changing the reaction rate (Moore and Pearson, 1981 However, the equilibrium position itself is not affected (Daintith, 1990).

Catalytic systems are divided into two major categories; homogeneous and heterogeneous. A homogeneous catalyst has the same phase as the reaction mixture it is affecting and is usually a dissolved species, whereas a heterogeneous catalyst is an insoluble solid and the catalytic action occurs on, or very close to, its surface (Campbell, 1988). The abiotic systems that are reviewed in this paper involve oxidation-reduction reactions between inorganic and organic components, i.e., there is proton and electron transfer. Oxidative processes result in electron loss and reductive processes result in electron gain. The oxidized component (oxidant) is the electron acceptor and the reduced component (reductant) is the electron donor (Sparks, 1995). In soils and sediments, soil organic matter is the source of electrons and soil minerals are the electron acceptors.

Although the significance of the association between mineral colloids and organics was recognized over six decades ago (Demolon and Barbier, 1929; Mattson, 1932; Waksman and Iyer, 1933), abiotic transformations of organic material in soil have often been ignored in the past because of the experimental difficulty of distinguishing abiotic processes from microbiological ones (McBride, 1994) especially since they often occur together. For example, the oxidative polymerization of phenols (an important precursor reaction in the formation of humic substances) is catalysed both by enzymes and abiotic (inorganic) catalysts (Dec and Bollag, 1990; Huang, 1990; Bollag, 1992; Shindo and Huang, 1992; Pal et al., 1994; Bollag et al., 1995; Wang and Huang, 1997). Presently, the oxidative polymerization of polyphenols in soils is thought to be one of

the major processes of formation of humic substances (Wang et al., 1986). Many soil inorganic components including oxides, hydroxides, oxyhydroxides, short-range ordered (SRO) minerals, clay-size layer silicates, primary minerals and natural soils have been shown to possess the ability to abiotically transform organic material in soils. The catalytic activity of clays is a function of their ability to behave as Brönsted acids (proton donors) or Lewis acids (electron acceptors). Transition metal ions in particular, have several oxidation states whose stability allows them to act as catalysts in naturally occurring redox reactions (Huang, 2000). Indeed metal ions in general and transition metal ions in particular can catalyze a wide variety of organic and inorganic reactions in soil and aquatic environments (Siegel, 1976; Bartlett, 1986; Mortland, 1986; Schwertmann et al., 1986; Huang, 1990, 1991; McBride, 1994; Stone and Torrents, 1995; Smolen and Stone, 1998).

#### 2.3.3.1.1 Short-Range Ordered Metal Oxides

Short-range ordered (SRO) mineral colloid forms in soil include metal oxides, aluminosilicates, and carbonates. These minerals have a relatively large surface area and charge density and therefore readily react with organic compounds. In soils SRO minerals frequently occur as coatings on crystalline minerals and, therefore, in addition to abiotic transformations of organic compounds, they can alter the surface properties and reactivity of crystalline minerals. As a consequence the effect of these colloids can be out of all proportion to their actual content in a soil (Huang, 1995).

The tremendous significance, in particular, of Mn oxides and oxyhydroxides in environmental health is a function of two conditions - they are present in a wide variety of soil environments (McKenzie, 1971, 1989) and they are extremely reactive - the most

important abiotic redox active mineral found in many soils and sediments (Risser and Bailey, 1992) - able to oxidize many environmentally important organic compounds and inorganic ions that include pollutants toxic to living organisms. In natural environments, Mn oxides exist as coatings on soils or sediments and as discrete particles (Crerar and Barnes, 1974; McKenzie, 1989).

Scheffer et al. (1959) investigated the formation of model humic substances by the catalytic oxidative polymerization of hydroquinone at pH 3 to 7 and room temperature using various iron oxides and oxyhydroxides (ferrihydrite, goethite, maghemite, hematite and lepidocrocite). The catalytic oxidative power is ferrihydrite > goethite > maghemite > lepidocrocite > hematite. Coupled with Ziechmann's work of the same period, this marked the beginning of the use of the phrase "abiotic formation of humic substances" in the literature (Wang et al., 1986). Iron oxides can adsorb a large variety of naturally occurring and anthropogenically produced organic compounds (Schwertmann et al., 1986). The causes of high energy levels of these iron oxide catalysts are lattice disturbance (i.e., lattice disorder, transitional condition, contamination by SRO materials, mixed crystallization) and development of large surface area (Huang, 1990). Particularly active sites are the points, holes, edges and corners of the soil minerals (Huang, 1990).

Adsorption may not only immobilize organics such as herbicides but also lead to their catalytic transformation (Schwertmann et al., 1986). Amberger and Vilsmeier (1978) studied the catalytic influence of synthetic proto-ferrihydrite and goethite on the transformation of cyanamide into urea or dicyanamide and guanylurea. They found that the mode of action of ferrihydrite was probably the result of its larger surface area and higher water content compared to goethite.

The manganese oxide minerals birnessite, cryptomelane, and pyrolusite are found widely distributed in soils and sediments (McKenzie, 1971, 1989). They are powerful oxidizers (oxidant strength decreases in the order Mn(III/IV) oxides > Co(III) oxides > Fe(III) oxides (Sparks, 1995)). Poorly or noncrystalline Fe, Al, Mn, and Si oxides (commonly found in soils) catalyze the browning of hydroquinone (Shindo and Huang, 1982). Hydroquinone is considered to be an important precursor for the formation of humic substances in natural environments (Flaig et al., 1975). Shindo and Huang (1982) found that Mn (IV) oxide exerted an extremely powerful effect on the abiotic browning of hydroquinone solution over normal soil pH ranges. They attributed the browning reaction to two processes:

1. Mn (IV) oxide catalyzed the oxidative polymerization of hydroquinone, acting as a Lewis acid by accepting electrons from the hydroquinone;

2. The oxidative polymerization was increased by a pH increase caused by reduction of the Mn (IV) oxide.

The effect of Fe oxide on hydroquinone was much less pronounced and only occurred under acidic conditions, whereas Al and Si oxides did not exhibit any activity. Subsequently Shindo and Huang (1984a) found that Mn (IV) oxides (birnessite, cryptomelane and pyrolusite) were the most reactive in promoting the polymerization of hydroquinone, resorcinol and catechol when compared to SRO Fe (III), Al and Si oxides.

Shindo and Higashi (1986) also studied the varying ability of SRO Mn (IV), Fe (III), Al and Si oxides, montmorillonite and tephroite to catalyze the abiotic transformation of hydroquinone and again noted the powerful promoting effect of Mn(IV) oxide. Al and Si oxides did not form humic polymers presumably because

by adsorption of low molecular weight polymers they suppressed further humification processes.

Stone and Morgan (1984) studied the reduction and dissolution of manganese (III) or (IV) oxide suspensions by hydroquinone in order to determine the kinetics and mechanism of the solubilization reaction. The reductive dissolution of Mn oxides by substituted phenols was investigated by Stone (1987). McBride (1987) investigated the adsorption and oxidation of catechol and hydroquinone by Fe and Mn oxides. He proposed that a $Fe^{3+}$-hydroquinone complex was formed at Fe oxide surfaces. which existed for long enough to allow electron transfer.

Stone (1987) assessed the importance of manganese dioxide in the abiotic degradation of phenolic pollutants. Reaction kinetics of manganese (III/IV) with 11 substituted phenols was examined. Alkyl. alkoxy and other electron donating substituents on phenols made them susceptible to oxidative degradation by the Mn oxides. However phenols substituted by electron-withdrawing groups such as carboxyl. aceto. nitro. chloro and others degraded more slowly. Significantly even the most refractory of the substituted phenols studied - *p*-nitrophenol - reacted. albeit slowly with manganese (III/IV) oxides. The postulated mechanisms for the surface chemical reactions for chlorophenols are:

(1) Precursor complex formation:

$$>Mn^{III} + ArOH \underset{k_{-1}}{\overset{k_1}{\rightleftharpoons}} (>Mn^{III}.ArOH)$$

(2) Electron transfer:

$$(>Mn^{III},ArOH) \underset{k_{-2}}{\overset{k_2}{\rightleftharpoons}} (>Mn^{II},ArO^{\bullet}) + H^+$$

(3) Release of phenoxy radical:

$$(>Mn^{II},ArO^{\bullet}) \underset{k_{-3}}{\overset{k_3}{\rightleftharpoons}} >Mn^{II} + ArO^{\bullet}$$

(4) Release of reduced Mn(II):

$$>Mn^{II}\text{-}OH_2 \underset{k_{-4}}{\overset{k_4}{\rightleftharpoons}} Mn^{2+} (+ \text{free underlying site})$$

(5) Coupling and further oxidation:

$ArO^{\bullet} + ArO^{\bullet} \Rightarrow$ quinones, dimers, and polymeric oxidation products (humic polycondensates)

where > denotes bonds between surface metal centres and the oxide lattice.

The successor complex to electron transfer $\{(>Mn^{II},ArO^{\bullet})\}$ may be either inner-sphere or outer-sphere and Mn (IV) oxide surface sites may participate in analogous reactions (Ulrich and Stone, 1989).

Ulrich and Stone (1989) studied the adsorption and oxidation of chloro-substituted phenols by Mn(III/IV) oxides. Chlorophenols are highly toxic compounds which frequently present environmental pollution problems because of their widespread use as insecticides, herbicides, fungicides and as intermediates in industrial syntheses. Chlorophenols can be degraded by certain bacteria and fungi (Baker and Mayfield, 1980; Boyd et al., 1989) but their persistence in natural environments indicates that conditions for their biotic degradation are often adverse. The impact of Mn oxides on degradation of chlorophenols may be a major factor in

the detoxification of these compounds in natural environments, particularly in zones of accumulation of Mn oxides (Ulrich and Stone, 1989).

The mineral-catalyzed oxidation and polymerization of both natural and xenobiotic phenolic compounds has been the focus of numerous other studies (Lehmann et al. 1987; McBride, 1987, 1989b, 1989c; Naidja et al. 1997, 1999; Shindo and Huang, 1982, 1984a, 1985a; Stone, 1987; Stone and Morgan, 1984a, 1984b; Ulrich and Stone, 1989; Wang and Huang, 1992). The results clearly show the catalytic power of Fe oxides, silicate clays and in particular Mn oxides.

According to Schnitzer (1982), humic acids are formed from simple phenols and phenolic acids via the formation of a semiquinone radical. Coupling of semiquinones originating from diphenols can lead to the formation of stable humic polymers under the catalytic action of Mn (IV) oxides (Huang, 1990). In the abiotic (free of microbial growth) Mn (IV) oxide-pyrogallol system, $CO_2$ is released apparently because of the ring cleavage of pyrogallol and subsequent formation of aliphatic compounds (Wang and Huang, 1992). This process could partly explain the aliphaticity of humic substances in soils which has been noted as a result of NMR studies (Hatcher et al., 1981; Wilson and Goh, 1977b). Therefore the soil mineral abiotic transformation of polyphenols resulting in ring cleavage may be an important pathway of C turnover in the natural environment (Wang and Huang, 1992).

Sunda and Kieber (1994) examined the oxidative degradation of humic substances by Mn oxides. Low molecular weight carbonyl compounds including pyruvate, acetone, formaldehyde and acetaldehyde were produced by the oxidation of natural organic matter. Oxidation of fulvic acids led to formation of pyruvate and acetaldehyde.

Many bacteria can, while oxidizing thermodynamically unstable Mn (II) to Mn oxides, deposit the oxides on their surfaces (Ghiorse, 1985). This process appears to account for most Mn oxidation in natural waters (Tebo and Emerson, 1985) and sediments (Kepkay, 1985). It is speculated (Sunda and Kieber, 1994) that the deposition of Mn oxides on bacterial surfaces represents a means for the bacteria to degrade refractory, non-available sources of organic carbon into simpler molecules which can be utilized by the bacteria. This "symbiotic process" illustrates the use of a metal oxide catalyst by a biogenic medium.

Shindo and Huang (1984b) found that birnessite catalysed the abiotic formation of nitrogenous polymers in hydroquinone-glycine systems at common soil pH ranges. They proposed the following processes as taking place:

1. The birnessite (Mn(IV) oxide) acts as a Lewis acid and accepts electrons from hydroquinone which is oxidized and then polymerized (Shindo and Huang, 1982).
2. Polymer-N and $NH_3$-N are formed by the reaction of glycine with hydroquinone. During the oxidative polymerization of hydroquinone, the glycine is incorporated into the nitrogenous polymer. Glycine is partially decarboxylated and deaminated (Figure 2.14) and reacts with quinonic C=O during the polymerization process (Shindo and Huang, 1984b).

Birnessite also catalyzes the polycondensation of pyrogallol and glycine under abiotic conditions and the nitrogenous polymers formed are similar to natural humic polycondensates (Wang and Huang, 1987a). The amino acid is deaminated and decarboxylated (Figure 2.14) and this process which is catalysed by birnessite may be a significant new pathway of C turnover and N transformation in nature (Figure 2.15)

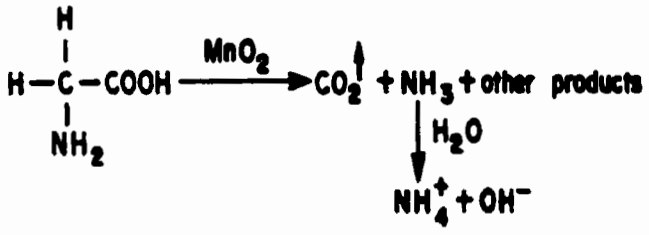


**Figure 2.14** Decarboxylation and deamination of glycine catalyzed by birnessite (Wang and Huang, 1987a).

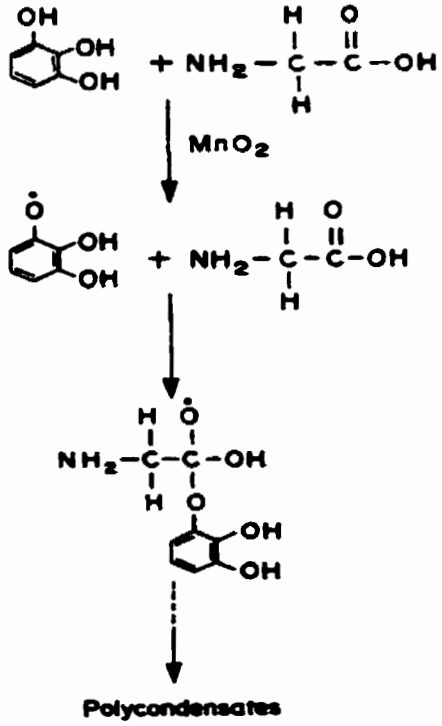


**Figure 2.15** Reaction of pyrogallol-derived free radicals with glycine (Wang and Huang, 1987a).

Wang and Huang (1997) also noted that birnessite strongly promoted incorporation of alkyl C and N into humic polycondensates via the interaction of glycine with pyrogallol. $^{14}C$ tracer experiments also showed that carboxyl C from glycine was incorporated into the humic polymers.

#### 2.3.3.1.2 Other minerals

Early research on catalytic oxidative polymerization of phenolics by clay-size layer silicates leading to formation of humic polycondensates was carried out by Kumada and Kato (1970), Wang and Li (1977), Wang et al. (1978a, 1978b), and Pinnavaia et al. (1974). Kumada and Kato (1970) observed the "browning effect" of various clay minerals and metal oxides on pyrogallol. Wang and Li (1977) and Wang et al. (1978a, 1978b, 1980) found that clay minerals catalyzed the abiotic formation of humic polycondensates through processes of oxidative polymerization involving common naturally occurring phenolic compounds. Clay minerals such as muscovite can catalyze the oxidation of some humic substance precursors (Filip et al. 1977). Ca-illite can accelerate the formation of N-containing humic polymers from systems containing phenolic compounds and amino acids at neutral pH (Wang et al., 1985). Shindo and Huang (1985b) examined 14 inorganic materials including clay and primary minerals for catalytic power in oxidatively polymerizing hydroquinone. Of all the minerals investigated, Mn oxide was the most effective in promoting oxidative polymerization of hydroquinone although the clay minerals montmorillonite, vermiculite, illite and kaolinite all had some effect. The 2:1 layer silicates were more effective than 1:1 layer silicates (e.g., kaolinite) because of their greater specific surface and increased probability of lattice imperfections (Thomas and Thomas, 1967). Montmorillonite, a

smectite type clay, has been known for a long time to exhibit marked solid acidity (Izumi et al., 1992). It was used as a catalyst for the cracking of hydrocarbons prior to replacement by synthetic silica-alumina and zeolites. The catalytic power of montmorillonite is governed by particle size, cation exchange capacity, and the position of isomorphous substitution (Izumi et al., 1992).

Wang and Huang (1986) discovered that in aqueous solution and at near neutral pH (6.5), hydroquinone - a known humic substance precursor (Flaig et al., 1975; Hayes and Swift, 1978) - can be transformed into humic polycondensates which are deposited in the interlayers of nontronite (Fe(III) bearing smectite) saturated with calcium, the most common and abundant exchangeable cation found in soils and sediments. Since micro-organism growth was not observed in the systems studied, it was concluded that the processes were abiotic in nature (Wang and Huang, 1986). Heating the complex to between 150 and 500°C caused collapse of d-spacing due to decrease in organic carbon content. Humic macromolecules present in the Ca-nontronite interlayers were not entirely decomposed even after heating at 350°C. This suggests that humic polycondensates present in organo-mineral complexes are stabilized by the inorganic structures and can be protected from degradation under natural conditions. X-ray diffraction evidence showed that heating at 500°C destroyed the humic macromolecule interlayers.

Fe (III) on the edges and internal and external planar surfaces (Lewis acid sites) of Ca-nontronite promote the abiotic polymerization of hydroquinone (Wang and Huang, 1987b). Treating Ca-nontronite with sodium metaphosphate (which blocks the edges of the mineral) caused a significant decrease in, but did not completely prevent, the formation of humic polymers. A synergistic effect of Ca-nontronite and atmospheric

$O_2$ was noticed since polymerization of hydroquinone was substantially lower in a $N_2$ atmosphere. Wang and Huang (1989) studied the catalytic activity of several Ca-exchanged minerals with respect to their ability to abiotically transform pyrogallol. Catalytic activity as evinced by $CO_2$ release from ring cleavage of pyrogallol, and the quantity of humic polycondensates formed was Ca-nontronite > Ca-kaolinite > Ca bentonite.

The polycondensation of glycine and pyrogallol was strongly promoted by nontronite (Wang and Huang, 1991). The nontronite-catalyzed ring cleavage of polyphenolics was further investigated by Wang and Huang (1994) in abiogenic or abiotic systems. The influence of the polyphenolic structure and functionality on their ring cleavage was examined and it was determined that the ease of cleavage of the polyphenolics was pyrogallol > catechol > hydroquinone. The proposed reaction processes are shown in Figure 2.16.

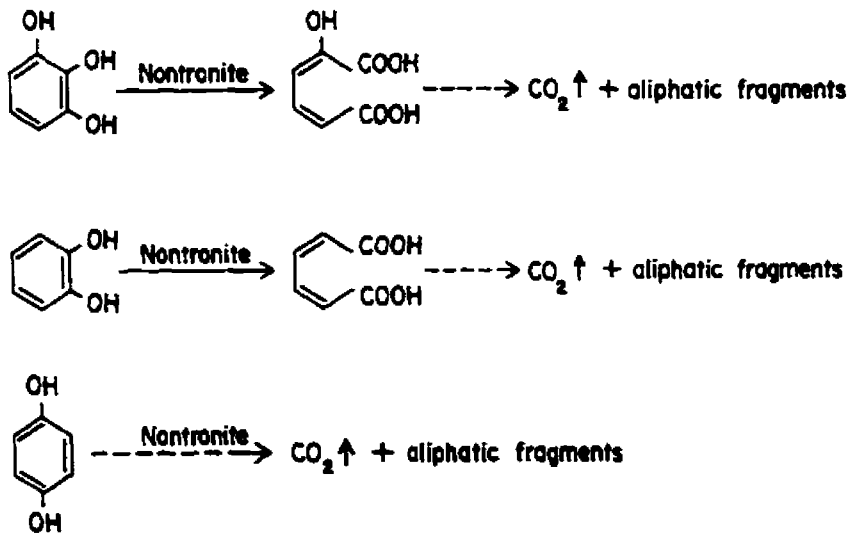


**Figure 2.16** Proposed reaction processes for the ring cleavage of polyphenols and subsequent release of $CO_2$ (Wang and Huang, 1994).

Primary minerals occur widely in soil and sediment environments (Paul and Huang, 1980). Therefore, the effect of primary minerals on natural and anthropogenic organic compounds is of significance to environmental health. Shindo and Huang (1985b) investigated the catalytic effects of primary minerals (quartz, feldspars, micas, pyroxenes, amphiboles and olivines) on hydroquinone polymerization under abiotic conditions. Of all the minerals tested, tephroite exhibited the strongest effect on hydroquinone increasing total yields of HA by greater than ninefold. The proposed reasons are (Shindo and Huang, 1985b):

1. Tephroite is a Mn bearing silicate.
2. It is probable that part of the Mn in tephroite is present in the form of higher valency states which are extremely reactive.
3. The oxidation of diphenols is thermodynamically unfavourable.

Wang et al. (1983) found that rates of polymerization of phenolic compounds in the presence of an Inceptisol (low organic matter content) and the $H_2O_2$ treated silt fraction of a Mollisol followed the order vincinal trihydroxy > vincinal dihydroxy > meta-dihydroxy > monohydroxy phenolics. The polymerization rate for meta-dihydroxy phenolics was orcinol > resorcinol > 3,5-dihydroxybenzoic acid. Electron releasing methyl group substituents increased polymerization rate while electron withdrawing carboxyl substituents reduced the rate (Wang et al., 1983).

In summary, phenolic compounds undergo oxidative coupling reactions during the process of humification. The process requires catalysts which may be biotic in nature (oxidoreductive enzymes) synthesized by soil microorganisms (Sjoblad and Bollag, 1981) or abiotic in nature (clay minerals or metal oxides) and present in soils (Huang, 2000).

### 2.3.3.2 The Maillard reaction

The Maillard reaction was initially proposed by Maillard (1912, 1913) who investigated the formation of yellow-brown to dark-brown "pigments" or melanoidins upon refluxing solutions of glucose and lysine together. The basic pathways of the Maillard reaction are summarized in Figure 2.17.

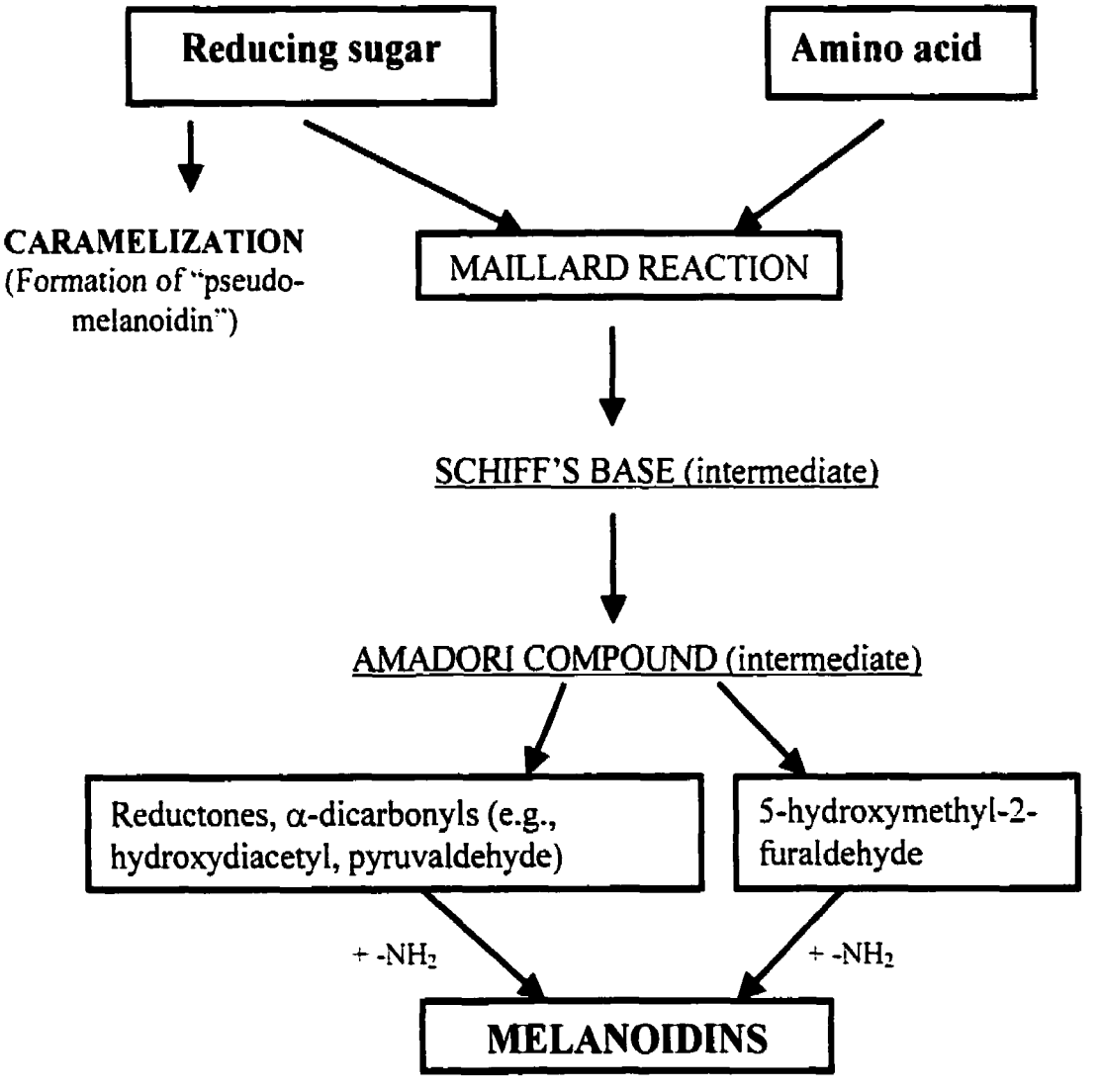


**Figure 2.17** The Maillard reaction summarized (adapted from Ikan et al., 1996).

The initial reaction in the Maillard reaction is the condensation of a reducing sugar with an amine which involves the addition of the amine to the aldehyde group of the sugar and formation of the Schiff base (Figure 2.18). This subsequently forms a N-substituted glycosylamine which then undergoes the Amadori rearrangement forming an N-substituted-1-amino-1-deoxy-2-ketose (Figure 2.18).

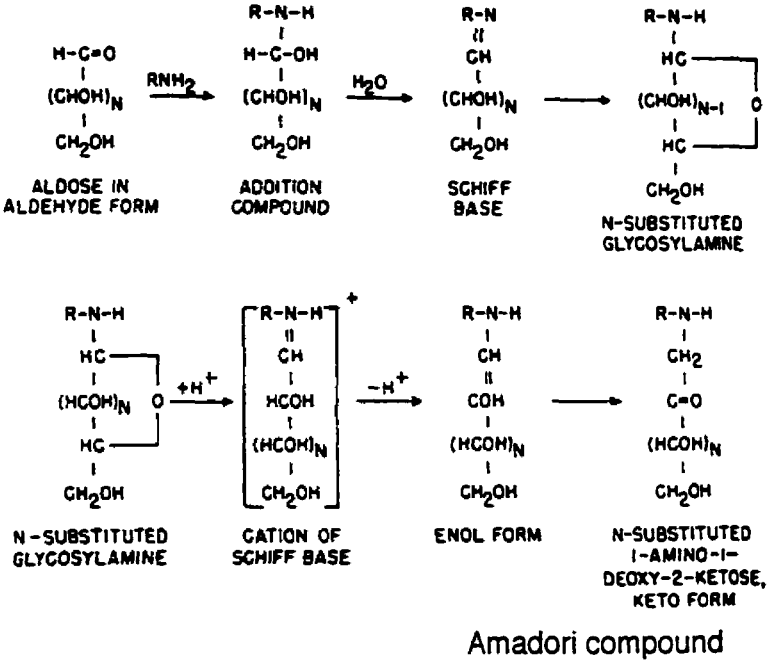


**Figure 2.18** Formation of some intermediate compounds from sugar-amine condensation (Hodge, 1953).

The Amadori adduct can then (a) fragment with liberation of the amine and formation of 3C aldehydes and ketones such as acetal, glyceraldehyde, and dihydroxyacetone, (b) lose two water molecules and form reductones, or (c) lose three

water molecules and form 3-hydroxymethyl furfural (Hodge, 1953). All of the above compounds are extremely reactive and can undergo polycondensation reactions in the presence of amino compounds to form high molecular weight brown coloured melanoidins of indeterminate structure (Figure 2.19).

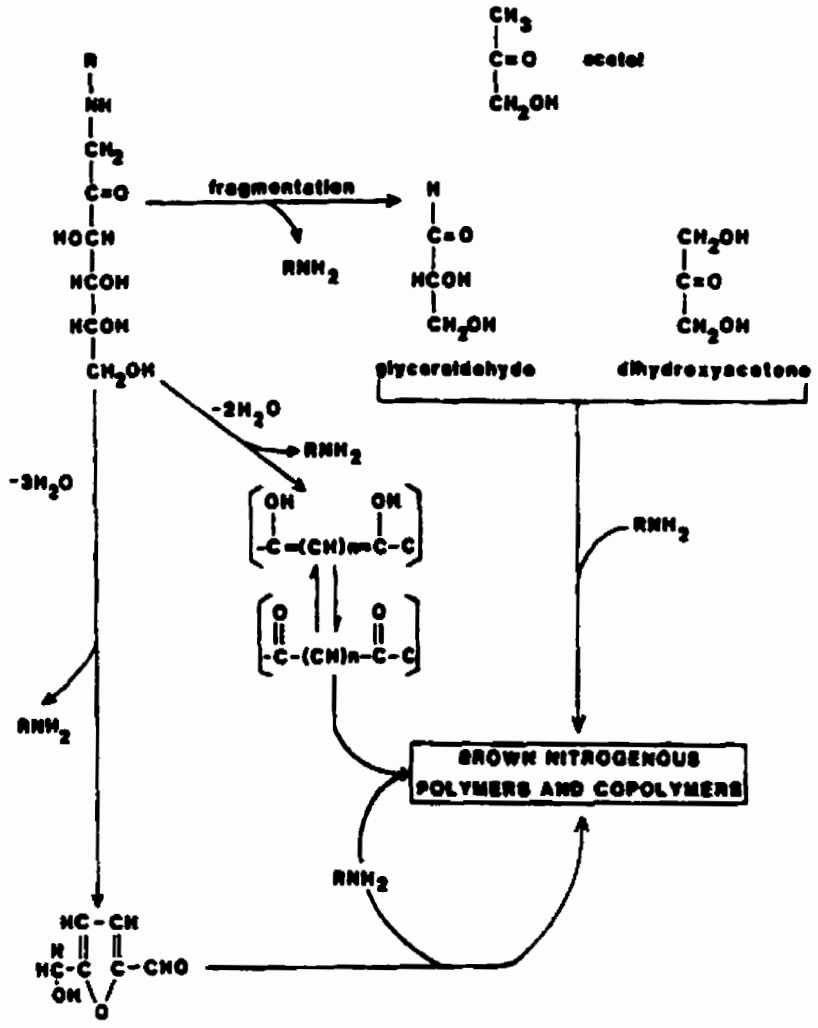


**Figure 2.19** Pathways for the formation of brown nitrogenous polymers (melanoidins) from the product of the Amadori rearrangement (Stevenson, 1994).

In addition, carbohydrates on their own can undergo dehydration reactions leading to the formation of phenols and quinones (Popoff and Theander, 1976). The mechanism is shown below (Figure 2.20).

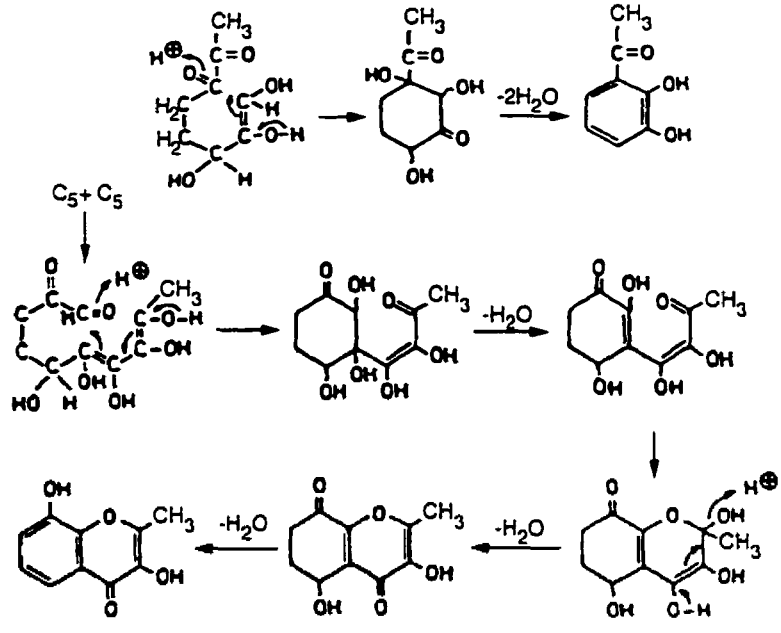


**Figure 2.20** Reactions leading to formation of phenols and quinones from carbohydrates; $C_5$ = pentose sugar (Popoff and Theander, 1976).

Since Maillard's pioneering work, evidence has accumulated which suggests that natural humic substances may be produced by condensation reactions between sugars and amino acids (Hodge, 1953; Ikan et al., 1996). Further support is lent by the presence of humic substances in marine environments where carbohydrates and proteins, because of their abundance, are more probable precursors of humic substances than are lignin or phenolic polymers (Nissenbaum and Kaplan, 1972; Hedges and Parker, 1976; Ikan et al.,

1996). For example, proteins and carbohydrates are the principal constituents (up to 80% of dry cell material) of marine organisms such as algae (Harvey, 1969). Marine floras such as *Spartina alterniflora* contain and release the chemical precursors of melanoidins, i.e., sugars and amino acids (Ikan et al., 1990).

Additional evidence for the contribution of melanoidin-type structures to humic substances was supplied by thermal (Ioselis et al. 1981) and spectroscopic studies (Rubinstzain et al. 1984). Further, the chemical and physical properties of both natural and synthetic humic substances were examined by spectroscopic (IR, UV, $^{13}$C-CPMAS NMR, ESR), chromatographic (GC and GC/MS), thermogravimetric (TG, DTG, TG-EGD-MS), pyrolytic (stepwise, Rock Eval, Curie point), oxidative ($KMNO_4$) and isotopic methods by Ikan et al. (1992). Ikan et al. (1996) noted that $^{13}$C-CPMAS NMR spectra of melanoidins were remarkably similar to some humic acids. They suggested, therefore, that the Maillard reaction (of sugars and amino acids) plays a more significant role in the formation of the skeletal matrix structure of humic substances than previously thought. Evershed et al. (1997) have recently detected the presence of Maillard reaction products in decayed plant materials from an archaeological site dating from ancient Egypt. However, there are significant gaps in knowledge and, the catalytic role of minerals common in soils and sediments in the Maillard reaction and the resultant formation of humic substances in nature is little understood and the effect of light in promoting such catalysis is unknown.

There have been very few studies to investigate the possible mechanisms of formation of melanoidins under naturally occurring conditions. On the basis of rate studies, Hedges (1978) suggested that melanoidins should form more readily in seawater or in marine sediments (pH ~ 8), than in terrestrial waters or soils which are generally

more acidic (Becking et al. 1960). Hedges (1978) concluded that the reaction of basic amino acids with sugars was kinetically favoured and resulted in the formation of predominantly aliphatic nitrogen-rich polycondensates. Such characteristics are shared in particular by humic substances found in marine environments (Nissenbaum and Kaplan, 1972; Rashid and King, 1970; Stuermer and Harvey, 1974; Stuermer and Payne, 1976). Hedges (1978) also reported that the relative affinities of kaolinite and montmorillonite for dissolved melanoidins varied with pH, and montmorillonite adsorbed more melanoidins than did kaolinite. Partitioning between aqueous solutions and clay minerals could produce 100 to 1000 fold concentrations of the melanoidin polymers in the particulate phase where a significant portion of the molecules may be selectively adsorbed on the basal surface of expandable clay minerals (Hedges, 1978).

Taguchi and Sampei (1986) reacted glucose (1.5M) and glycine (1.5M) and glucose (1.5M) and alanine (1.5M) (90 °C ± 0.5 °C for 408 hours 18 minutes) to synthesize melanoidins. They subsequently examined the roles of montmorillonite and calcium carbonate in accelerating the above reactions (under conditions of 90 °C ± 0.5°C for 131 hours 36 minutes) and found that the rate of melanoidin formation was much higher in the presence of montmorillonite. However the $CaCO_3$ association reactions of the same experiments showed extremely low rates of melanoidin formation (Taguchi and Sampei, 1986). Collins et al. (1992) presented experimental evidence for condensation reactions between sugars and proteins in carbonate skeletons. They postulated that fossil biomaterials such as shells protected proteins and polysaccharides from microbial degradation. Mixtures of protein, polysaccharides and finely ground calcite crystals in sealed glass vials were heated at 90°C. On the basis of the yield of melanoidins obtained they estimated that at the global scale roughly $2.4 \times 10^6$ tons of

calcified tissue matrix glycoproteins were annually processed through the melanoidin pathway.

Arfaioli et al. (1999) studied humic-like compounds formed by the action of clay minerals and exchangeable cations on D-glucose and L-tyrosine. Ten grams of montmorillonite or kaolinite made homoionic using Ca, Al or Cu(II) chlorides were reacted with one gram each of L-tyrosine and D-glucose in a small volume of water (replenished regularly) at 70°C for 30 days. Humic and fulvic acids were extracted from the mineral-organic complexes. Arfaioli et al. (1999) found that Cu-systems showed the largest degree of humification probably as a result of the complexing power of Cu ions overcoming all other factors.

Mayer (1994) examined the relationship between mineral specific surface area and organic carbon concentration for sediments and soil A horizons from around the world. He found that most of the mineral surface area was found to be present within pores <8 nm wide and hypothesized that if organic matter in soils or sediments was present in a highly dispersed state such as a monolayer, then the organic coatings on the mineral grains probably resided on adsorption sites within the small (<8 nm) pores. The organic matter was, therefore, protected from hydrolytic enzymes produced by microorganisms, which were too large to enter the pores. Bosetto et al. (1997) also postulated that in soils with a large number of pores <0.1μm in diameter which are inaccessible to microbes, simple compounds such as amino acids could escape microbial attack and undergo polycondensation reactions.

Although the Maillard reaction is perceived to be an important pathway in humification processes, it is slow under ambient conditions (Hedges, 1978). In addition, in aquatic environments the significance of the rate of polycondensation of dissolved

free sugars and amino acids at the very low concentrations found in such natural systems remains obscure (Hedges, 1988). Active microbial recycling of the precursor carbohydrates and proteins is also a problem. However, minerals common in soils and sediments could catalyze the Maillard reaction and the resultant formation of humic substances in nature, while at the same time protecting the substrates against microbial action. Moreover, polyphenols that have been shown to be important precursors in the abiotic formation of humic substances (Shindo and Huang, 1982), could also interact with the Maillard reaction and form humic polycondensates. Birnessite is a widely occurring manganese oxide mineral (McKenzie, 1989) and has marked catalytic activity in the abiotic transformation (oxidative polymerization) of phenolic compounds to humic materials (Huang, 1995).

## 2.4 Photochemistry of Humic Substances and Manganese (IV) Oxides

Photochemical reactions involve the absorption of light of a particular wavelength by chromophores (Wershaw, 1994). All molecules absorb light at short enough wavelengths but the energy difference between the highest occupied molecular orbital (HOMO) and the lowest unoccupied molecular orbital (LUMO) is difficult to calculate accurately for even small molecules (Warren, 1994). This absorption raises the electrons in the chromophore molecule to a higher energy state. In the simplest approximations of such a system (the "particle in a box" model) the energy for a transition is approximately $n^2(1.5 \times 10^{-18}$ J) where n = principal quantum number (Warren, 1994). As the excited molecule returns to the ground state, energy is dissipated

in the form of heat, light, energy transfer or decomposition of the molecule often accompanied by the formation of reactive free radical species (Wershaw, 1994).

Mn (IV) oxides are semiconductors and Stone (1986) notes that their semiconducting properties are of potential importance in reductive dissolution reactions. Band gap energies for Mn (IV) oxides vary from 0.26 to 0.7 eV and the average vibrational energy of molecules is approximately 0.026 eV at ambient temperature (25°C). Therefore, the bandgap energy of Mn oxides is potentially low enough for thermal or photochemical energy to excite electrons into the conduction band at 25°C. Once this occurs, electrons can be transferred from one manganese centre to another. The electron transfer results in the creation of reactive electron holes on the manganese oxide surface and permits the increased reaction of reductant molecules on the oxide surface.

Humic substances are known to be rich in stable free radicals which probably influence their behaviour in polymerization-depolymerization reactions, and reactions with organics such as pesticides and pollutants (Schnitzer, 1978). Photoreduction of Mn oxides by marine fulvic acid was first observed by Sunda et al. (1983) and is more rapid at lower pH values, possibly as a result of greater adsorption of fulvic acid on Mn oxide surfaces (Stone and Morgan, 1984). Rates of Mn (IV) oxide reduction increased considerably with increasing light intensity and with the addition of marine humic acid. The significance of the photoactivated reduction of manganese oxides to $Mn^{2+}$ lies in the dissolution of Mn oxides entering the surface of the ocean and prevention of appreciable oxidation of $Mn^{2+}$ to Mn oxide precipitates which would sink to the ocean bottom and thereby be lost to the water column. In surface waters where the effect of sunlight is important, photoactivated reduction by dissolved organic compounds would redissolve freshly formed Mn oxides - this process explains the dominance of dissolved over

particulate forms of manganese in surface seawater (Sunda et al, 1983). Therefore the photocatalyzed reduction of Mn oxides in surface seawaters by dissolved organic compounds retains soluble Mn ion in the photic zone where it is of essential use to marine phytoplankton (Sunda et al, 1983).

The reductive dissolution of $\gamma$-MnOOH and $\beta$-$MnO_2$ in the presence of oxalate occurs thermally at pH values from 4 to 6 (Xyla et al. 1992). A precursor surface complex with oxalate was formed followed by electron transfer and release of the reduced metal centre into solution. A strong pH dependence, which paralleled pH dependence of oxalate adsorption on the oxide surface, was demonstrated by the rates of reductive dissolution which were markedly higher at low pH values (Xyla et al. 1992). In contrast to other studies where natural reductants were utilized, only a slight photochemical enhancement of the reductive dissolution was noted.

Lee and Huang (1995) investigated the photochemical and associated thermal effects on the role of birnessite in catalyzing the abiotic transformation of four polyphenols (hydroquinone, resorcinol, catechol and pyrogallol). They found that increasing light intensities from 0 (dark) to 500 $\mu E\ m^{-2}\ s^{-1}$ (lower limit of a cloudy day according to Sunda et al. (1983) caused an increase in abiotic formation of $CO_2$ in the birnessite-polyphenol and polyphenol systems. Likewise increase in temperature from 5 to 45°C at a light intensity of 0 $\mu E\ m^{-2}\ s^{-1}$ also caused increased release of $CO_2$. There was a synergistic effect of birnessite and O2 in the abiotic ring cleavage of polyphenols (Lee and Huang, 1995). Polyphenolic photofragmentation probably caused the observed decrease in absorbances (at 472 and 664 nm) of the supernatants in the birnessite-polyphenol and polyphenol systems as light intensity was increased (despite increase in

absorbance as temperature was increased from 5 to 45°C in the dark) (Lee and Huang, 1995).

Photoprocesses affecting natural organic matter and pesticides in water phase are summarized in Table 2.3. The use of light as an aid to degradation and oxidation of various organics has been the focus of research by Hidaka et al. (1996) who examined the photocatalytic degradation of surfactants in the presence of $TiO_2$ suspensions. Hilgendorff et al. (1996) studied the photocatalytic decomposition of tetrachloromethane on semiconducting $TiO_2$-particles. They found that effectiveness of $CCl_4$ mineralization increased markedly with decreasing concentration of molecular oxygen. The photocatalytic degradation of atrazine has been investigated using nanosized iron under simulated solar radiation (Pulgarin et al. 1996). The initial degradation rate was observed to be pseudo-first order.

**Table 2.3** Photoprocesses affecting natural organic matter and pesticides in the water phase (Andreux et al. 1995)

| Substrates | Products | Probable mechanisms and effects |
|---|---|---|
| Natural organic chromophores | $^1C + {}^1HO_2$; $C + {}^1O_2^-$ | Transfer (H, electron, energy) to $^1O_2$; initiation of numerous reactions |
| Petroleum hydrocarbon (RH, ArH) | ROO· | Oxygen addition; oxidized organic radicals |
| Pesticides (disulfoton) | Disulfoton sulfoxide | Singlet oxygen; changes in properties and toxicity |
| Herbicides (2,4-D; 2,4,5-T) | Oxidation and reduction products | Direct photolysis; complex |
| Pentachlorophenol | Phenols, quinones, acids | Direct photolysis; changes in properties and toxicity |
| PCBs, DDT | Complex | Direct or sensitized photolysis; dehydrochlorination |

## 2.5 Molecular Topological Analysis

### 2.5.1 Introduction

Computational chemistry simulates chemical structures and reactions numerically, based in full or in part on the fundamental laws of physics. Chemical phenomena can be studied in principle by running calculations on computers rather than by examining reactions and compounds experimentally. Ideally, not only stable molecules but also in some cases short-lived unstable intermediates and even transition states can be so modelled. As a consequence information about molecules and reactions can be obtained that is impossible by observation alone (Foresman and Frisch, 1996).

There are two major areas within the field of computational chemistry which are devoted to the structure of molecules and their reactivity: (1) molecular mechanics and (2) electronic structure theory. They share some goals which are summarized below, but the calculations are very different in nature:

1. Computing the energy of a particular molecular structure (i.e., the arrangement of atoms, nuclei and electrons in space).
2. Performing geometry optimizations that locate the lowest energy molecular structure in close proximity to the specified starting structure.
3. Computing the vibrational frequencies of molecules resulting from interatomic motion within the molecule.
4. Computing everything that can be measured (chemical shifts, solvent effects etc.).

### 2.5.2 Molecular Mechanics

Molecular mechanics simulations utilize the laws of classical physics in order to predict molecular structures and properties. Various commercially available computer programs such as MM3, Hyperchem, Quanta, Sibyl and Alchemy use molecular mechanics methods. Each particular method is characterized by a force field consisting of the following components.

(1) An equation set that defines how the potential energy of a molecule varies with the positions of its component atoms.

(2) A series of atom types that define the element characteristics within a particular chemical context. Atom types prescribe different characteristics for an element depending upon its environment. Hybridization, charge and the types of atoms to which it is bonded define the atom type.

(3) One or several parameter sets that fit the equations and atom types to experimental data. Parameter sets define force constants (the values used in the equations to relate atomic characteristics to energy components and structural data such as bond lengths and angles).

Molecular mechanics calculations perform calculations based upon nuclear interactions and electronic effects are implicitly, rather than explicitly, included in force fields through parametrization. Therefore, molecular mechanics computations can be used for large systems containing thousands of atoms. However, because of this approximation there are several limitations:

1. Each force field can achieve good results only for a small class of molecules that are closely related to those for which it was parametrized. No force field can be applied in a general manner for all molecular systems that are of interest.

2. Because molecular mechanics computations neglect electrons, they cannot consider chemical problems where electronic effects are dominant i.e., they cannot be used to investigate processes involving bond formation and/or bond breaking. In addition, molecular properties dependent on subtle electronic details cannot be reproduced by molecular mechanics methods.
3. Force fields are relatively correct only in cases where the atoms in a molecule are slightly displaced from their equilibrium positions.

### 2.5.3 Electronic Structure Methods

Electronic structure computations utilize the laws of quantum mechanics rather than classical physics as the basis for their calculations. Quantum mechanics theory states that the state of a quantum mechanical molecule may be obtained by solving for the Schrödinger equation:

$$H\psi = E\psi$$

where $\psi$ is the wavefunction , E is the energy and H the Hamiltonian operator.

In the Born-Oppenheimer approximation electrons in a molecule move in the electrostatic field of atomic nuclei. The state of the molecule is represented by a many-electron wavefunction and the Hamiltonian contains two terms: the electron kinetic energy term and the electron-electron and electron-nucleus potential interaction term. It should be noted that for any but the smallest systems exact solutions to the Schrödinger equation are not computationally practical i.e., are beyond the capabilities of even the most powerful present day supercomputers.

Electronic structure methods are divided into two types according to their mathematical approaches:

1. Semi-empirical methods such as AM1, MINDO/3 and PM3 which are used in programs such as MOPAC, AMPAC, Hyperchem and Gaussian involve parameters derived from experimental data to simplify the computations. They solve for an approximate form of the Schrödinger equation, e.g., in the case of the present dissertation the glucose-glycine system, that relies on the availability of appropriate parameters for the chemical system involved.
2. *Ab initio* methods, unlike molecular mechanics or semi-empirical methods, involve no experimental parameters in their computations. Instead their operations utilize only the laws of quantum mechanics i.e., the first principle in the name *ab initio*, and the values of a limited number of physical constants: The speed of light, the masses and charges of electrons and nuclei, and Planck's constant.

In summary, semi-empirical methods provide a reasonably quantitative description of a molecular system and fairly accurate quantitative predictions of energies and structures for systems where good parameter sets are available. *Ab initio* computations provide accurate, quantitative predictions for a broad range of systems and are not limited to any particular class of system. However, system size can be a serious limiting factor and in practice, systems that are over fifty atoms in size or that contain elements of high atomic number may be too much to handle for even the most powerful supercomputers available for analysis.

# 3. Experiments, Results and Discussion

## 3.1 The Effect of Birnessite on the Maillard Reaction at Ambient Light Conditions.

### 3.1.1 Introduction

The Maillard reaction was initially proposed by Maillard (1912, 1913) who investigated the formation of yellow-brown to dark-brown "pigments" or melanoidins upon refluxing solutions of glucose and lysine together. Since then, evidence has accumulated which suggests that natural humic substances may be produced by condensation reactions between sugars and amino acids (Hodge, 1953; Ikan et al., 1996). However, the catalytic role of minerals common in soils and sediments in the Maillard reaction and the resultant formation of humic substances in nature remains to be uncovered.

The objective of this research unit was to investigate birnessite catalysis of the Maillard reaction between glucose and glycine and the resultant formation of humic substances under conditions of ambient light intensity, and varying pH and temperature.

Glucose and glycine were used in this study because they are present in plant and microbial polymers. Structural components of plants and microbial carbohydrates are relatively rich in glucose (McKeague et al., 1986; Cheshire, 1979). Proteinaceous material in soil originates from animals, plants, and microorganisms; proteins and peptides of plant tissues are rich in glycine and other amino acids (McKeague et al., 1986). Manganese

oxides are common mineral components of soils and birnessite, a short-range ordered and tetravalent Mn oxide, is one of the most widely occurring forms (McKenzie, 1989).

### 3.1.2 Materials and Methods

Chemicals were purchased from Sigma Chemical Co. (St. Louis, MO). All chemical reagents used were ACS reagent grade or purer.

**Preparation of Birnessite**

Birnessite was synthesized according to the method recommended by McKenzie (1971). It was characterized by X-ray diffractometry and Fourier transform infrared absorption (FTIR) spectroscopy. The X-ray diffractogram exhibited peaks at 0.720 nm, 0.360 nm and 0.243 nm which are characteristic for birnessite. The FTIR spectra had absorption bands at 3431, 1624 and 524 $cm^{-1}$ which are diagnostic for birnessite (Potter and Rossman, 1979).

**Effect of Birnessite on the Maillard Reaction**

Utensils, birnessite and double-deionized water were sterilized by autoclaving and 0.02% w/v thimerosal was added to each sample as antiseptic. Two and a half grams of birnessite were suspended in 80 mL of glucose-glycine (0.05 mole each, 1:1 molar ratio) solution. The pH was adjusted to 6.00 or 7.00 by the addition of 0.1M HCl or 8.00 by the addition of 0.1 M NaOH, and double-deionized water was added to make a total volume of 100 mL. The flasks were sealed and placed on an oscillating water bath at 25 or 45°C. The system was allowed to react for 15 (45°C), 30 (25°C) or 60 (25°C) d. Ambient light intensity over the samples ranged from 0 to 3.1 ± 0.9 $\mu E\ s^{-1}\ m^{-2}$. At the end of the reaction period, the supernatant liquid phase was separated from the solid phase by centrifugation

at 25000 g for 35 to 40 minutes. The following control experiments were carried out under the same conditions as above:

Control 1- duplicated above conditions but contained no birnessite.

Control 2 - duplicated above conditions but consisted of birnessite and water alone.

Control 3 - was not sterilized and did not contain antiseptic.

The solid phases were lyophilized (freeze dried) and the following analyses performed:

(a) Visible absorption spectroscopy, pH, Eh, pE + pH and Mn of supernatants: Supernatants of the reaction systems were analyzed by visible absorption spectrophotometry using a Beckman DU 650 microprocessor controlled spectrophotometer (Beckman, Fullerton, CA). The pH and Eh of suspensions of the systems was measured and the Mn (i.e., Mn (II) or $Mn^{2+}$) content of the supernatants was determined at 279.5 nm by atomic absorption spectroscopy.

(b) Electron paramagnetic resonance (EPR) spectroscopy of solid (lyophilized) and liquid phases: The reaction systems were investigated by electron paramagnetic resonance spectrometry using a Bruker B-ER418S spectrometer (Bruker Analytik, Rheinstetten/Karlsruhe Germany) operating in the field modulation mode at 100 KHz and a frequency of 9 to 10 GHz (X band) at room temperature. The microwave frequencies were measured with an EIP model 548A microwave frequency counter. The field positions were calibrated using a Bruker NMR Gaussmeter ER035M and corrections. The relative positions of the sample and the NMR probe were adjusted using 1,1-Diphenyl-2-picryl-hydrazil (DPPH) as a standard.

(c) $^{13}C$ nuclear magnetic resonance (NMR) spectroscopy of liquid phase samples containing no Mn: Analysis was performed on a Bruker Avance 500 spectrometer (Bruker

Analytik, Rheinstetten/Karlsruhe Germany) with a supercooled magnet of field strength 11.74 Tesla operating at 125.77 MHz for $^{13}C$. Deutero-chloroform ($CDCl_3$) was used as external standard.

(d) $^{55}Mn$ cross polarization magic angle spinning (CPMAS) NMR of the lyophilized solid phase: Analysis was performed on a Bruker Avance 500 spectrometer (Bruker Analytik. Rheinstetten/Karlsruhe Germany) with a $^{55}Mn$ probe. Manganese (II) sulphate and birnessite were used as standards.

(e) Fourier transform infra-red (FTIR) spectroscopy: FTIR spectra of samples of the lyophilized solid phase of the reaction systems were obtained using KBr disks (200 mg) containing 0.5% w/w sample on a Biorad 3240 SPS microprocessor-controlled spectrometer (Cambridge. MA). Disks were flushed with dry $N_2$ gas for 10 min prior to analysis in order to remove atmospheric $CO_2$ and moisture.

(f) X-ray Absorption Near-Edge Structure (XANES) spectroscopy: X-ray-absorption near-edge spectroscopy experiments were carried out at the MRL (UIUC)/Lucent Technologies beam line X16-C at the National Synchrotron Light Source. Brookhaven National Laboratory (BNL). Upton. NY. The X-ray energy varied from 200 eV below to 1000 eV above the absorption K-edge of Mn ($E_K$ = 6540 eV) using a Si (111) double-crystal monochromator. To minimize thickness effect in the XANES experiment. the powdered samples were ground. sieved through 200 mesh. and spread onto Scotch tape. Up to 16 layers were folded to acquire a total thickness of the sample corresponding experimentally to $\Delta\mu x \sim 1$. where $\Delta\mu$ is the absorption edge jump at the Mn K-edge energy. and $x$ is the thickness of the sample. The data were obtained in the transmission mode. using gas-filled ionization chambers as detectors. Data from the pre-edge and near-edge regions (-30 eV < $E-E_K$ < 40 eV) were acquired with a 0.5 eV energy increment. The data in the extended

energy range (40 eV < $E-E_K$ < 1000 eV) were acquired with a 2 eV increment. Up to 3 measurements were averaged for the same sample to improve the signal-to-noise ratio. To correct for a small angular drift of the monochromator crystals between the scans, all data sets were aligned versus their absolute energy and interpolated to the same energy grid before the averaging. The X-ray absorption coefficient of Mn metal foil, placed downstream of the sample, was measured in the transmission mode simultaneously with all the samples and was used as a reference for the alignment of energies.

**Examination of microbial activity**

Samples of the above-mentioned reaction systems were incubated for 6 or 15 d (after reaction period was complete) at 37°C under aerobic or anaerobic conditions on Trypticase Soy Agar (TSA) plates to test for abiotic conditions. TSA is a nonselective growth medium suitable for the cultivation of a wide variety of microorganisms (Dandurand and Knudsen, 1997). No culturable, chemolithotrophic micro-organisms were detected indicating that all reactions were abiotic in nature.

### 3.1.3 Results and Discussion

#### 3.1.3.1 Visible absorption spectroscopy of supernatants and related solution phase analysis

Table 3.1.1 shows the effect of birnessite on the browning of glucose-glycine, glucose and glycine systems at initial pH values of 6.00, 7.00 and 8.00 at 45°C for a period of 15 d. Compared to the control solution, which contained no Mn (IV) oxide, the addition of birnessite to the glucose-glycine system markedly increased the extent of browning. In the glucose-glycine-birnessite systems with initial pH of 6.00, 7.00 and 8.00, the final pH values ranged from 7.78 to 8.40.

**Table 3.1.1** Effect of birnessite on the glucose-glycine, glucose, and glycine solutions at initial pH values of 6.00, 7.00 and 8.00 following reaction for 15 d at 45°C

| Treatment† | Absorbance 400 nm | Absorbance 600 nm | pH | Eh (mV) | Mn ($\mu g\ mL^{-1}$) | pH + pE |
|---|---|---|---|---|---|---|
| **Initial pH 8.00** | | | | | | |
| Glucose + glycine + birnessite | 12.6 ± 0.2 | 0.85 ± 0.04 | 8.40 ± 0.07 | 159 ±12 | 8740 ± 185 | 10.92 ± 0.26 |
| Glucose + glycine | 0.66 ± 0.02 | 0.129 ± 0.005 | 7.91 ±0.08 | 408 ±8 | 0 | 14.27 ±0.20 |
| Glucose + birnessite | 0.098 ± 0.002 | 0.041 ± 0.002 | 7.62 ±0.10 | 294 ±11 | 2845 ±82 | 12.28 ±0.23 |
| Glucose | 0.054 ± 0.002 | 0.027 ± 0.001 | 7.39 ±0.05 | 397 ±9 | 0 | 13.68 ±0.19 |
| Glycine + birnessite | 0.02 | Colourless‡ | 8.12 ±0.06 | 378 ±7 | 9.7 ±0.5 | 14.11 ±0.17 |
| Glycine | 0.02 | Colourless‡ | 7.86 ±0.04 | 395 ±10 | 0 | 14.12 ±0.20 |
| **Initial pH 7.00** | | | | | | |
| Glucose + glycine + birnessite | 10.4 ± 0.3 | 0.74 ± 0.01 | 7.89 ±0.08 | 151 ±16 | 8286 ±108 | 10.28 ±0.32 |
| Glucose + glycine | 0.34 ± 0.02 | 0.093 ± 0.005 | 7.03 ±0.05 | 428 ±11 | 0 | 13.81 ±0.22 |
| Glucose + birnessite | 0.043 ± 0.002 | 0.027 ± 0.001 | 7.47 ±0.08 | 283 ±7 | 2797 ±75 | 11.96 ±0.20 |
| Glucose | 0.038 ± 0.002 | 0.022 ± 0.001 | 6.69 ±0.04 | 408 ±9 | 0 | 13.16 ±0.19 |
| Glycine + birnessite | 0.02 | Colourless‡ | 7.46 ±0.04 | 404 ±6 | 20.9 ±0.8 | 13.86 ±0.13 |
| Glycine | 0.02 | Colourless‡ | 6.95 ±0.05 | 396 ±10 | 0 | 13.23 ±0.21 |
| **Initial pH 6.00** | | | | | | |
| Glucose + glycine + birnessite | 10.1 ± 0.3 | 0.53 ± 0.01 | 7.78 ±0.09 | 160 ±11 | 7622 ±85 | 10.32 ±0.27 |
| Glucose + glycine | 0.113 ± 0.01 | 0.042 ± 0.002 | 5.86 ±0.07 | 446 ±16 | 0 | 12.39 ±0.22 |
| Glucose + birnessite | Colourless‡ | | 6.41 ±0.11 | 286 ±12 | 2575 ±41 | 10.94 ±0.30 |
| Glucose | Colourless‡ | | 5.85 ±0.10 | 410 ±8 | 0 | 12.35 ±0.23 |
| Glycine + birnessite | 0.02 | Colourless‡ | 6.70 ±0.06 | 352 ±6 | 40.9 ±1.5 | 12.28 ±0.18 |
| Glycine | Colourless‡ | | 5.87 ±0.07 | 402 ±10 | 0 | 12.24 ±0.23 |

† Laboratory ambient light intensity was 0 to 3.1 ± 0.9 $\mu E\ s^{-1}\ m^{-2}$.

‡ The supernatant was visibly colourless with absorbance < 0.01 at the wavelengths studied.

In contrast to the glucose-glycine-birnessite system, the pH values of the glucose-glycine-system, which had initial pH of 6.00, 7.00 and 8.00, ranged from 5.86 to 7.91. Furthermore, the pH + pE values (Table 3.1.1) of the glucose-glycine-birnessite system were much lower (10.28 to 10.92) compared to the glucose-glycine system containing no birnessite (12.39 to 14.27). Since pE + pH = 20.78 + ¼ $O_2$ (g) and this value is derived from the transformation of $H^+$ to form $H_2O$, it is a measure of the redox status of a system (Lindsay, 1979). Therefore the pE + pH of the glucose-glycine-birnessite systems with initial pH's of 6.00, 7.00 and 8.00 were consistently lower than the corresponding glucose-glycine system. There were large amounts of Mn (i.e., Mn (II)) in the supernatants of the glucose-glycine-birnessite systems in the pH range studied (Table 3.1.1). The supernatant of the glucose-birnessite system exhibited a similar but much less advanced trend compared to the glucose-glycine-birnessite system for the pH + pE values and Mn content. The presence of glycine in the glucose-glycine-birnessite system increased the reduction of Mn(IV) to Mn(II), and greatly increased the extent of browning compared to the glucose-birnessite system. There was only slight evidence of reaction in the glycine-birnessite system at 45°C.

Table 3.1.2 summarizes the effect of birnessite on the glucose and glucose-glycine system at the initial pH values of 6.00, 7.00 and 8.00 at the end of the reaction period of 30 d at 25°C. There is a similiar pattern to that exhibited at 45°C, though the extent of browning in all the systems was much less. Figure 3.1.1 shows the absorbance versus wavelength plots for the glucose-glycine-birnessite and glucose-glycine systems with initial pH values of 6.00, 7.00 and 8.00 at the end of 15 d at 45°C and at the end of 30 d at 25°C. It is clear that birnessite exerted a marked catalytic effect on the extent of browning, and therefore, on polycondensation in the Maillard reaction between glucose

and glycine at 25 and at 45°C, which is the approximate temperature of the soil surface on a day when the ambient air temperature is 25°C (Baver, 1956), and therefore is a surficial soil temperature frequently encountered in tropical and subtropical areas, and even in temperate areas during the summer months.

**Table 3.1.2** Effect of birnessite on the glucose-glycine and glucose systems (initial pH values of 6.00, 7.00, 8.00) following reaction for 30 d at 25°C

| Treatment† | Absorbance | | pH | Mn | Eh | pH + pE |
|---|---|---|---|---|---|---|
| | 400 nm | 600 nm | | ($\mu g\ mL^{-1}$) | (mV) | |
| **Initial pH 8.00** | | | | | | |
| Glucose + glycine + birnessite | 0.148 ± 0.009 | 0.046 ± 0.002 | 8.08 ± 0.07 | 2215 ± 64 | 340 ± 9 | 13.82 ± 0.22 |
| Glucose + glycine | 0.065 ±0.005 | 0.022 ±0.002 | 7.81 ± 0.14 | 0 | 389 ± 7 | 14.38 ± 0.26 |
| Glucose + birnessite | Colourless‡ | | 7.76 ± 0.10 | 909 ± 7 | 360 ± 10 | 13.84 ± 0.27 |
| Glucose | Colourless‡ | | 7.53 ± 0.08 | 0 | 390 ± 9 | 14.11 ± 0.23 |
| **Initial pH 7.00** | | | | | | |
| Glucose + glycine + birnessite | 0.114 ±0.007 | 0.023 ±0.001 | 7.39 ± 0.11 | 2341 ± 56 | 380 ± 6 | 13.80 ± 0.21 |
| Glucose + glycine | 0.026 ±0.001 | 0.011 ±<0.001 | 7.06 ± 0.05 | 0 | 407 ± 12 | 13.98 ± 0.25 |
| Glucose + birnessite | Colourless‡ | | 6.85 ± 0.09 | 1001 ± 17 | 362 ± 11 | 12.96 ± 0.28 |
| Glucose | Colourless‡ | | 6.65 ± 0.07 | 0 | 399 ± 7 | 13.40 ± 0.19 |
| **Initial pH 6.00** | | | | | | |
| Glucose + glycine + birnessite | 0.064 ±0.003 | 0.022 ±0.001 | 6.67 ± 0.07 | 2012 ± 76 | 413 ± 8 | 13.64 ± 0.21 |
| Glucose + glycine | Colourless‡ | | 6.55 ± 0.05 | 0 | 438 ± 9 | 13.95 ± 0.23 |
| Glucose + birnessite | Colourless‡ | | 6.22 ± 0.05 | 981 ± 28 | 370 ± 6 | 12.47 ± 0.15 |
| Glucose | Colourless‡ | | 5.81 ± 0.01 | 0 | 411 ± 6 | 12.75 ± 0.11 |

† Laboratory ambient light intensity was 0 to 3.1 ± 0.9 $\mu E\ s^{-1}\ m^{-2}$.
‡ The supernatant was visibly colourless with absorbance < 0.01 at the wavelengths studied

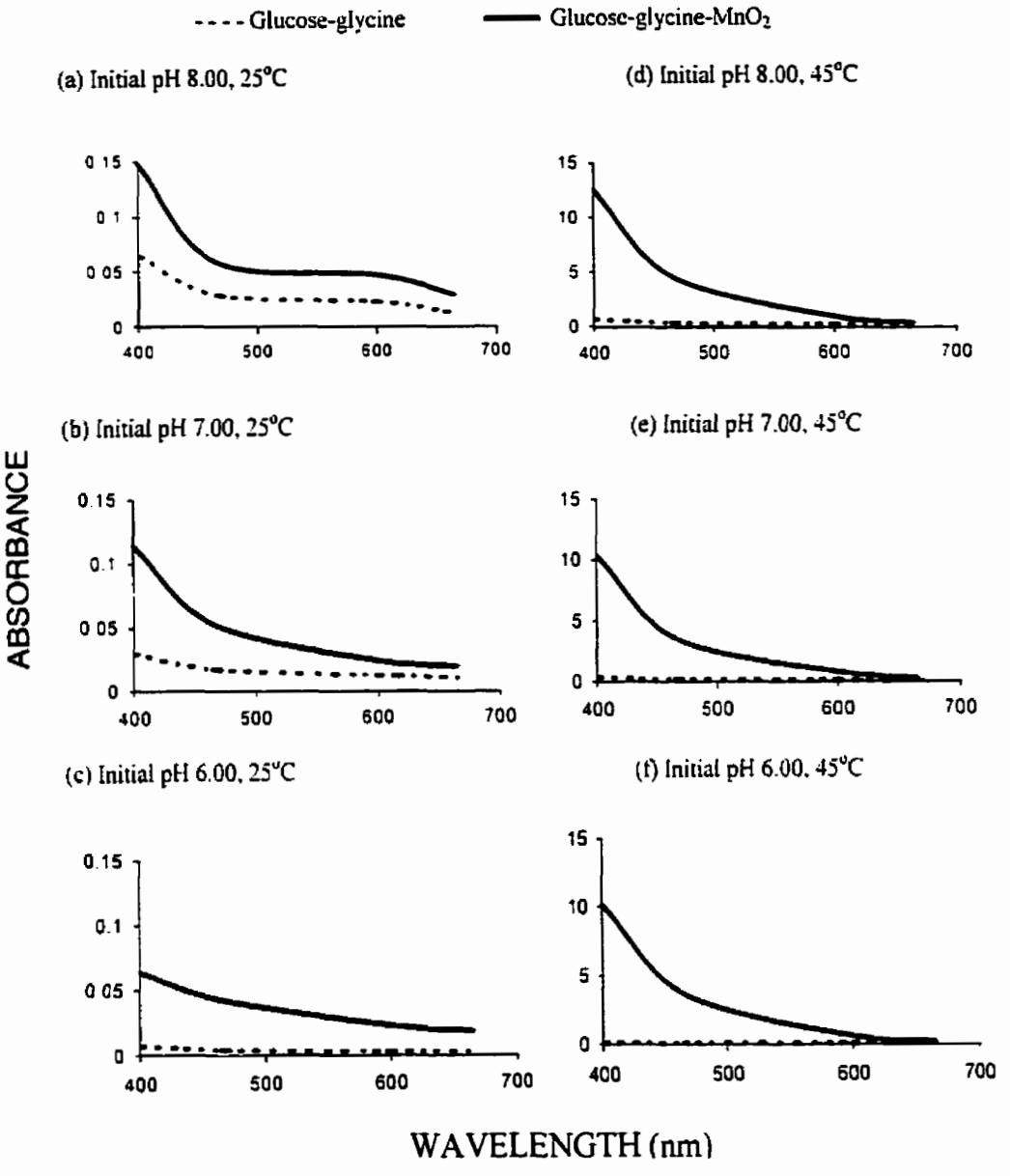


**Figure 3.1.1** Absorbance versus wavelength plots of products of Maillard reaction between glucose and glycine as influenced by birnessite catalysis under laboratory ambient light intensity. (a), (b) and (c): 30 day reaction period. (d), (e) and (f): 15 day reaction period.

### 3.1.3.2 Electron paramagnetic resonance (EPR) spectroscopy

In EPR spectroscopy, Mn(II) in solution gives a characteristic six-line hyperfine pattern spaced at 90 gauss and centred on g = 2 (Lipard and Berg, 1994). The EPR evidence confirms the presence of Mn(II) in the supernatants of the glucose-glycine-birnessite and glucose-birnessite systems at 45°C and 25°C (Figures 3.1.2 to 3.1.4). EPR spectroscopic analysis of the freeze dried solid phase of the glucose-glycine-birnessite, glucose-birnessite and glycine-birnessite systems at 45°C indicates that the presence of Mn(II) was most pronounced in the glucose-glycine-birnessite system (Figure 3.1.5). XANES spectroscopic data confirms this as discussed in Section 3.1.3.5. It is not possible at the moment to prove the existence of organic free radicals in the sediments because of the masking effect of Mn(II).

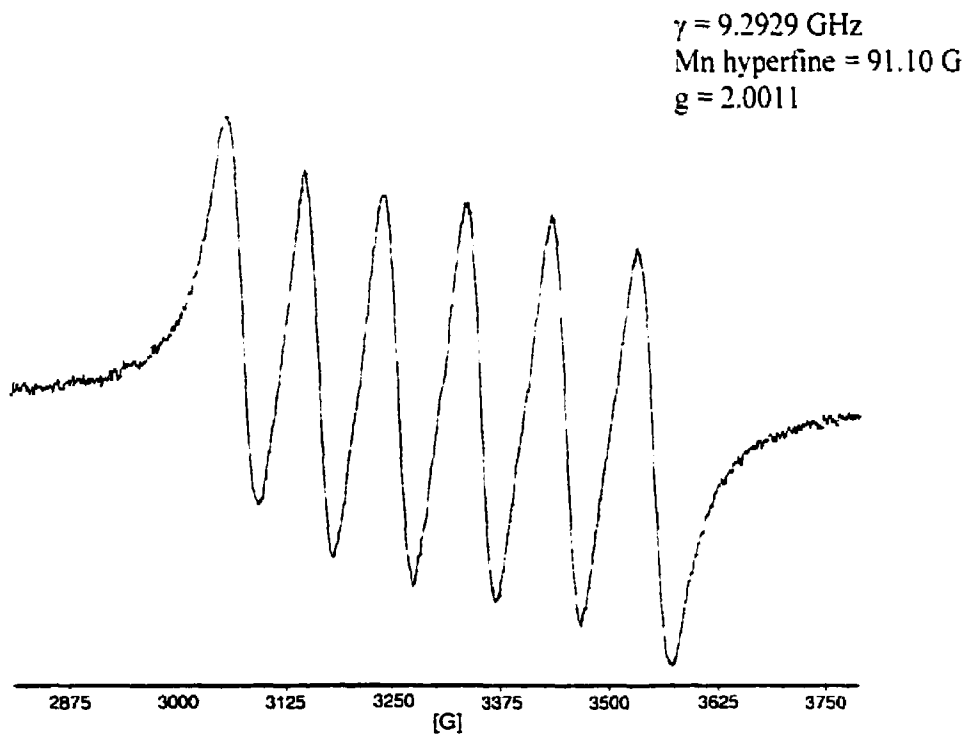


**Figure 3.1.2** The EPR spectrum of the supernatant of the glucose-glycine-birnessite system following reaction at 45°C for 15 d at an initial pH of 7.00.

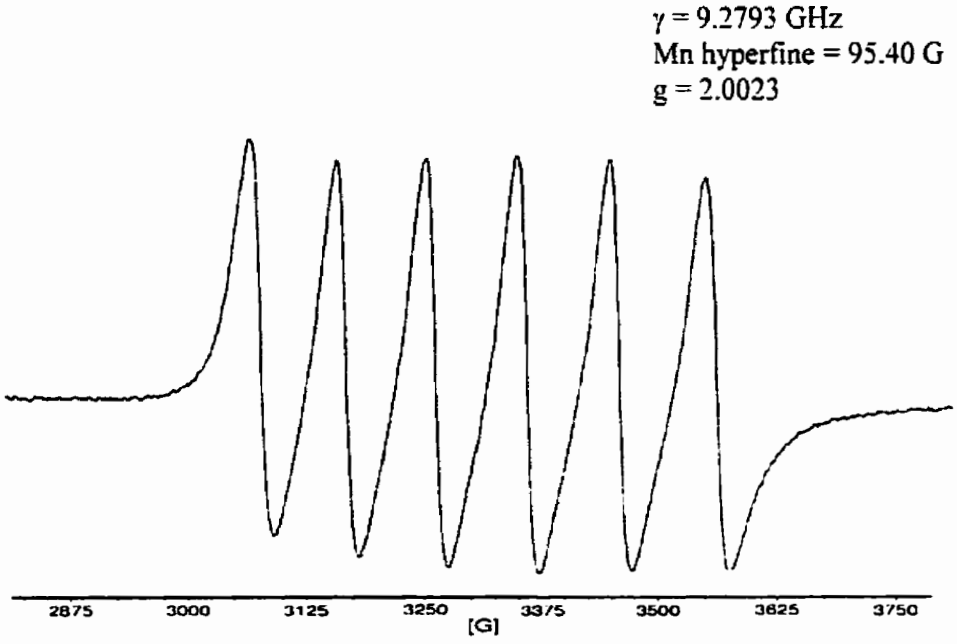


**Figure 3.1.3** The EPR spectrum of the supernatant of the glucose-birnessite system following reaction at 45°C for 15 days at an initial pH of 7.00.

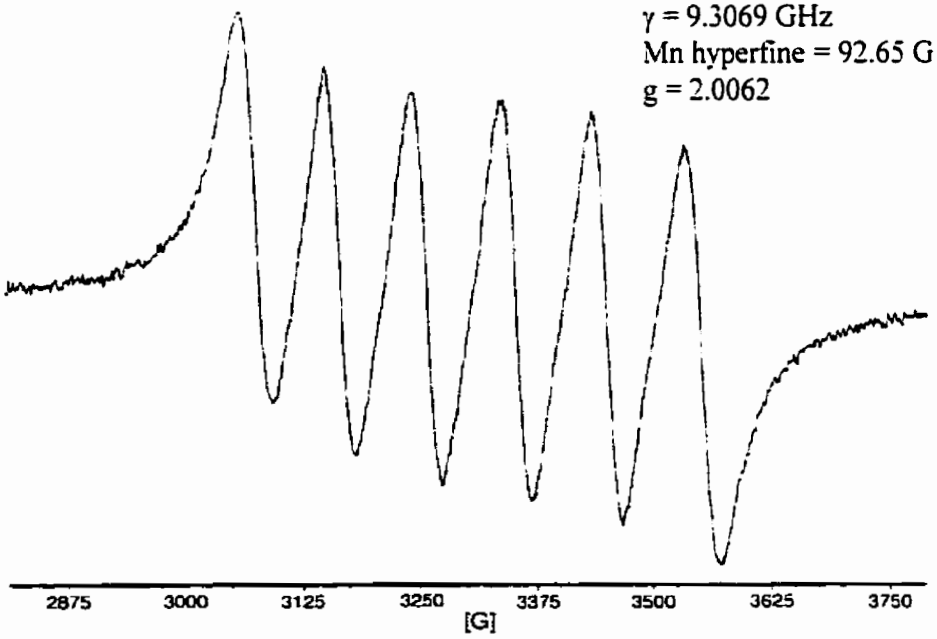


**Figure 3.1.4** The EPR spectrum of the supernatant of the glucose-glycine-birnessite system following reaction at 25°C for 30 days at an initial pH of 7.00.

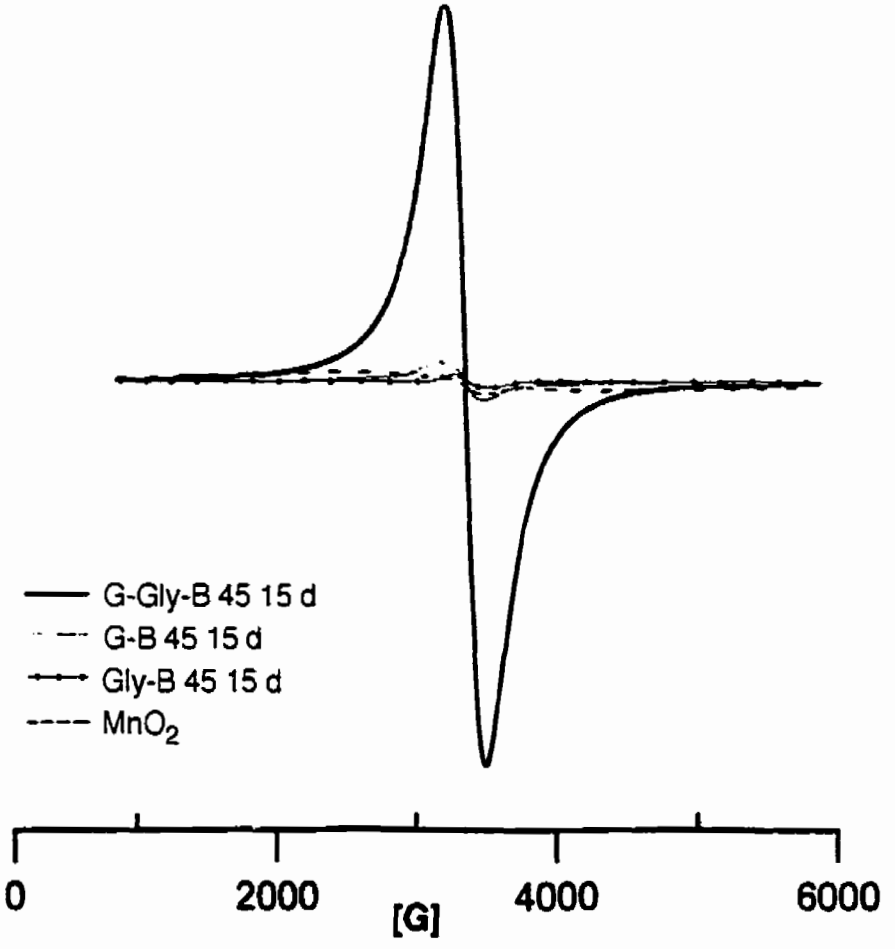


**Figure 3.1.5.** EPR spectra of lyophilized sediments of glucose-glycine-birnessite (GGlyB), glucose-birnessite (GB), glycine-birnessite (GlyB) and birnessite (B) systems at 45°C for 15 days and at an initial pH of 7.00.

### 3.1.3.3 Nuclear Magnetic Resonance spectroscopy

There is some indication of the formation of the Amadori compound N-(1-deoxy-D-fructos-1-yl)-glycine (fructosylglycine) in the glucose-glycine reaction system with an initial adjusted pH of 8.00, which was heated at 45°C for a period of 310 h, (Figure 3.1.6 and Table 3.1.3). The peaks at 53.77, 64.65, 64.80, 69.81 71.52, 72.68 and 72.97 ppm can be assigned to fructosylglycine carbons (Mossine et al., 1994) The $^{13}C$ NMR data also indicate that various tautomeric forms exist in the reaction system (peaks at 64.65 and 64.80 ppm from ring carbon C-6 of $\alpha$ and $\beta$-D-fructopyranose CHOH moieties). Mossine et al. (1994) prepared pure solutions of fructosylglycine among other Amadori compounds and noted that it contained $\alpha$ and $\beta$ pyranose and $\alpha$ and $\beta$ furanose carbons.

$^{13}C$ NMR spectroscopy in solution was also carried out for the glucose-glycine-birnessite system under the same conditions as above. However the presence of substantial amounts of Mn(II) caused severe paramagnetic interference and a poor signal to noise ratio. In addition, the presence of Mn(II) ions in the solution caused a shift downfield of approximately 8 ppm for all signals and might have caused suppression of some signals. Therefore solution $^{13}C$ NMR cannot be used to study the formation of reaction products in the systems containing birnessite.

| Shift range (ppm) | Possible assignation |
|---|---|
| 41.76 | α-Carbon in glycine |
| 57-64 | $C_6$ carbon in saccharides |
| 65-85 | Ring carbon of saccharides |
| 90-110 | Anomeric (O-C-O) carbon in saccharides |
| 172.52 | Carboxyl carbon |

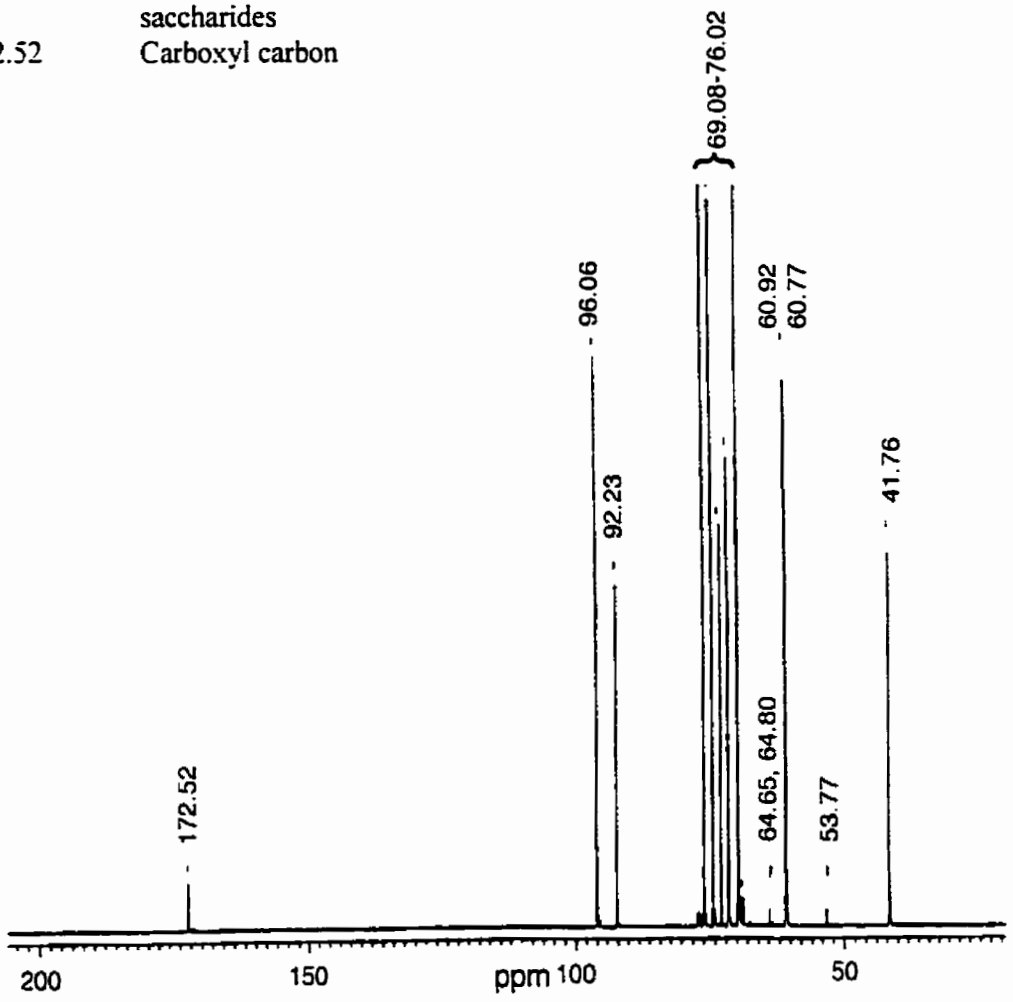


**Figure 3.1.6** 125 MHz high resolution $^{13}C$ solution NMR spectrum of the supernatant of the glucose-glycine system at initial pH 8.00, 45°C for 310 h. Refer to Table 3.1.3 for detailed peak assignations.

**Table 3.1.3** 125 MHz high resolution $^{13}C$ solution NMR peak assignations for the reaction products of the supernatant of the glucose-glycine system (initial pH 8.00 and at 45°C for 310 h)†

| Chemical shift (ppm) | Assignation |
|---|---|
| 41.76 | α-carbon of glycine |
| 53.77 | Ring carbon C-1 of β-D-fructopyranose moiety in N-(1-deoxy-D-fructos-1-yl)-glycine |
| 60.77 | C-6 carbon of α-[D] glucose ($CH_2OH$) |
| 60.92 | C-6 carbon of β-[D] glucose ($CH_2OH$) |
| 64.65, 64.80 | Ring carbon C-6 of α and β-D-fructopyranose (CHOH) moieties in N-(1-deoxy-D-fructos-1-yl)-glycine and related structures |
| 69.08, 69.55, 69.76, | Ring carbon (CHOH) of carbohydrate |
| 69.81 | Ring carbon C-5 of β-D-fructopyranose moiety or related carbon |
| 71.52, 71.68 | Ring carbon C-4 of α-D-fructopyranose (CHOH) moiety in N-(1-deoxy-D-fructos-1-yl)-glycine and related carbon |
| 72.97 | Ring carbon C-3 of α-D-fructopyranose (CHOH) moiety in N-(1-deoxy-D-fructos-1-yl)-glycine or related carbon |
| 74.01 | Ring carbons of carbohydrate (CHOH) and related structures |
| 74.36 | Ring carbons of carbohydrate (CHOH) and related structures |
| 76.02 | Ring carbon C-2 of β-[D] glucose (CHOH) |
| 92.23 | Anomeric C- 1 carbon (carbon singly bonded to two oxygens) of β-[D] glucose |
| 96.06 | Anomeric C- 1 carbon (carbon singly bonded to two oxygens) of α-[D] glucose |
| 172.52 | Carboxyl carbon from glycine |

†Assignations were based on $^{13}C$ NMR shift values from Levy et al. (1980), Kalinowski et al. (1988), Malcolm (1989), and Mossine et al. (1994).

$^{55}$Mn NMR results indicate the presence of Mn(II) in the lyophilized sediment samples of the glucose-glycine-birnessite system which was heated at 100°C for a period of 3 hours at an initial pH of 8.00 (Figure 3.1.7). The spectrum of the sediment is similiar to a control spectrum of a Mn(II) salt. The glucose-birnessite system was also heated at 100°C for a period of 3 hours at an initial pH of 8.00: the spectrum is similiar to that of birnessite (Mn(IV) oxide) (Figure 3.1.7). This indicates that in the case of the glucose-glycine-birnessite system, reduction of Mn(IV) to Mn(II) occurs to a much greater extent than in the glucose-birnessite system. These results were confirmed unequivocally for reactions conducted at 25°C and 45°C and investigated by XANES spectroscopy.

### 3.1.3.4 Fourier transform infrared absorption spectroscopy

Figure 3.1.8 shows the FTIR spectra of the solid phase of the glucose-glycine-birnessite, the glucose-birnessite and the glycine-birnessite systems at an initial pH 7.00 after reaction for 15 d at 45°C and of a control sample of pure birnessite. Band assignations are shown in Table 3.1.4. The FTIR spectrum of the control sample of birnessite (Figure 3.1.8 (a) is very similiar to that reported in the literature (Potter and Rossman, 1979). The broad absorption band with a maximum at 3431 $cm^{-1}$ is caused by hydroxide ion, or water, in a specific crystallographic site while the small band with the maximum at 1624 $cm^{-1}$ is ascribed to less ordered water. The broad band at 524 $cm^{-1}$ is attributed to vibrations of the $MnO_6$ octahedral framework of birnessite.

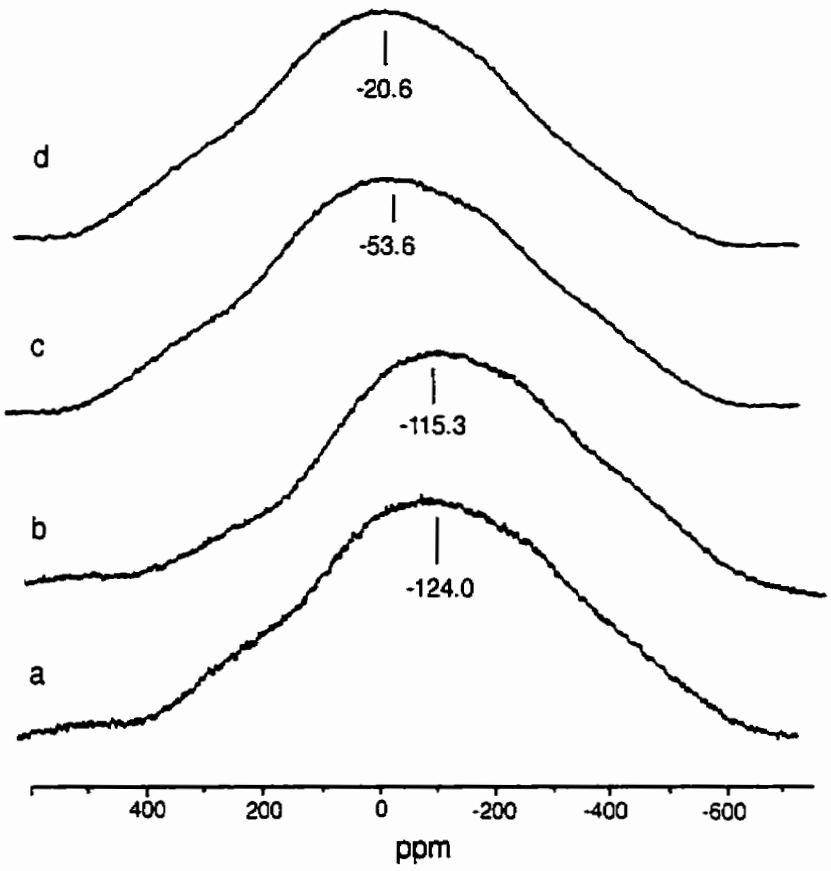


**Figure 3.1.7** $^{55}$Mn CPMAS NMR spectra of the lyophilized sediment of the (a) birnessite [Mn (IV) oxide] heated at 100°C for 3 h at an initial pH of 8.00. (b) glucose-birnessite system heated at 100°C for 3 h at an initial pH of 8.00. (c) manganese (II) sulphate, and (d) glucose-glycine-birnessite system heated at 100°C for 3 h at an initial pH of 8.00.

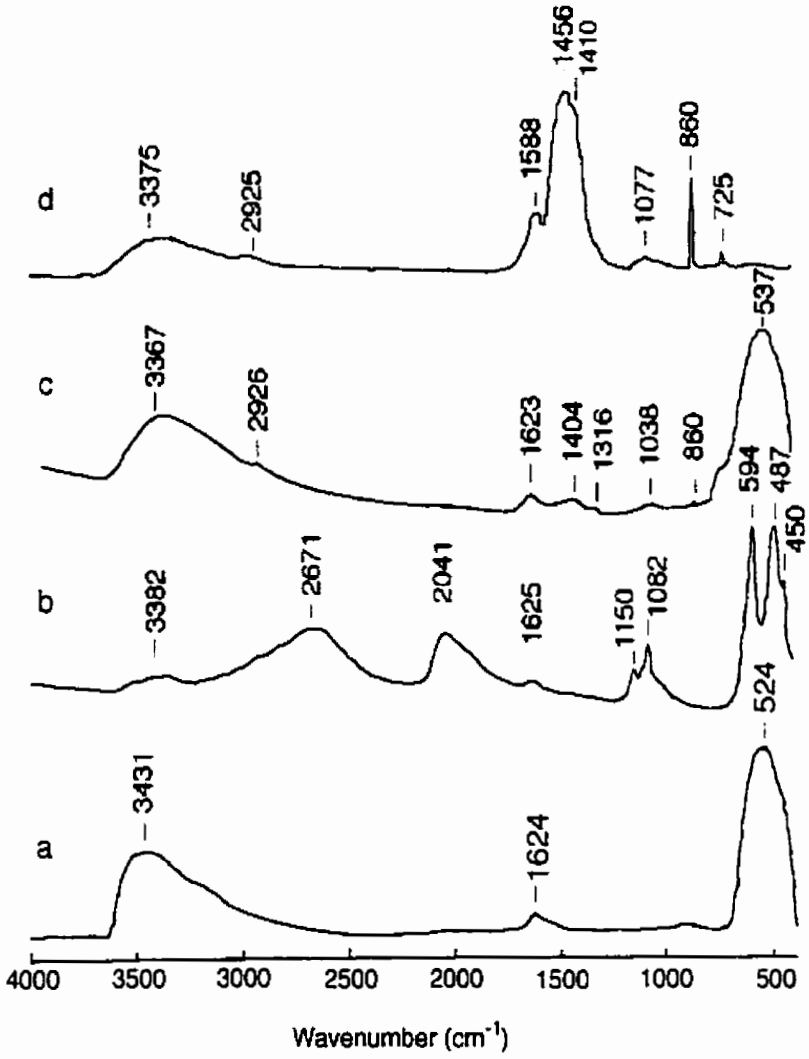


**Figure 3.1.8** FTIR spectra of (a) birnessite, (b) glycine-birnessite, (c) glucose-birnessite, (d) glucose-glycine-birnessite. Samples (b) – (d) were at an initial pH of 7.00 and were allowed to react at 45°C for 15 d.

The spectrum of the glycine-birnessite system, (Figure 3.1.8 b) is different from the other spectra. Absorption bands at 3367 (possible overlap of birnessite and organic OH), 2671, 2041, 1625, 1150, and 1082 $cm^{-1}$ (Figure 3.1.8 b and Table 3.1.4) arise from the presence of organic reaction products in the solid phase. The strong absorption bands at 450,

**Table 3.1.4** Assignations of FTIR absorption bands of the solid phase of the systems: (a) pure birnessite, (b) glycine-birnessite, (c) glucose-birnessite, and (d) glucose-glycine-birnessite[†]

| (a) Birnessite | | (b) Glycine + birnessite | | (c) Glucose + birnessite | | (d) Glucose + glycine + birnessite | |
|---|---|---|---|---|---|---|---|
| Wavenumber ($cm^{-1}$) | Relative Intensity | Wavenumber ($cm^{-1}$) | Relative Intensity | Wavenumber ($cm^{-1}$) | Relative Intensity | Wavenumber ($cm^{-1}$) | Relative Intensity |
| 524 (vibrations of $MnO_6$ octahedra) | Broad, strong | 450 (Mn-O interactions) | Moderate | 537 (vibrations of $MnO_6$ octahedra) | Broad, strong | 725 (Mn-O interactions or carbohydrate ring stretch) | Weak |
| 1624 (less ordered water) | Broad, weak | 487 (Mn-O interactions) | Strong | 860 (Mn-O interactions or carbohydrate ring stretch) | Weak | 860 (Mn-O interactions or carbohydrate ring stretch) | Moderate, sharp |
| 3431 (-OH, $H_2O$ adsorbed on birnessite) | Broad, very strong | 594 (Mn-O interactions) | Strong | 1038 (carbohydrate C-O-stretch) | Weak | 1077 (aliphatic C-C stretch or OH of polysaccharide) | Broad, moderate |
| | | 1082 (aliphatic C-C stretch and OH deformation and C – O stretch) | Moderate | 1316 (CH and $CH_2$ or OH in-plane deformation | Weak | 1410 (sym – $COO^-$ stretch) | Shoulder |
| | | 1150 (OH deformation and C – O stretch) | Strong | 1404 (sym – $COO^-$ stretch) | Weak | 1456 (-CH bending of $CH_2$) | Strong |
| | | 1625 ($NH_3^+$ asymm. deformation or $COO^-$ asymm. stretch) | Strong | 1623 ($COO^-$ asymm. stretch) | Weak | 1588 (Aromatic C=C stretch and/or asym – $COO^-$ stretch) | Strong |
| | | 2041(asymm. $NH_3^+$ deformation and $NH_3^+$ hindered rotation) | Broad, strong | 2926 (-$CH_2$- sym stretch) | Very weak | 2925 (-$CH_2$- sym stretch) | Weak |
| | | 2671 ($NH_3^+$ stretch overlapped with carboxyl) | Broad, strong | 3367 (stretching vibration of H-bonded OH) | Broad, strong | 3375 (stretching vibration of H-bonded OH) | Broad, strong |
| | | 3382 (H-bonded OH from COOH) | Broad, weak | | | | |

[†]Samples (b) – (d) were at an initial adjusted pH of 7.00 and were allowed to react at a temperature of 45°C for a period of 15 d. The assignations are based on Colthup et al. (1990) and Wang and Huang (1992).

487, and 594 $cm^{-1}$, are probably from Mn – O interactions (Colthup et al., 1990). The results are interesting because the FTIR spectrum of the solid phase of the glycine-birnessite indicates that there is significant reaction between glycine and birnessite even though the results from visible absorption and atomic absorbance spectroscopy do not indicate the presence of significant reaction products in the supernatant. It is known that birnessite decarboxylates and deaminates glycine (Wang and Huang, 1987a).

The spectrum of the glucose-birnessite system (Figure 3.1.8 c), is quite different from that of the glucose-glycine-birnessite system (Figure 3.1.8 d), since it still shows the presence of birnessite (broad absorption band at 537 $cm^{-1}$ indicative of vibrations of $MnO_6$ octahedra) in the system but the appearance of new absorption bands at 3367 (possible overlap of birnessite and organic OH), 2926, 1623, 1404, 1316, and 1038 $cm^{-1}$ (Figure 3.1.8 c and Table 3.1.4) indicates the presence of organic reaction products in the solid phase. The weak absorption band at 860 $cm^{-1}$ is probably from carbohydrate ring stretching and/or Mn–O interactions (Colthup et al., 1990).

In the glucose-glycine-birnessite system (Figure 3.1.8 d and Table 3.1.4), absorption bands at 725 and 860 $cm^{-1}$ are present, probably from carbohydrate ring stretching and/or Mn–O interactions (but not from birnessite) (Colthup et al., 1990). Absorption bands at 3375, 2925, 1588, 1456, 1410, and 1077 $cm^{-1}$ (Figure 3.1.8 d and Table 3.1.4) from the organic components are present. The absence of a band at approximately 1714 $cm^{-1}$ (undissociated carboxyl) in (Figure 3.1.8 d), is consistent with the system pH being near or above 7 (Wang and Huang, 1992) and therefore, the carboxyl groups are present in dissociated form (absorption bands at 1409 and 1589 $cm^{-1}$) (Colthup et al., 1990). No absorption bands arising from birnessite were detected in the spectrum. The spectra of the solid phase of the glucose-glycine-birnessite system at initial pH 6.00, 7.00, and 8.00 (after reaction for 15 d at 45°C) are qualitatively identical (Figure 3.1.9).

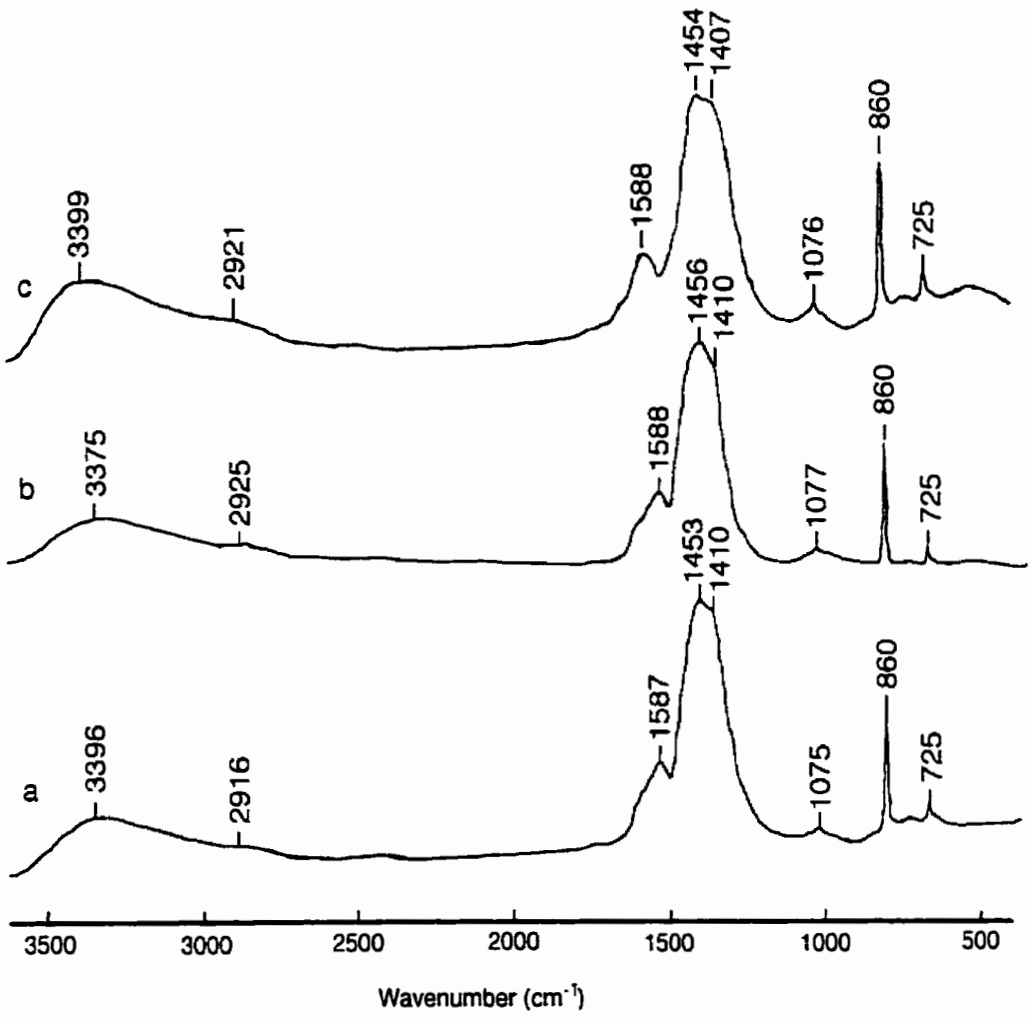


**Figure 3.1.9** FTIR spectra of the solid phase of the glucose-glycine-birnessite systems at initial pH (a) 6.00, (b)7.00, and (c) 8.00.

### 3.1.3.5 X-ray absorption near-edge structure spectroscopy

After normalizing by the absorption edge step, the resultant X-ray absorption near-edge structure (XANES) data are plotted in Figure 3.1.10. Several features in the spectra, in the energy region between 6545 and 6565 eV indicate that Mn ions are present in different oxidation states in all samples. The energy corresponding to the positions of $Mn^{2+}$ and $Mn^{4+}$ states are indicated by the arrows. These positions are

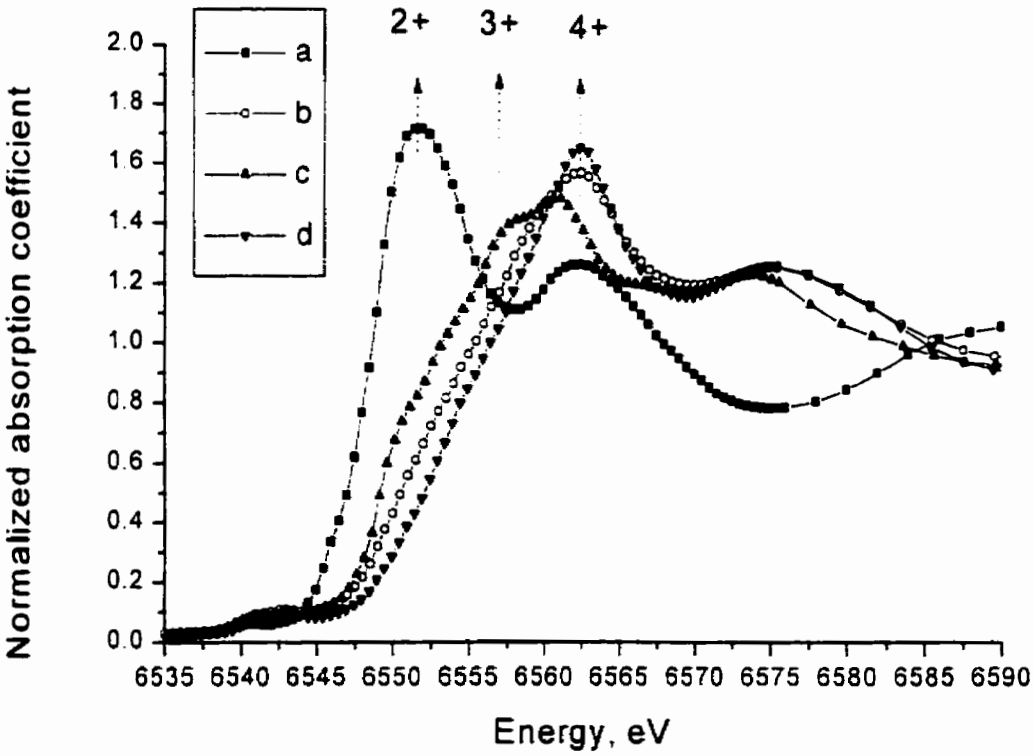


**Figure 3.1.10** The XANES region of the X-ray absorption coefficients in solid phase samples: (a) glucose-glycine birnessite, (b) glucose-birnessite, and (c) glycine-birnessite); all at initial pH 7.00, 45°C, 15 d and ambient light conditions (0 to 3.1 ± 0.9 μE $s^{-1}$ $m^{-2}$) and (d) pure birnessite as control.

in good agreement with those obtained in several reference compounds, containing Mn in different oxidation states, by Manceau et al. (1992a). The position of the $Mn^{3+}$ oxidation state was linearly interpolated, to a good approximation, and is shown in Figure 3.1.10 as well. The XANES spectra for the systems at 45°C were also analyzed by quantitative techniques and the results are summarized in Table 3.1.5. The following points are of particular interest. Birnessite, although nominally described as $MnO_2$, which assumes a Mn(IV) oxidation state, contains substantial quantities of Mn of lower oxidation states. The results are in agreement with the findings of Drits et al. (1997) and Nesbitt and Banerjee (1998) who also noted the presence of significant amounts of Mn (II) and particularly Mn (III) in samples of synthetic birnessite.

In the solid phase of the glucose-birnessite system (Table 3.1.5) there is a slight increase in the amount of reduced Mn (II). On the other hand, AA spectroscopy (Table 3.1.1), indicates that most of the Mn (II) entered the liquid phase and did not remain adsorbed on the surface of the birnessite. The most striking feature of the glycine-birnessite spectrum is the substantial presence of Mn (III)) as well as an increase in the amount of Mn (II) present (Table 3.1.5). This contrasts with the results from AA spectroscopy (Table 3.1.1) which indicate the presence of only small amounts of Mn (II) in solution. Therefore, unlike the glucose-birnessite system where most of the reduced Mn (i.e., $Mn^{2+}$) entered the liquid phase, in the glycine-birnessite system, the Mn (II) that was formed remained adsorbed on the surface of the birnessite and did not enter solution.

Finally, in the glucose-glycine-birnessite system there was a dramatic increase in the amount of Mn (II) formed both in the solid phase and in the liquid phase (results from AA spectroscopy, Table 3.1.1). It is important to note that there was still 39% Mn

(IV) present presumably in the form of birnessite, but because of the surface coating of reaction products it was not detected by other analytical methods such as FTIR spectroscopy (Figure 3.1.8 and Table 3.1.4). It can be concluded that the presence of both a reducing sugar and an amino acid is necessary to trigger the increase in catalytic action of birnessite thereby accelerating the Maillard reaction.

**Table 3.1.5** Content of Mn oxidation states (II) to (IV) in solid phase samples as determined by quantitative XANES analysis: (a) glucose-glycine birnessite, (b) glucose-birnessite, and (c) glycine-birnessite: all at initial pH 7.00, 45°C, 15 d and ambient light conditions (3.1 ± 0.9 μE $s^{-1}$ $m^{-2}$) and (d) pure birnessite as control

| Sample | Mn (II) content g $kg^{-1}$ | Mn (III) content g $kg^{-1}$ | Mn (IV) content g $kg^{-1}$ |
|---|---|---|---|
| (a) pure birnessite | 130 | 310 | 560 |
| (b) glucose-birnessite | 170 | 300 | 530 |
| (c) glycine-birnessite | 210 | 440 | 350 |
| (d) glucose-glycine birnessite | 500 | 110 | 390 |

The increased degree of browning in the glucose-glycine-birnessite system compared to the glucose-glycine system containing no Mn(IV) oxide may be attributed to three simultaneous processes:

(a) The birnessite acts as a Lewis acid which accepts electrons from glucose and probably initially oxidizes it to D-gluconic acid. Then, decarboxylation with loss of carbon dioxide occurs and/or there is further oxidation and formation of, e.g., α-dicarbonyl compounds. Simultaneously or subsequently a complex poly-

condensation process involving glycine proceeds on the surface of birnessite with the formation of coloured Maillard reaction products,

(b) The polycondensation is accelerated by an increase in pH as a result of the reduction of Mn(IV) to Mn(II):

$$MnO_2 + 4H^+ + 2e^- \rightleftharpoons Mn^{2+} + 2H_2O$$

For a range of amino acids in the Maillard reaction, the rate of polycondensate formation increased with increasing pH (Hedges, 1978). Glucose polymerized with itself at an appreciable rate only at pH 8 or above and Hedges (1978) considered that at this pH a significant amount of the polycondensate formed could result from glucose-glucose condensations.

(c) The Mn(II) formed also catalyzes the polycondensation reaction between glucose and glycine.

Birnessite, as shown in this study, is a powerful catalyst in the Maillard reaction (abiotic browning) between glucose and glycine at temperatures of 25°C and 45°C. The approximate temperature of the soil surface on a day when the ambient air temperature is 25°C is approximately 45°C (Baver, 1956), and therefore is a temperature frequently encountered in surface horizons of tropical and subtropical soils, and even temperate soils during the summer months.

## 3.2 Effect of Light on the Heterogeneous Catalytic Action of Birnessite in the Maillard Reaction.

### 3.2.1 Introduction

In the previous unit the catalytic effect of birnessite in promoting the Maillard reaction between glucose and glycine at 25 and 45°C and ambient light intensity of 0 to 3.1 ± 0.9 $\mu E\ s^{-1}\ m^{-2}$ was demonstrated. Mn (IV) oxides are semiconductors and the bandgap energy of Mn oxides is potentially low enough for thermal or photochemical energy to excite electrons into the conduction band. Photoreduction of Mn oxides by marine fulvic acid, and marine humic acid was observed by Sunda et al. (1983). They noted that reaction rates increased considerably with increasing light intensity. Stone and Morgan (1984) noted that dissolution of Mn oxides by a marine fulvic acid increased significantly upon exposure to strong illumination. Lee and Huang (1995) noted a significant photochemical and thermal effect on the role of birnessite in catalyzing the abiotic transformation of four polyphenols (hydroquinone, resorcinol, catechol and pyrogallol). Therefore light exerts an additional stimulatory effect on oxidative processes involving manganese (IV) oxides.

The importance of photochemical reactions has been well documented (Crosby, 1972, 1979; Engelhart et al., 1986; Andreux et al., 1995) except for the influence of sunlight on chemical reactions occurring at the soil- and water-atmosphere interfaces. Biochemical, physical and chemical processes in soil and related environments are all affected by light to a greater or lesser degree. The effect of light on birnessite catalysis of the Maillard reaction remains to be uncovered. The objective of the present study was to investigate birnessite

catalysis of the Maillard reaction under conditions of darkness and exposure to moderate light conditions.

### 3.2.2 Materials and Methods

The experimental procedure closely parallels that of Section 3.1. Light intensities in the environment chamber were measured using a LI-COR (model LI-250) light meter (LI-COR, Lincoln, NB) Light intensities were adjusted by increasing or decreasing distance from the light fixtures to the samples while adjusting for any change in temperature.

**Examination of microbial activity**

Samples of the reaction systems (at the end of the reaction periods) were incubated for 6 d under aerobic or anaerobic conditions on Trypticase Soy Agar (TSA) plates to test for abiotic conditions. TSA is a nonselective growth medium suitable for the cultivation of a wide variety of microorganisms (Dandurand and Knudsen, 1997). Using a bent glass rod, a small portion of the experimental suspensions was spread on TSA plates at the beginning and the end of the reaction period to examine whether there had been any microbial growth in the systems. No culturable, chemolithotrophic micro-organisms were detected indicating that all reactions were abiotic in nature.

**Effect of light on birnessite catalysis of the Maillard reaction**

Two and a half grams of birnessite were suspended in 85 mL of glucose:glycine (1:1 molar ratio, 0.05 mole each) solution. The pH was adjusted to 7.00 and double-deionized water was added to a total volume of 100 mL. The flasks were sealed and placed on an oscillating wrist action shaker in an environment chamber with constant light intensity 168 ± 2 μE $s^{-1}$ $m^{-2}$ or 500 ± 5 μE $s^{-1}$ $m^{-2}$. For conditions of darkness (0 μE $s^{-1}$ $m^{-2}$) the flasks were wrapped in aluminium foil, ensuring that temperatures inside the

flasks were within the reaction range of systems exposed to light. In comparison the intensity of the midday sun is approximately 2000 μE $s^{-1}$ $m^{-2}$ and the lower limit of the light intensity on a typical cloudy day is approximately 500 μE $s^{-1}$ $m^{-2}$ (Sunda et al., 1983). The system was allowed to react for 30 or 60 days at 25.5 ±0.5°C. At the end of the reaction period, the supernatant liquid phase was separated from the solid phase by centrifugation at 25 000 g for 35 to 40 minutes. The solid phase was lyophilized and the following analyses were carried out:

(a) Visible absorption spectroscopy of supernatants.
(b) pH, Eh, pE + pH, and Mn content of supernatants.
(c) EPR of the liquid phase.
(d) FTIR of the solid phase.
(e) XANES of the solid phase.

The instrumentation and operating conditions for the above analyses has been described previously in Section 3.1.2.

### 3.2.3 Results and Discussion

#### 3.2.3.1 Visible absorption spectroscopy and related solution phase analysis

The results are shown in Tables 3.2.1 and 3.2.2 and Figures 3.2.1 and 3.2.2. The spectrophotometric absorbance of reaction products from glucose and glycine in the presence of birnessite was compared to the absorbance of glucose and glycine alone. In the range 400 to 600 nm the absorbance of the reaction products of the system containing birnessite was consistently higher than for the control system of glucose and glycine at 0, 168 and 500 μE $s^{-1}$ $m^{-2}$. The highest absorbance after 30 days

**Table 3.2.1** Effect of light (0, 168, and 500 μE $s^{-1}$ $m^{-2}$) on the glucose-glycine-birnessite system and the control system (no birnessite) at the initial pH 7.00 and at the end of the reaction period of 30 days at 25.5 ± 0.5°C

| Treatment | Absorbance 400 nm | Absorbance 600 nm | Mn (μg $mL^{-1}$) | pH | Eh (mV) | pE + pH |
|---|---|---|---|---|---|---|
| Glucose + glycine + birnessite (500 μE $s^{-1}$ $m^{-2}$) | 0.303 ±0.010 | 0.041 ±0.003 | 4512 ± 134 | 7.68 ±0.07 | 320 ±11 | 13.09 ±0.26 |
| Glucose + glycine (500 μE $s^{-1}$ $m^{-2}$) | 0.042 ± 0.002 | 0.012 ± 0.001 | 0 | 7.04 ±0.05 | 409 ±8 | 13.94 ±0.18 |
| Glucose + glycine + birnessite (168 μE $s^{-1}$ $m^{-2}$) | 0.162 ± 0.007 | 0.033 ± 0.003 | 4254 ± 77 | 7.65 ± 0.08 | 328 ± 10 | 13.19 ± 0.25 |
| Glucose + glycine (168 μE $s^{-1}$ $m^{-2}$) | 0.030 ± 0.001 | 0.011 | 0 | 6.94 ± 0.05 | 425 ± 13 | 14.12 ± 0.27 |
| Glucose + glycine + birnessite (0 μE $s^{-1}$ $m^{-2}$) | 0.121 ± 0.006 | 0.023 ± 0.002 | 2475 ± 111 | 7.59 ± 0.07 | 364 ± 12 | 13.74 ± 0.27 |
| Glucose + glycine (0 μE $s^{-1}$ $m^{-2}$) | 0.032 ± 0.001 | 0.012 ± 0.001 | 0 | 7.01 ± 0.06 | 431 ± 9 | 14.29 ± 0.21 |

**Table 3.2.2** Effect of light (0 and 500 μE $s^{-1}$ $m^{-2}$) on the glucose-glycine-birnessite system and the control system (no birnessite) at the initial pH 7.00 and at the end of the reaction period of 60 days at 25.5 ± 0.5°C

| Treatment | Absorbance 400 nm | Absorbance 600 nm | Mn (μg $mL^{-1}$) | pH | Eh (mV) | pH + pE |
|---|---|---|---|---|---|---|
| Glucose + glycine + birnessite (light) | 3.08 ± 0.2 | 0.173 ± 0.01 | 5119 ± 204 | 7.98 ± 0.07 | 218 ±12 | 11.65 ± 0.25 |
| Glucose + glycine (light) | 0.089 ±0.005 | 0.023 ±0.001 | 0 | 6.75 ±0.10 | 377 ±17 | 13.14 ±0.39 |
| Glucose + glycine + birnessite (dark) | 0.530 ±0.007 | 0.064 ±0.001 | 3283 ±167 | 7.66 ±0.09 | 329 ±13 | 13.23 ±0.32 |
| Glucose + glycine (dark) | 0.092 ±0.004 | 0.019 ±0.001 | 0 | 7.09 ±0.04 | 390 ±8 | 13.67 ±0.17 |

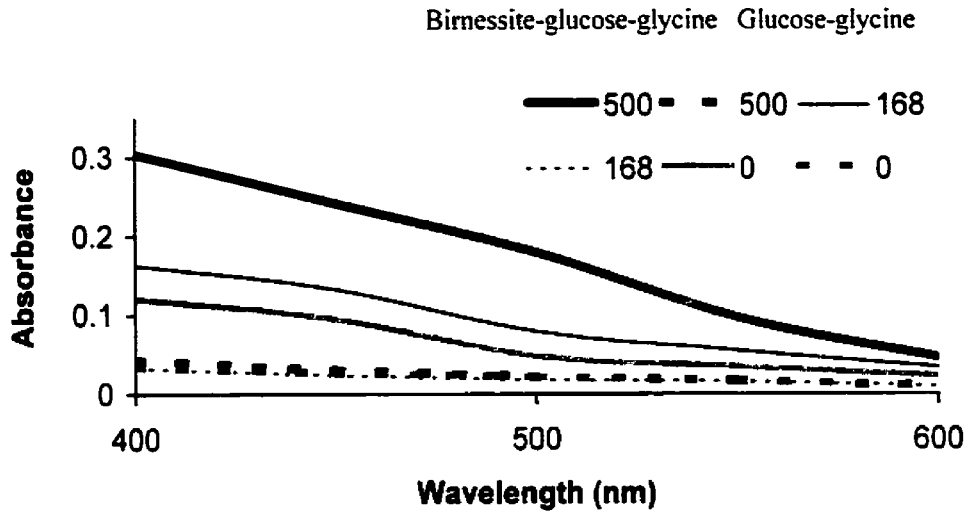


**Figure 3.2.1** Effect of birnessite on the absorbance of the glucose-glycine solution at the initial pH 7.00 and 25.5 ±0.5°C, at the end of a 30 day reaction period under light intensity of 0 (darkness), 168 and 500 μE $s^{-1}$ $m^{-2}$.

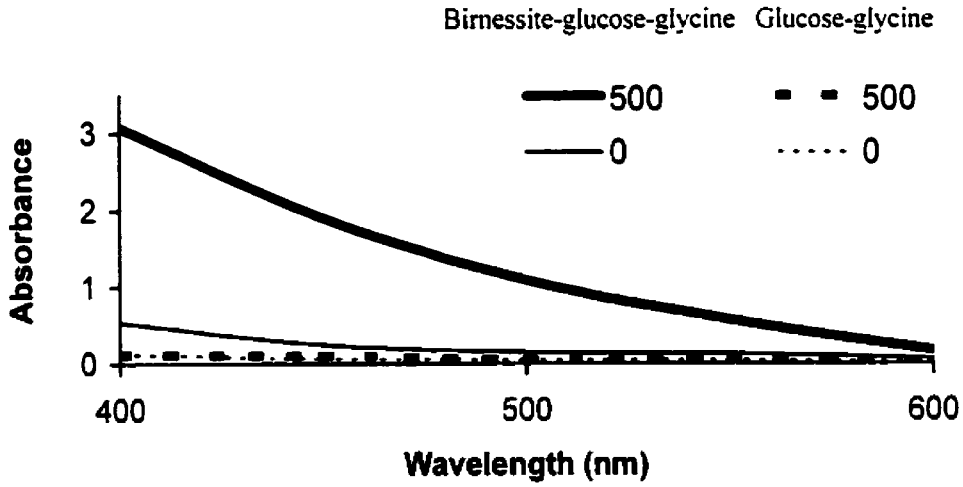


**Figure 3.2.2** Effect of birnessite on the absorbance of the glucose-glycine solution (control) at the initial pH 7.00 and 25.5 ± 0.5°C, at the end of a 60 day reaction period under light intensity of 0 (darkness), and 500 μE $s^{-1}$ $m^{-2}$.

was in the glucose-glycine-birnessite system at 500 μE $s^{-1}$ $m^{-2}$. The data indicate that humification of glucose and glycine through their polycondensation was significantly enhanced by the presence of birnessite, especially in the presence of light.

### 3.2.3.2 Electron paramagnetic resonance spectroscopy

EPR analysis (Figure 3.2.3) confirms the presence of Mn (II) both in the supernatant of the glucose-glycine-birnessite system at 168 μE $s^{-1}$ $m^{-2}$, 25°C for 30 days, and at 0 μE $s^{-1}$ $m^{-2}$ (not shown).

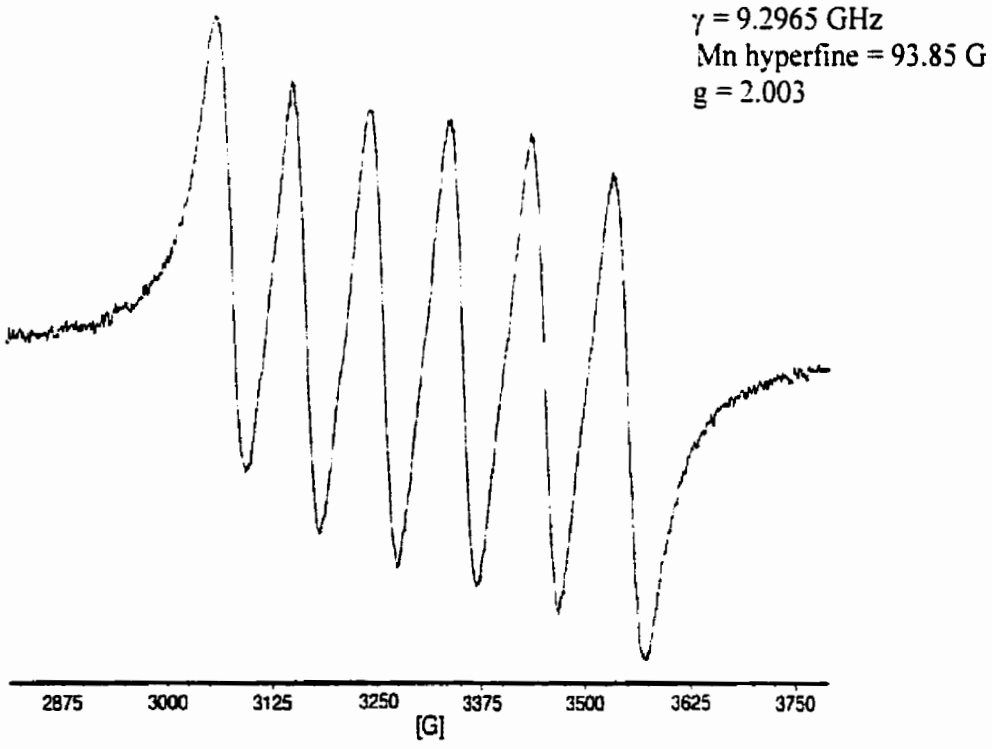


**Figure 3.2.3** The EPR spectrum of the supernatant of the glucose-glycine-birnessite system exposed to light at 168 μE $s^{-1}$ $m^{-2}$ at the initial pH of 7.00 and 25.5 ± 0.5°C for 30 d.

### 3.2.3.3 Fourier transform infrared absorption spectrophotometry

Figure 3.2.4 shows the FTIR spectra and Table 3.2.3 the absorption band assignations of the solid phase of the glucose-glycine-birnessite system exposed to 0, 168 and 500 $\mu E\ s^{-1}\ m^{-2}$ and of pure birnessite exposed to 500 $\mu E\ s^{-1}\ m^{-2}$ at the initial pH of 7.00 and 25 ± 0.5°C for 60 days. The FTIR spectrum of the birnessite exposed to light at 500 $\mu E\ s^{-1}\ m^{-2}$ (Figure 3.2.4 a) is identical to that of a control sample of birnessite and to a sample of birnessite exposed to 168 $\mu E\ s^{-1}\ m^{-2}$ (not shown), and is very similiar to that reported in the literature (Potter and Rossman, 1979), indicating that light alone has no effect. The broad absorption band with a maximum at 3448 $cm^{-1}$ is caused by hydroxide ion, or water, in a specific crystallographic site while the small band with a maximum at 1628 $cm^{-1}$ is ascribed to less ordered water. The broad band at 521 $cm^{-1}$ is attributed to vibrations of the $MnO_6$ octahedral framework of birnessite.

The spectrum of the glucose-glycine-birnessite system at 0 $\mu E\ s^{-1}\ m^{-2}$ (Figure 3.2.4 b) still shows the presence of birnessite (broad absorption band at 510 $cm^{-1}$) in the system but the appearance of new absorption bands at 3378, 2910, 1601, 1448, 1410, 1074, and 1032 $cm^{-1}$ (Table 3.2.3) indicates the presence of organic reaction products in the solid phase. The absorption band at ca. 500 $cm^{-1}$, which is indicative of vibrations of $MnO_6$ octahedra is absent in both the solid phases of the glucose-glycine-birnessite system exposed to light at 168 and 500 $\mu E\ s^{-1}\ m^{-2}$ (Figure 3.2.4 c and d). Absorption bands at 721 and 859 $cm^{-1}$ (168 $\mu E\ s^{-1}\ m^{-2}$), and 496, 724, 813, and 860 $cm^{-1}$ (500 $\mu E\ s^{-1}\ m^{-2}$), probably from carbohydrate ring stretching and/or Mn–O interactions (Colthup et al., 1990), are present.

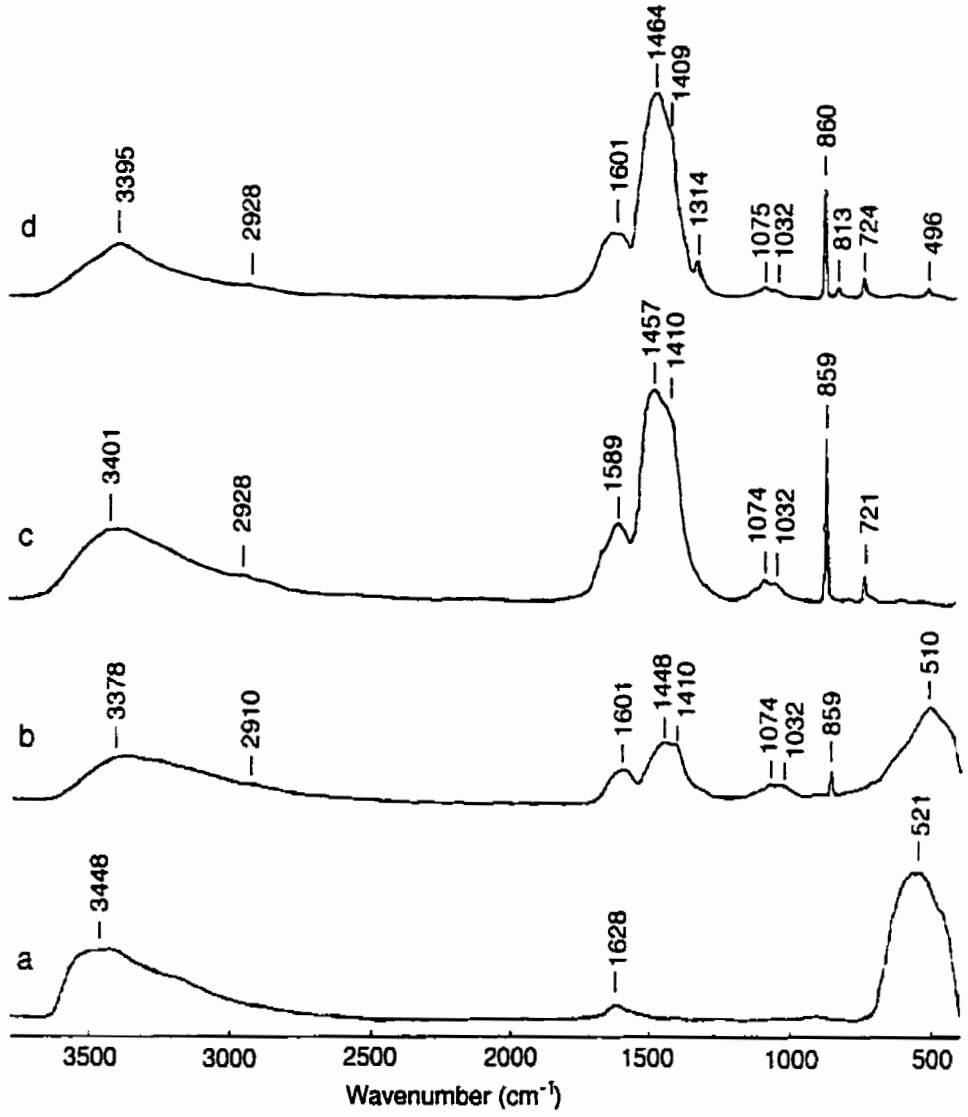


**Figure 3.2.4** FTIR spectra of (a) pure birnessite exposed to 500 μE $s^{-1}$ $m^{-2}$ (60 d) and of the solid phase of the glucose-glycine-birnessite system exposed to (b) 0 μE $s^{-1}$ $m^{-2}$ (60 d), (c) 168 μE $s^{-1}$ $m^{-2}$ (58 d), and (d) 500 μE $s^{-1}$ $m^{-2}$ (60 d) at the initial pH of 7.00 and 25.5 ±0.5°C. The FTIR spectra of birnessite not exposed to light was similar to (a).

**Table 3.2.3.** Assignations of FTIR absorption bands of the solid phase of the systems: (a) pure birnessite exposed to 500 μE $s^{-1}$ $m^{-2}$ (60 d) and of the solid phase of the glucose-glycine-birnessite system exposed to (b) 0 μE $s^{-1}$ $m^{-2}$ (60 d). (c) 168 μE $s^{-1}$ $m^{-2}$ (58 d), and (d) 500 μE $s^{-1}$ $m^{-2}$ (60 d) at the initial pH of 7.00 and 25.5 ± 0.5°C [†]

| (a) Birnessite | | (b) Glucose + glycine + birnessite (0) | | (c) Glucose + glycine + birnessite (168) | | (d) Glucose + glycine + birnessite (500) | |
|---|---|---|---|---|---|---|---|
| Wavenumber ($cm^{-1}$) | Relative Intensity | Wavenumber ($cm^{-1}$) | Relative Intensity | Wavenumber ($cm^{-1}$) | Relative Intensity | Wavenumber ($cm^{-1}$) | Relative Intensity |
| 521 (vibrations of $MnO_6$ octa-hedra) | Broad, strong | 510 (vibrations of $MnO_6$ octa-hedra) | Broad, strong | 721 (Mn-O interactions or carbohydrate ring stretch) | Weak, sharp | 496 (Mn-O interactions) | Weak |
| | | 859 (Mn-O interactions or carbohydrate ring stretch) | Weak, sharp | 859 (Mn-O interactions or carbohydrate ring stretch) | Strong, sharp | 724 (Mn-O interactions or carbohydrate ring stretch) | Weak, sharp |
| 1628 (less ordered water) | Broad, weak | 1032 (carbo-hydrate -C-O- stretch) | Weak, broad | 1032 (carbo-hydrate -C-O- stretch) | Weak, broad | 813 (Mn-O interactions or carbohydrate ring stretch) | Weak |
| 3448 (-OH, $H_2O$ adsorbed on birnessite) | Broad, very strong | 1074 (aliphatic C-C stretch) | Weak, broad | 1074 (aliphatic C-C stretch) | Weak, broad | 860 (Mn-O interactions or carbohydrate ring stretch) | Strong, sharp |
| | | 1410 (sym $-COO^-$ stretch) | Moderate, broad | 1410 (sym $-COO^-$ stretch) | Strong | 1032 (carbo-hydrate -C-O- stretch) | Weak, broad |
| | | 1448 (-CH bending of $CH_2$) | Moderate, broad | 1457 (-CH bending of $CH_2$) | Strong, broad | 1075 (aliphatic C-C stretch) | Weak, broad |
| | | 1601 (Aromatic C=C stretch and/or asym $-COO^-$ stretch) | Moderate, broad | 1589 (Aromatic C=C stretch and/or asym $-COO^-$ stretch) | Strong | 1314 ($CH_2$ deformation and/or CH and $CH_2$ wag, and/or OH in-plane defor-mation | Weak, sharp |
| | | 2910 (-$CH_2$- sym stretch) | Very weak | 2928 (-$CH_2$- sym stretch) | Very weak | 1409 (sym $-COO^-$ stretch) | Strong |

Table 3.2.3 continued

| | | | | | |
|---|---|---|---|---|---|
| 3378 (stretching vibration of H-bonded OH) | Broad, moderate | 3401 (stretching vibration of H-bonded OH) | Broad, strong | 1464 (-CH bending of $CH_2$) | Strong, broad |
| | | | | 1601 (Aromatic C=C stretch and/or asym $-COO^-$ stretch) | Moderate, broad |
| | | | | 2928 (-$CH_2$- sym stretch) | Very weak |
| | | | | 3395 (stretching vibration of H-bonded OH) | Broad, moderate |

[†] The assignations are based on Colthup et al. (1990) and Wang and Huang (1992).

Absorption bands at 3401, 2928, 1589, 1457, 1410, 1074, and 1032 $cm^{-1}$ (168 $\mu E\ s^{-1}\ m^{-2}$), and 3395, 2928, 1601, 1464, 1409, 1314, 1075, and 1032 $cm^{-1}$ (500 $\mu E\ s^{-1}\ m^{-2}$) (Figure 3.2.4 c and d and Table 3.2.3) from the organic components were observed. The absence of a band at ca. 1714 $cm^{-1}$ (associated with undissociated carboxyl) (Figure 3.2.4 b, c and d) is consistent with the system pH being near or above 7 (Wang and Huang, 1992) and therefore, the carboxyl groups are present in dissociated form (absorption bands at 1409 to 1410, 1589 to 1601 $cm^{-1}$) (Colthup et al., 1990). The FTIR spectroscopic data confirm that not all the reaction products were in the supernatant, but some were present in the solid phase. The results also indicate that the reductive dissolution of birnessite was promoted by the presence of light.

### 3.2.3.4 X-ray absorption near-edge structure spectroscopy

X-ray absorption near-edge structure spectroscopic experiments were performed on the following solid phases all at an initial pH of 7.00 following reaction at 25°C for 60 d (Figure 3.2.5): Birnessite (500 μE $s^{-1}$ $m^{-2}$, 60 d), glucose-glycine birnessite (0 μE $s^{-1}$ $m^{-2}$, 60 d) and glucose-glycine birnessite (500 μE $s^{-1}$ $m^{-2}$, 60 d). Specific features in the

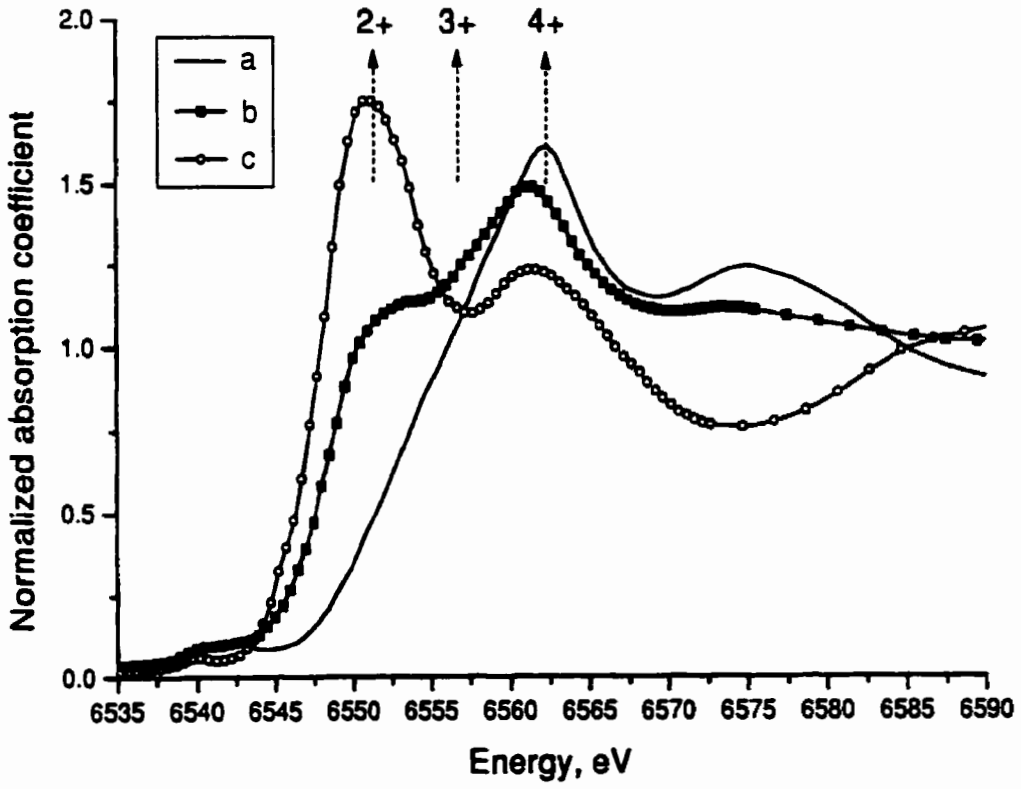


**Figure 3.2.5** XANES spectra of (a) birnessite exposed to 500 μE $s^{-1}$ $m^{-2}$, and the solid phase of the glucose-glycine-birnessite system exposed to (b) 0 μE $s^{-1}$ $m^{-2}$ (60 d), and (c) 500 μE $s^{-1}$ $m^{-2}$ (60 d). The reaction systems were at an initial pH of 7.00 and were maintained at 25.5 ± 0.5°C. The oxidation states of Mn (2+, 3+ and 4+) at respective energy levels are indicated by arrows.

spectra, in the energy region between 6545 and 6565 eV, indicate that the Mn ion was present in different oxidation states (Figure 3.2.5). In the XANES spectra, the presence of Mn(IV) was still detected, in the glucose-glycine-birnessite systems, whether exposed to 0, or 500 μE $s^{-1}$ $m^{-2}$, but Mn(IV) was dominant in the solid phase of the glucose-glycine-birnessite system at 0 μE $s^{-1}$ $m^{-2}$, whereas Mn(II) was the predominant species in the solid phase of the glucose-glycine-birnessite systems at 500 μE $s^{-1}$ $m^{-2}$.

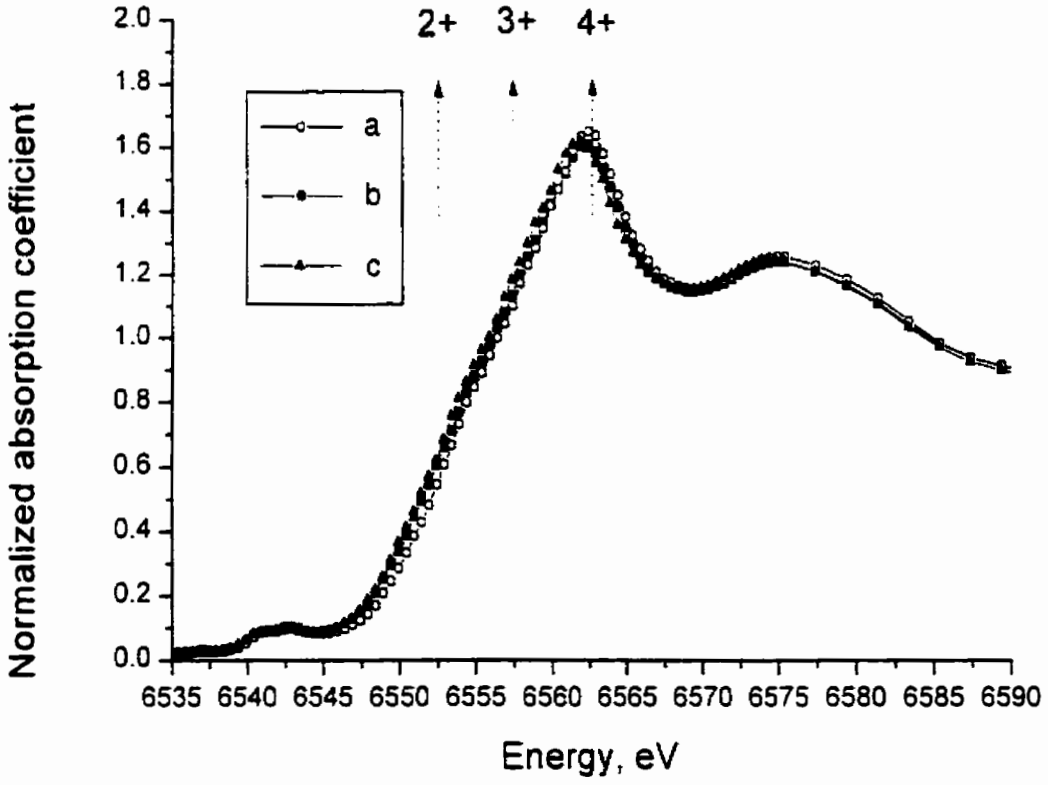


**Figure 3.2.6**. XANES spectra of (a) untreated birnessite, and (b) and (c) samples of birnessite at an initial pH of 7.00 exposed to 168 and 500 μE $s^{-1}$ $m^{-2}$, respectively, for 60 days at 25.5 ± 0.5°C.

Moroever, in the solid phase, XANES spectroscopic evidence shows that whether exposed to light or not, Mn(IV) in birnessite was partially reduced to Mn(II) in the glucose-glycine-birnessite system.

Control systems of birnessite and water alone, at an initial pH of 7.00 were also exposed to light intensities of 168 and 500 $\mu E\ s^{-1}\ m^{-2}$ for a period of 60 days at 25°C. The spectra were examined by XANES spectroscopy and were found to be identical to a sample of pure birnessite (Figure 3.2.6). Therefore light alone had no effect on birnessite.

The data indicate that light accelerated the rate at which electrons were transferred from glucose to the surface of the birnessite leading to the following reductive reaction:

$$MnO_2 + 4H^+ + 2e^- \longrightarrow Mn^{2+} + 2H_2O$$

As a consequence of the consumption of $H^+$, the pH of the system increased, further driving the polycondensation reaction of glucose and glycine. The glucose was apparently oxidized to D-gluconic acid initially and then, either further oxidized to α-dicarbonyl compounds or decarboxylated with loss of carbon dioxide. Simultaneously or subsequently a complex polycondensation process between glucose and glycine resulted in the formation of Maillard reaction products. The Mn(II) released into solution may form complexes with intermediate Maillard reaction products and further catalyze the Maillard reaction. Arfaioli et al. (1999) noted the ability of Cu(II) ion to catalyze the formation of humic-like substances in a system containing glucose and tyrosine.

Light intensity of 168 or 500 $\mu E\ s^{-1}\ m^{-2}$ exerted a positive effect on the browning of the glucose-glycine-birnessite system compared to the same system which was kept in

the dark. As a consequence, the reductive dissolution of the birnessite and release of Mn (II) to the supernatant was increased. Even in complete darkness birnessite catalyzed the browning reaction between glucose and glycine. Therefore, birnessite catalysis of the Maillard reaction can occur in soil or sediment environments at any depth, but the presence of sunlight should strongly accelerate the reaction.

## 3.3 Molecular Topological Analysis of a Maillard Reaction Intermediate

### 3.3.1 Introduction

In molecular modelling, atomic scale systems are being considered and the only theoretical method that allows rigorous calculation of energies is quantum mechanics. *Ab initio* quantum mechanical methods are so termed because they use no empirical data other than the masses of elementary particles, elementary charge, Planck's constant and the speed of light (Teppen, 1998). The level of complexity of many chemical compounds and the large variety of their possible chemical reactions can obscure the simple fact that a molecule contains nothing more than atomic nuclei and an electron density cloud obeying the Pauli exclusion principle. Since the distribution of the atomic nuclei is deducible from the electron density, it follows that all information on the reactivity of the molecule can be obtained from the electron density (Mezey et al., 1996). The local maxima of electron densities are believed to coincide with the nuclear locations. Since no other particles are moving in the electrostatic field of the atomic nuclei, the electron density charge cloud contains all the information about a particular molecule (Mezey, 1998; Mezey et al., 1998).

The theory and computational techniques of molecular electron density shape analysis have briefly been described in Section 2.5. More detailed and advanced treatments are described in the literature (Mezey, 1987, 1988, 1993). With today's

computer technology, it is possible to calculate the shape of a molecule. The shape is defined by Molecular Iso-Density Contours (MIDCO's) which are electron density contour faces where along each surface the electron density is constant. A contour surface of lower density encloses surfaces of higher density analogous to a series of Russian wooden dolls (Mezey, 1993). The density value along each MIDCO is specified in atomic units (a.u.), defined as one electronic charge in one cubic bohr (i.e., electron/bohr$^3$), where the conversion to SI units gives 1 a.u. of electron density = 1.08 x $10^{12}$ C/m$^3$. One bohr is defined as the Bohr radius of the hydrogen atom. Therefore, at different density levels, different shapes exist.

Shape group analysis, a method proposed by Mezey (1986), presents a discrete representation of molecular shape and allows for easy comparison of molecular shapes. Shape analysis methods are based on detailed, high quality quantum chemical computations of the three-dimensional electron density clouds of the molecules involved (Mezey et al., 1998). To date, molecular topological information on the Maillard reaction is lacking. The establishment of a quantitative shape-activity relationship (QShAR) for the formation of the Amadori compound, which is an intermediate compound formed in the Maillard reaction. from the starting molecules glucose and glycine will provide a fundamental insight into the nature of the initial part of the Maillard reaction.

The computations in this dissertation considered the condensation reaction path between one molecule of glucose and one molecule of glycine leading to the formation of the Amadori compound and the splitting off of a molecule of water (Figure 3.3.1).

The objectives of these computations were: (1) To investigate how the atomic configuration in the two molecules (glucose and glycine) changes along the reaction path, and (2) to gain insight into how the energy of the system changes as the reaction path proceeds.

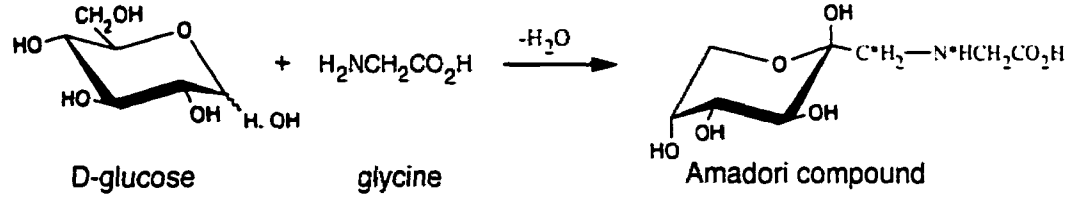


**Figure 3.3.1** Formation of the Amadori compound from glucose and glycine (Mossine et al., 1994). Note that a molecule of water is split off. The relevant carbon and nitrogen atoms considered in this section are designated with a *.

### 3.3.2 Materials and Methods

To achieve the objectives outlined above, the following methodology was employed:

1. Molecular models were constructed using Hyperchem.
2. The molecules were optimized using Gaussian quantum chemical optimization.

The electron density computations presented here are based on the quantum chemistry program system Gaussian 92 which provides the molecular wavefunctions (Foresman and Frisch, 1996). The computations were carried out on a Digital DEC 3000 (Digital, Canada) workstation featuring an Alpha 20164 processor and 125 MHz clock.

### 3.3.3 Results and Discussion

Molecular Iso-Density Contours for glucose, glycine, and fructosylglycine with electron density thresholds of $\rho = 0.1$ atomic units were constructed and are shown in Figure 3.3.2. It is evident that the hydrogen atoms are spatially very close to the bonding atoms C, N and O. All the bonds are covalent in nature. Originally in order to achieve the objectives outlined above (Section 3.3.1), an *ab initio* method – restricted Hartree-Fock with basis set STO-3G (Slater type orbitals) – was attempted. A basis set is a mathematical representation of the atomic orbitals within a molecule. However, the slowness of these computations, coupled with Hartree self-consistent field convergence and geometry problems which arose, led to the selection of a semi-empirical (AM1) method.

In this method, the starting point was the optimized Amadori compound with a bond distance between the C atom of glucose and the N atom of glycine (Figure 3.3.1 and Figure 3.3.3) of 1.443 Å. The distance between the two bonding atoms (see Figure 3.3.3) i.e., C* and N*, was then incrementally increased by manually inputting the bond distance parameter into the AM1 program and "locking it in" while all the other parameters were optimized. The goal was to observe what occurred when the distance between the glucose and glycine components of the Amadoric compound (i.e., the C-N bond distance) was increased from 1.443 Å and how this change influenced the internal coordinates of the atoms in the Amadori compound and also the mutual orientation of these two constituent components. However, as the distance increases the energy minimum becomes unstable and the Gaussian program has a problem finding this minimum. This is because when the two components (glucose and glycine) are separated

by a certain distance (which is approximately twice the optimal C*-N* bond distance in the Amadori compound i.e., ~ 2.8Å) they hardly interact with each other. Therefore the

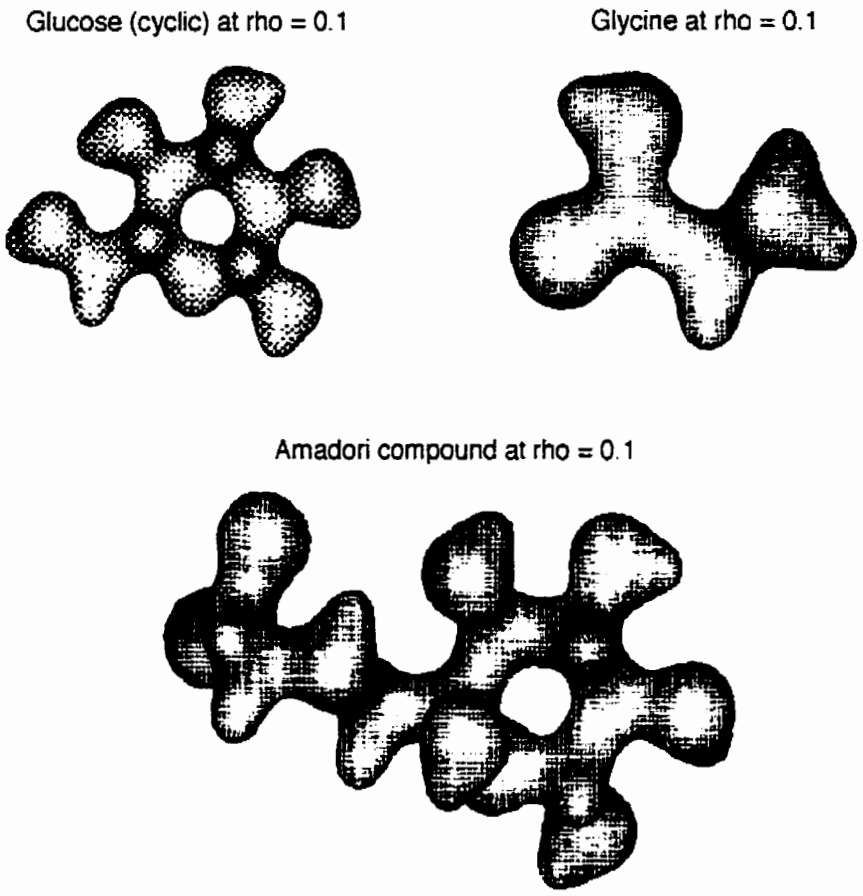


**Figure 3.3.2** Three MIDCO's of glucose, glycine, and their Amadori product N-(1-deoxy-D-fructos-1-yl)-glycine (fructosylglycine).

the energy minimum becomes very shallow and difficult to localize. The results of modelling the Amadori compound N-(1-deoxy-D-fructos-1-yl)-glycine or fructosylglycine using AM1 computations (conformations 1 – 9 from 1.443 Å to 3.2Å) are shown in Figure 3.3.3 below.

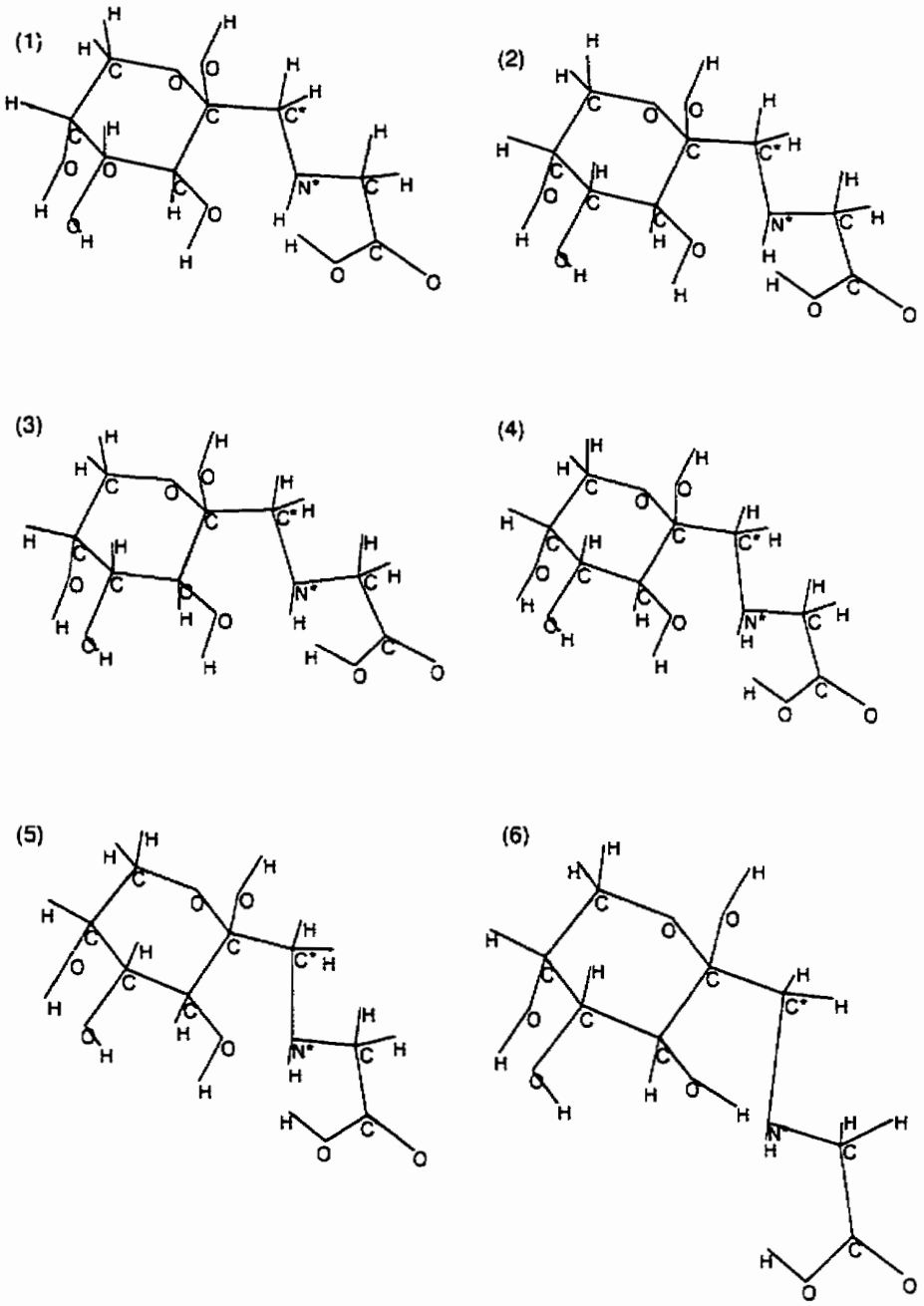


**Figure 3.3.3** Amadori compound modelled at different C* – N* bond (distances in Å) (1) 1.443 (optimized i.e., the optimal bond distance for the Amadori compound using AM1 quantum mechanical computations), (2) 1.6, (3) 1.7, (4) 1.8, (5) 1.9, (6) 2.0, (7) 2.4, (8) 2.8, (9) 3.2. Note the change in the conformation from 2.8 Å (8) onwards. All the models are planar representations of the 3-dimensional structures.

Figure 3.3.3 continued

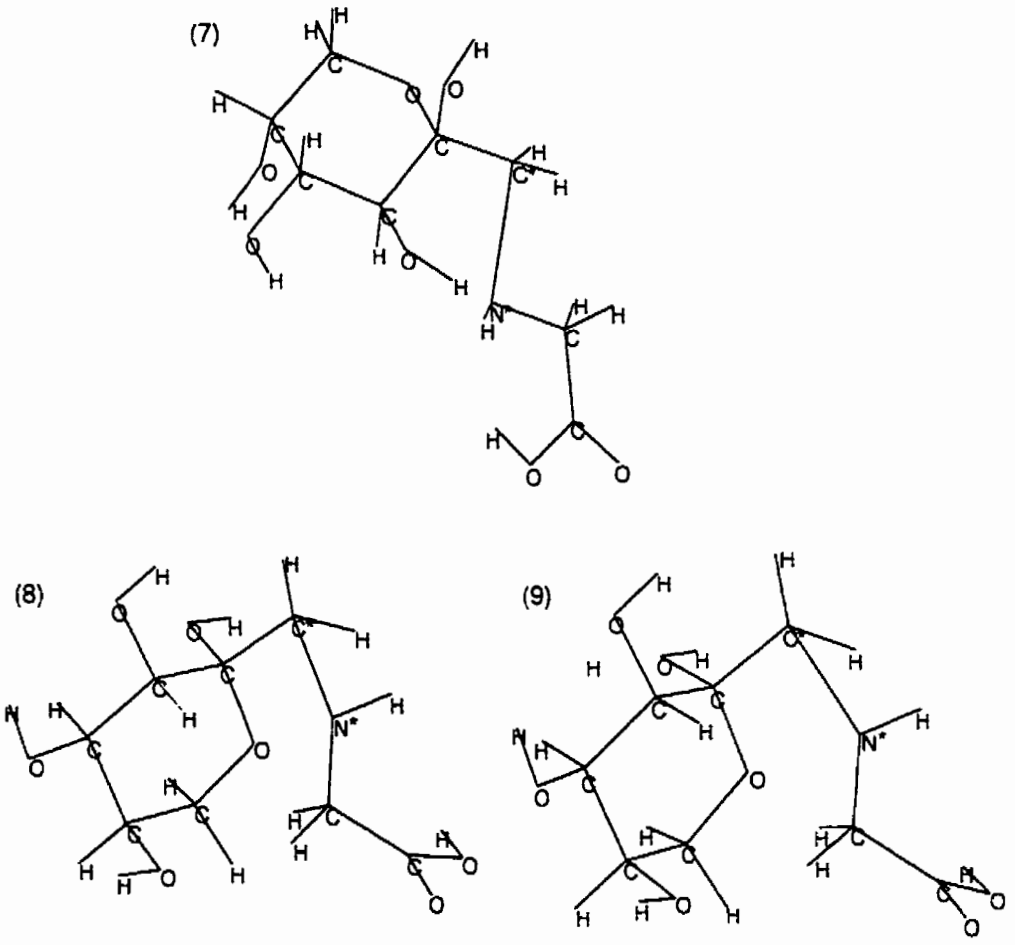


It is noted that from 2.8 Å (0.28 nm) (Figure 3.3.3 (8)) there is a significant change in the conformation of the molecule. This is due to a change from tetrahedral ($sp^3$) to trigonal ($sp^2$) in the carbon atom which is bonded to nitrogen. The bond distance between the C of glucose and the N of glycine has increased to such an extent that the C atom no longer "sees" the N atom and there is no fourth ligand present to require the C

atom to have tetrahedral coordination. The energies of the conformations (1) to (9), i.e., the ground state electron energy of each particular conformation in Figure 3.3.3, at 0 K (i.e., absolute zero temperature), were calculated using the AM1 method included in the Gaussian 92 program package. The results are given in Table 3.3.1 and plotted in Figure 3.3.4. Note that the AM1 program calculates the optimized C-N bond distance for the Amadori compound to be 1.443 Å and gives the ground state electron energy of the molecule. The effect of thermal vibrations on the computations was not taken into consideration.

**Table 3.3.1** Energies of Amadori compound fructosylglycine (FG) at different C – N bond distances (Figure 3.3.3) and for glucose, glycine and water

| Compound | C-N bond distance (Å) | Energy (Hartrees)[†] | Energy (kJ $mol^{-1}$)[†] |
|---|---|---|---|
| Glucose | | -0.471949 | $-1.239102 \times 10^{3}$ |
| Glycine | | -0.156299 | $-4.103630 \times 10^{2}$ |
| Water | | -0.094429 | $-2.479223 \times 10^{2}$ |
| FG[‡] (1) (optimized) | 1.443 | -0.522628 | $-1.372160 \times 10^{3}$ |
| FG (2) | 1.6 | -0.507973 | $-1.333683 \times 10^{3}$ |
| FG (3) | 1.7 | -0.489623 | $-1.285505 \times 10^{3}$ |
| FG (4) | 1.8 | -0.469304 | $-1.231577 \times 10^{3}$ |
| FG (5) | 1.9 | -0.449311 | $-1.179665 \times 10^{3}$ |
| FG (6) | 2.0 | -0.430752 | $-1.130939 \times 10^{3}$ |
| FG (7) | 2.4 | -0.377001 | $-9.898161 \times 10^{2}$ |
| FG (8) | 2.8 | -0.338246 | $-8.880649 \times 10^{2}$ |
| FG (9) | 3.2 | -0.315178 | $-8.274998 \times 10^{2}$ |

[†]1 Hartree = 2625.50 kJ $mol^{-1}$

[‡]Fructosylglycine molecular information in Figure 3.3.3.

The results (Table 3.3.1), were used to create a plot of [E(water) + E(complex)] - [E(glucose) + E(glycine)] (kJ $mol^{-1}$) vs. C-N bond distance (Å) (Figure 3.3.4). The complex is the Amadori compound, fructosylglycine which is formed from glucose and glycine with the splitting off of a molecule of water (Figure 3.3.1). To simplify the computations, the points in Figure 3.3.4 were obtained by assuming that a molecule of water does not interact with fructosylglycine. In reality this only holds true for the ground state of the fructosylglycine, i.e., at a C-N bond distance of 1.443 Å.

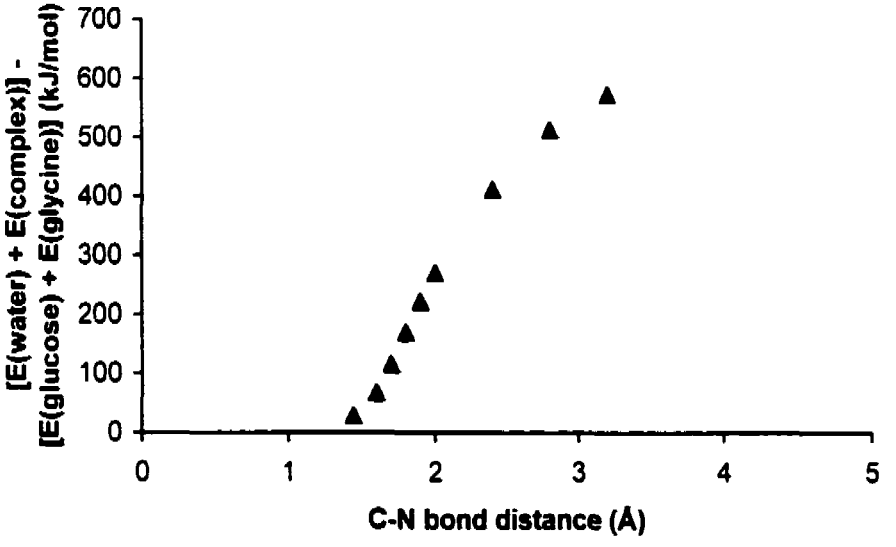


**Figure 3.3.4** Plot of energies of Amadori compound at different C-N bond distances. The energy of each conformation is defined as the ground state electronic energy of the conformation at 0 K (absolute zero temperature).

Originally it was intended to include the effect of water, i.e., to place a water molecule into the Amadori compound complex and perform computations with this

augmented system in order to observe how water splits off from glucose and glycine during the formation of the Amadori compound (Figure 3.3.1). Problems encountered with computations involving just glucose and glycine caused this to be set aside. MIDCO's were calculated for glucose, glycine and the complex fructosylglycine (FG). The calculations (Table 3.3.1 and Figure 3.3.4) show that FG, water, glucose, and glycine as separate entities are very close to each other in terms of their ground state energy. The results indicate that the potential energy barrier will be high (Figure 3.3.4) and therefore the reaction between glucose and glycine alone to form FG is very slow at room temperature. Example calculations are shown below.

E(water) + E(optimized complex)* = -0.617057 Hartree = $-1.620083 \times 10^3$ kJ $mol^{-1}$

E(glucose) + E(glycine) = -0.628248 Hartree = $-1.649465 \times 10^3$ kJ $mol^{-1}$

$\therefore$ [E(water) + E(optimized complex)*] – [E(glucose) + E(glycine)] = 29.382 kJ $mol^{-1}$

* - energy of FG complex where C-N bond distance is equal to 1.443Å

Based on quantum mechanical calculations (Table 3.3.1 and Figure 3.3.4) the Amadori compound is stable, i.e., the computations converge and the optimum C-N bond distance can be found, and this theoretical observation is in accord with experimental practice, i.e., the Amadori compound fructosylglycine can be isolated experimentally (e.g., O'Brien and Morrisey, 1997).

## 3.4 The Catalytic Role of Birnessite in Polycondensation of Glucose-glycine-catechol and the Formation of Humic Substances

### 3.4.1 Introduction

Many soil inorganic components including oxides, hydroxides, oxyhydroxides, short-range ordered (SRO) minerals, clay-size layer silicates, primary minerals and natural soils possess the ability to abiotically transform phenolic compounds and amino acids in soils (Wang et al., 1986; Huang, 1990, 2000). Birnessite is a powerful oxidizing agent (Shindo and Huang, 1982, 1984a, 1984b; Wang and Huang, 1987a, 1991, 1992). Oxidant strength for several metal oxides common in soils decreases in the order Mn(III/IV) oxides > Co(III) oxides > Fe(III) oxides (Sparks, 1995).

The polyphenol model of abiotic (mineral catalyzed) formation of humic substances has been well established (Huang, 1995, 2000). Sections 3.1 and 3.2 have demonstrated that birnessite catalysis of the Maillard reaction merits attention as an abiotic pathway for the formation of humic substances in soils and aquatic environments as shown in Section 3.1 and 3.2. It would be a logical step to attempt to integrate the two separate pathways into one combined pathway as the reaction would likely occur in nature. The objective of this research unit is to examine the catalytic effect of birnessite on the process of humification in the catechol-glucose-glycine ternary system

### 3.4.2 Materials and Methods

The procedure was very similiar to Section 3.1, i.e., 2.5 g of birnessite was suspended in 85 mL of glucose-glycine-catechol or glycine-catechol (1:1:1 or 1:1 molar ratio, 0.05 mole each) solution. The pH of the suspension was adjusted to 7.00 and double-deionized water was added to adjust the total volume to 100 mL. The flasks were sealed and placed on an oscillating water bath at 25 or 45°C. The system was allowed to react for 15 (45°C) or 30 or 60 (25°C) days. Ambient light intensity over the samples was 0 to 3.1 ± 0.9 $\mu E\ s^{-1}\ m^{-2}$. At the end of the reaction period, the supernatant liquid phase was separated from the solid phase by centrifugation at 25000 g for 40 minutes. The solid phase was lyophilized and the following analyses were carried out:

(a) Visible absorption spectroscopy of the supernatants,

(b) pH, Eh, pE + pH, and Mn content of the supernatants.

(c) EPR of the liquid phase.

(d) XANES of the solid phase, and

(e) FTIR of the solid phases and extracted humic and fulvic acids.

The experimental details for the visible absorption spectroscopic, pH, Eh, EPR, FTIR, and XANES analyses have been described in Sections 3.1 and 3.2.

(f) $^{13}C$ CPMAS NMR of the extracted fulvic acid from the glucose-glycine-birnessite system and of the humic acid from the glycine-catechol-birnessite system:

$^{13}C$ CPMAS NMR spectroscopic analysis was performed on a Bruker Avance 360 DRX spectrometer (Bruker Analytik, Rheinstetten/Karlsruhe Germany) with a supercooled magnet of field strength 8.46 Tesla operating at 90.57MHz for $^{13}C$.

Analysis was performed on extracted fulvic acid from the glucose-glycine-birnessite system and on humic acid from the glycine-catechol-birnessite system. A 4 mm Bruker probe and phase stabilized zirconium rotor was used. Chemical shifts are expressed relative to tetramethylsilane (TMS = 0 ppm). No rotor effects were observed.

Glucose-glycine-birnessite fulvic acid: The sample of fulvic acid was analyzed using a PAROPT (parameter optimization) program. After selection of an initial set of conditions the software allows the variation of key parameters such as contact time and relaxation delay in a search for optimal spectral conditions. For analysis of the sample of fulvic acid, the contact time was increased by intervals of 0.5 ms from 1 ms to 5.5 ms. The relaxation delay was similarly increased by increments of 0.5 s from 0.5 s to 4.0 s. Optimal spectral conditions were obtained using a contact time of 3.0 ms and relaxation delay of 2.0 s. In order to minimize the effect of spinning sidebands the sample was spun at 12 kHz.

Glycine-catechol-birnessite humic acid: The sample of humic acid was analyzed using a contact time of 3.0 ms and relaxation delay of 2.0 s with spin rate of 12 kHz.

(g) $^{14}C$ tracer analysis using $^{14}C$ uniformly labelled (UL) glucose was carried out on the following four systems at 45°C in order to monitor the evolution of $^{14}CO_2$:

(i) Glucose-glycine,

(ii) glucose-glycine-birnessite,

(iii) glucose-glycine-catechol, and

(iv) glucose-glycine-catechol-birnessite.

The procedure for experiments with $^{14}C$ UL glucose was as follows. $1.85 \times 10^6$ Bq (50 μCi, 50 μmol) of UL-$^{14}C$ D-glucose ($HO^{14}CH_2[^{14}CHOH]_4{}^{14}CHO$) of radiochemical purity ≥ 98% (HPLC) was purchased. 25 μmol of $^{14}C$-labelled glucose was diluted to 50 mL with double-deionized water and 12 μmol of UL-$^{14}C$ D-glucose were used as a tracer for each experimental batch. The experimental procedure then followed that given in Section 3 with one difference. An autoclaved polyethylene tube (of sufficient dimensions that it leaned against the wall of the reaction vessel without danger of its contents mixing with those of the vessel) containing 10 mL of 1/3M KOH was placed in each reaction flask, prior to closing, in order to absorb any $^{14}CO_2$ released. At the end of the 15 day reaction period, the KOH solutions were analyzed for $^{14}CO_2$ released using a Beckman LS3801 Liquid Scintillation Counter.

**Extraction of humic substances-**

The extraction of humic substances was carried out according to the procedure described by Wang and Huang (1989).

Extraction of humic acid (HA) and fulvic acid (FA) from the supernatant of the glucose-glycine-birnessite system and of humic acid (HA) from the supernatant of the glycine-catechol-birnessite system: The supernatant combined with its water extracts was acidified to pH 1.0 by the addition of 6 M HCl to precipitate HA and separate it from the FA which remained in solution. After standing for 24 h, any HA precipitate was separated from the supernatant by centrifugation at 2000g for 20 min (International No.1 centrifuge, International Equipment Company, Boston, MA). The HA was transferred to dialysis tubing (MWCO 1000) using double-deionized water

and was dialyzed against water until a negative chloride test was obtained (10% silver nitrate solution). After dialysis was completed, the HA was lyophilized.

The acidified FA, that remained in solution, was passed through a column of XAD-8 resin. The column was then washed with water until unadsorbed, low molecular weight reactants were removed and the pH was approximately 7. The FA was eluted from the XAD-8 column using 0.1 M NaOH until the eluate became colourless. The column was washed with water to neutral pH and the eluates were combined and immediately acidified with 6 M HCl to pH 1. The acidified FA was allowed to stand for 48 h with stirring and was then again passed through a column of XAD-8 resin. After washing with water the column was eluted with 0.1 M NaOH and the FA eluate was immediately passed through a second column containing IR-120 $H^+$-activated cation exchange resin to convert the Na-fulvate into the $H^+$ form. The FA solution was concentrated to a small volume on a rotary evaporator and then lyophilized. HF was not used in the purification process because no siliceous material was present.

### 3.4.3 Results and Discussion

#### 3.4.3.1 Visible absorption spectroscopy and related analyses

The results for the systems at 25 (60 days) and 45°C (15 days) are shown in Tables 3.4.1 to 3.4.4. Birnessite significantly promoted the browning of all systems (both at 25 and 45°C) compared to non-birnessite containing systems. This is due to the ability of birnessite to accelerate the polymerization of catechol and the

polycondensation of catechol with glucose and glycine or glycine and simultaneous reduction of Mn(IV) of birnessite to Mn(II) (Tables 3.4.1 to 3.4.4).

The browning was most pronounced in systems (both at 25 and 45°C) that contained catechol. The polycondensation of catechol, glycine and glucose or catechol and glycine was greatly accelerated by the catalytic action of birnessite. The highest degree of browning at 45°C was exhibited by the glycine-catechol-birnessite system; the polymerization and polycondensation products (humic substances) formed in this oxido-reductive catalytic reaction had the highest visible absorbances of all the systems studied.

The glucose-glycine-catechol-birnessite system exhibited lower absorbances in the range 400 to 600 nm compared to the glycine-catechol-birnessite system (Table 3.4.2). This is attributed to the humification (polycondensation) products in the former system having lower absorbances. Glucose apparently perturbed polymerization of catechol and polycondensation of glycine-catechol by birnessite. The glucose-glycine-birnessite system had the highest concentration of Mn in the supernatant indicating that in this system, oxidation/reduction and the subsequent Mn dissolution processes are particularly important. However, the products which are formed in the system had a lower absorbance in the range 400 to 600 nm than those produced in systems containing catechol. The formation of large amounts of Mn(II) in solution could also contribute to the acceleration of the Maillard reaction.

**Table 3.4.1** Increase in the visible absorbance in the glucose-glycine, glucose-glycine-birnessite, glucose-glycine-catechol and glucose-glycine-catechol-birnessite systems studied at 25°C for a period of 60 days†

| Reaction system | Absorbance | |
|---|---|---|
| | 400 nm | 600nm |
| | —— 10 days —— | |
| Glucose-glycine | <0.01 | <0.01 |
| Glucose-glycine-birnessite | 0.052 ±0.001 | 0.010 ±0.001 |
| Glucose-glycine-catechol | 2.67 ±0.11 | 1.23 ±0.07 |
| Glucose-glycine-catechol-birnessite | 31.8 ±2.0 | 8.85 ±0.71 |
| | —— 20 days —— | |
| Glucose-glycine | 0.01 | <0.01 |
| Glucose-glycine-birnessite | 0.104 ±0.004 | 0.020 ±0.001 |
| Glucose-glycine-catechol | 3.23 ±0.25 | 1.37 ±0.11 |
| Glucose-glycine-catechol-birnessite | 42.8 ±2.2 | 11.2 ±0.67 |
| | —— 30 days —— | |
| Glucose-glycine | 0.031 ±0.001 | 0.010 |
| Glucose-glycine-birnessite | 0.141 ±0.005 | 0.022 ±0.001 |
| Glucose-glycine-catechol | 3.53 ±0.29 | 1.52 ±0.10 |
| Glucose-glycine-catechol-birnessite | 45.0 ±2.1 | 12.2 ±0.8 |
| | —— 40 days —— | |
| Glucose-glycine | 0.042 ±0.003 | 0.016 ±0.001 |
| Glucose-glycine-birnessite | 0.171 ±0.005 | 0.033 ±0.002 |
| Glucose-glycine-catechol | 6.31 ±0.38 | 2.35 ±0.17 |
| Glucose-glycine-catechol-birnessite | 47.1 ±2.9 | 14.4 ±1.0 |
| | —— 50 days —— | |
| Glucose-glycine | 0.059 ±0.003 | 0.018 ±0.001 |
| Glucose-glycine-birnessite | 0.264 ±0.007 | 0.041 ±0.001 |
| Glucose-glycine-catechol | 8.17 ±0.39 | 2.95 ±0.21 |
| Glucose-glycine-catechol-birnessite | 68.8 ±3.1 | 25.1 ±1.4 |
| | —— 60 days —— | |
| Glucose-glycine | 0.077 ±0.004 | 0.021 ±0.001 |
| Glucose-glycine-birnessite | 0.367 ±0.006 | 0.067 ±0.002 |
| Glucose-glycine-catechol | 10.8 ±0.55 | 3.75 ±0.22 |
| Glucose-glycine-catechol-birnessite | 90.4 ±3.8 | 37.6 ±1.7 |

†The glycine-catechol-birnessite system was not studied at 25°C.

**Table 3.4.2** Increase in the visible absorbance in the glucose-glycine, glucose-glycine-birnessite, glucose-glycine-catechol, glucose-glycine-catechol-birnessite and glycine-catechol-birnessite systems at 45°C for a period of 15 days

| Reaction system | Absorbance 400 nm | 600nm |
|---|---|---|
| | 3 days | |
| Glucose-glycine | 0.019 ±0.001 | <0.01 |
| Glucose-glycine-birnessite | 0.337 ±0.002 | 0.090 ±0.001 |
| Glucose-glycine-catechol | 0.230 ±0.01 | 0.143 ±0.005 |
| Glucose-glycine-catechol-birnessite | 28.9 ±1.4 | 8.46 ±0.8 |
| Glycine-catechol-birnessite | 72.2 ±4.3 | 20.9 ±1.7 |
| | 6 days | |
| Glucose-glycine | 0.088 ±0.003 | 0.016 ±0.001 |
| Glucose-glycine-birnessite | 1.462 ±0.008 | 0.123 ±0.003 |
| Glucose-glycine-catechol | 0.560 ±0.010 | 0.152 ±0.005 |
| Glucose-glycine-catechol-birnessite | 40.4 ±2.1 | 9.21 ±0.7 |
| Glycine-catechol-birnessite | 92.3 ±4.5 | 24.5 ±1.7 |
| | 9 days | |
| Glucose-glycine | 0.179 ±0.007 | 0.044 ±0.002 |
| Glucose-glycine-birnessite | 5.72 ±0.14 | 0.31 ±0.01 |
| Glucose-glycine-catechol | 3.61 ±0.09 | 1.52 ±0.06 |
| Glucose-glycine-catechol-birnessite | 58.4 ±3.9 | 15.8 ±1.1 |
| Glycine-catechol-birnessite | 163.5 ±8.1 | 73.8 ±3.5 |
| | 12 days | |
| Glucose-glycine | 0.313 ±0.013 | 0.085 ±0.005 |
| Glucose-glycine-birnessite | 9.02 ±0.30 | 0.76 ±0.03 |
| Glucose-glycine-catechol | 4.05 ±0.21 | 1.72 ±0.10 |
| Glucose-glycine-catechol-birnessite | 64.7 ±1.4 | 19.9 ±1.03 |
| Glycine-catechol-birnessite | 186.0 ±10.8 | 88.7 ±4.1 |
| | 15 days | |
| Glucose-glycine | 0.362 ±0.018 | 0.103 ±0.006 |
| Glucose-glycine-birnessite | 14.7 ±0.68 | 1.50 ±0.10 |
| Glucose-glycine-catechol | 5.60 ±0.35 | 2.13 ±0.08 |
| Glucose-glycine-catechol-birnessite | 73.7 ±1.3 | 24.7 ±1.51 |
| Glycine-catechol-birnessite | 242.1 ±14.7 | 115.6 ±6.9 |

**Table 3.4.3** Final pH, redox status, and Mn content of supernatants in the glucose-glycine, glucose-glycine-birnessite, glucose-glycine-catechol, and glucose - glycine-catechol-birnessite systems studied at 25°C for the period of 60 days

| Treatment | Mn (μg $mL^{-1}$) | pH | Eh (mV) | pE + pH |
|---|---|---|---|---|
| Glucose + glycine | 0 | 7.11 ±0.05 | 411 ±12 | 14.03 ±0.23 |
| Glucose + glycine + birnessite | 2839 ±71 | 7.68 ±0.09 | 343 ±10 | 13.47 ±0.26 |
| Glucose + glycine + catechol | 0 | 6.42 ±0.08 | 296 ±10 | 11.42 ±0.25 |
| Glucose + glycine + catechol + birnessite | 3010 ±174 | 7.60 ±0.09 | 87 ±15 | 9.07 ±0.34 |

**Table 3.4.4** Final pH and Mn content of supernatants of glucose-glycine, glucose-glycine-birnessite, glucose-glycine-catechol, and glucose-glycine-catechol-birnessite systems at 45°C for the period 15 days

| Treatment | Mn (μg $mL^{-1}$) | pH |
|---|---|---|
| Glucose + glycine | 0 | 7.01 ±0.09 |
| Glucose + glycine + birnessite | 7803 ±74 | 7.98 ±0.11 |
| Glucose + glycine + catechol | 0 | 5.92 ±0.06 |
| Glucose + glycine + catechol + birnessite | 3222 ±120 | 7.21 ±0.13 |
| Glycine + catechol + birnessite | 3281 ±141 | 7.66 ±0.15 |

### 3.4.3.2 Electron paramagnetic resonance spectroscopy

EPR spectroscopic analysis of the glucose-glycine-birnessite supernatant both at 25 and 45°C was carried out and the results (presented and discussed in Section 3.1) clearly indicated the presence of Mn (II) in the supernatant.

### 3.4.3.3 X-ray absorption near-edge structure spectroscopy

XANES spectroscopic analyses were carried out on lyophilized samples of the solid phase of the reaction products of the glucose-glycine-catechol-birnessite system (60 days at 25°C and 15 days at 45°C) and on the glycine-catechol-birnessite system (15 days at 45°C). The XANES data indicate that there was substantial reduction of Mn (IV) in the birnessite to lower Mn oxidation states, particularly Mn (II) (Figure 3.4.1).

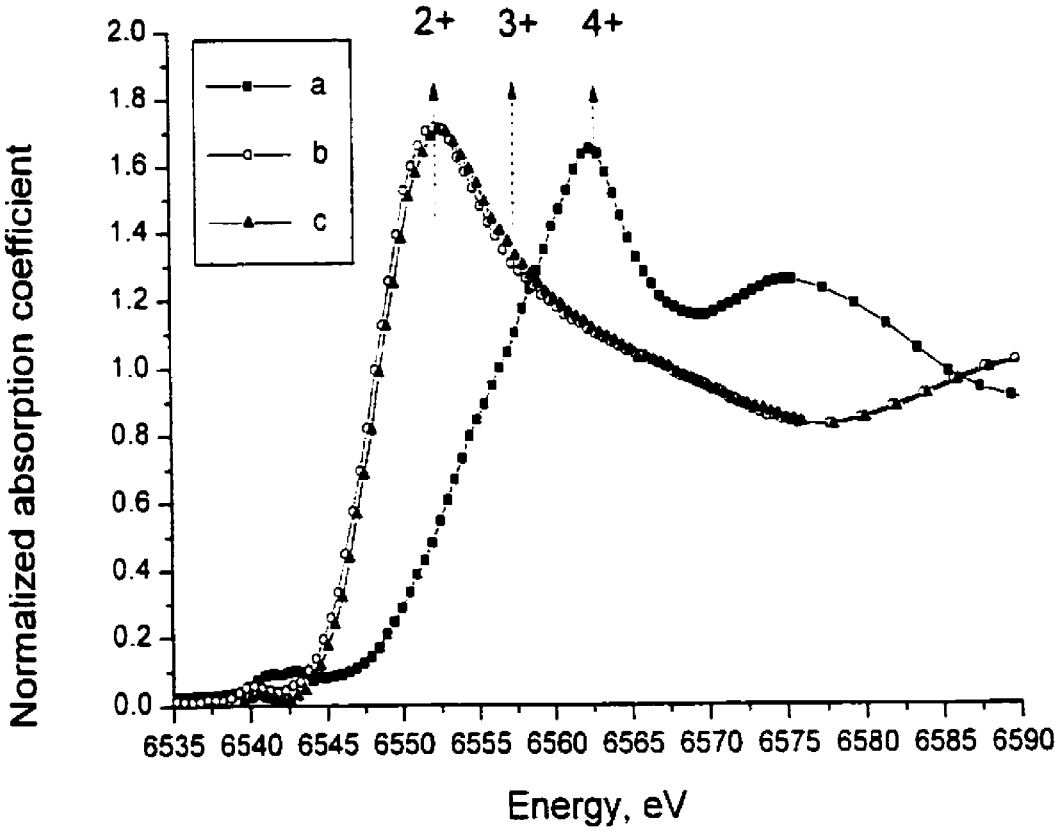


**Figure 3.4.1** XANES spectra of (a) control sample of pure birnessite, and the solid phase of the glucose-glycine-catechol-birnessite system reacted for (b) 60 days at 25°C and (c) 15 days at 45°C. The glycine-catechol-birnessite system (15 days at 45°C) is not shown but the spectrum is identical to treatments (b) and (c).

### 3.4.3.4 Fourier transform infrared absorption spectroscopy of the solid phases and extracted humic and fulvic acids

FTIR analysis was carried out on the lyophilized solid phase of the following systems all of which had the initially adjusted pH of 7.00: (a) glucose-glycine-catechol-birnessite (reacted at 25°C for 60 days), (b) glycine-catechol-birnessite (c) glucose-glycine-catechol-birnessite, and (d) glucose-glycine-birnessite (all reacted at 45°C for 15 days). At the qualitative level the spectra of the freeze-dried glucose-glycine-catechol-birnessite, Figure 3.4.2 a, (which was reacted at 25°C for 60 days), glycine-catechol-birnessite, Figure 3.4.2 b, and glucose-glycine-catechol-birnessite, Figure 3.4.3 c, (both of which were reacted at 45°C for 15 days) are very similiar. All three systems have weak bands at 576 or 591 $cm^{-1}$ which are assigned to Mn-O interactions. All other bands arise from organic components, i.e., phenolic OH, aromatic C=C, carboxylate, aliphatic $-CH_2$, hydroxyl, and the amino group (Table 3.4.5).

The spectrum of the solid phase of the freeze-dried glucose-glycine-birnessite system (Figure 3.4.2 d) has already been examined in Section 3.1 and is only briefly described here. Bands at 725 and 860 $cm^{-1}$ are assigned to Mn-O interactions or carbohydrate ring stretch (Table 3.4.5). Bands at 1077, 1410, 1456, 1588, 2925 and 3376 $cm^{-1}$ are assigned to organic components i.e., carbohydrate, aromatic C=C, carboxylate, aliphatic $-CH_2$, and hydroxyl (Table 3.4.5). The birnessite peak at 524 $cm^{-1}$ is absent in the FTIR spectrum though XANES indicates the presence of substantial amounts of Mn(IV).

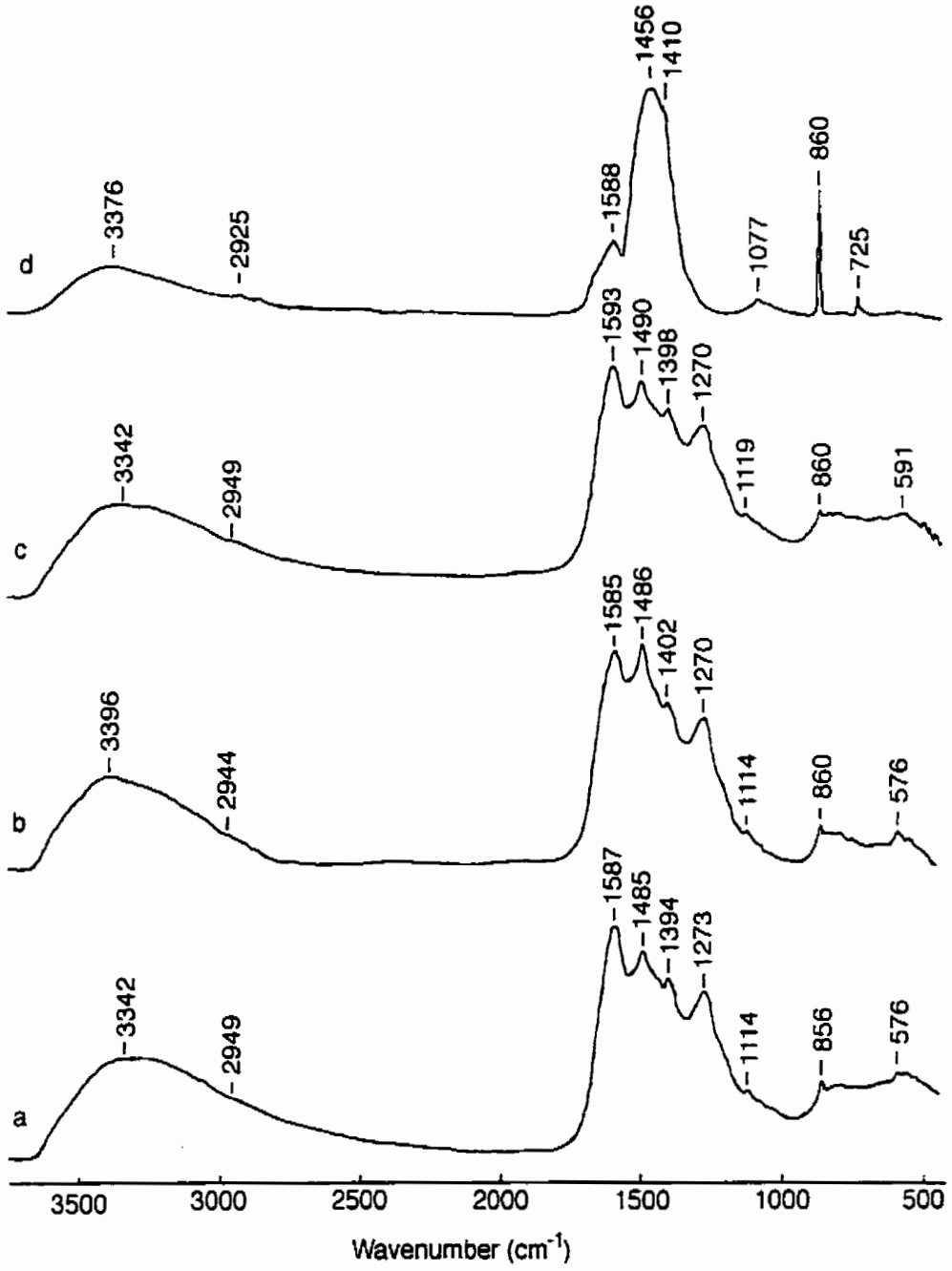


**Figure 3.4.2** FTIR spectra of (a) glucose-glycine-catechol-birnessite following reaction at 25°C for 60 days; (b) glycine-catechol-birnessite, (c) glucose-glycine-catechol-birnessite, and (d) glucose-glycine-birnessite all following reaction at 45°C for 15 days. All had the initial pH of 7.00.

**Table 3.4.5** Assignations of FTIR absorption bands of the solid phase of the systems with the initial pH of 7.00: (a) glucose-glycine-catechol-birnessite following reaction at 25°C for 60 days: (b) glycine-catechol-birnessite, (c) glucose-glycine-catechol-birnessite, and (d) glucose-glycine-birnessite all following reaction at 45°C for 15 days[†]

| (a) glucose-glycine-catechol-birnessite (25°C) | | (b) glycine-catechol-birnessite (45°C) | | (c) glucose-glycine-catechol-birnessite (45°C) | | (d) Glucose-glycine-birnessite (45°C) | |
|---|---|---|---|---|---|---|---|
| Wavenumber ($cm^{-1}$) | Relative Intensity | Wavenumber ($cm^{-1}$) | Relative Intensity | Wavenumber ($cm^{-1}$) | Relative Intensity | Wavenumber ($cm^{-1}$) | Relative Intensity |
| 576 (Mn-O interactions and/or phenolic C-OH) | Weak | 576 (Mn-O interactions and/or phenolic C-OH) | Broad | 591 (Mn-O interactions and/or phenolic C-OH) | Weak | 725 (Mn-O interactions or carbohydrate ring stretch) | Weak |
| 860 (Mn-O interactions or carbohydrate ring stretch) | Weak | 860 (Mn-O interactions or carbohydrate ring stretch) | Weak | 860 (Mn-O interactions or carbohydrate ring stretch) | Weak | 860 (Mn-O interactions or carbohydrate ring stretch) | Intense, sharp |
| 1114 (C-O stretch of COH and COC) | Weak | 1114 (C-O stretch of COH and COC) | Weak | 1119 (C-O stretch of COH and COC) | Weak | 1077 (aliphatic C-C stretch or OH of poly-saccharide) | Broad, moderate |
| 1273 (phenolic OH and C-O) | Strong | 1270 (phenolic OH and C-O) | Strong | 1270 (phenolic OH and C-O) | Strong | 1410 (sym – $COO^-$ stretch) | Shoulder |
| 1394 (sym. $COO^-$ stretch) | Strong | 1402 (sym. $COO^-$ stretch) | Strong | 1398 (sym. $COO^-$ stretch) | Strong | 1456 (-CH bending of $CH_2$) | Strong |
| 1485 (sym. $NH_3$ deformation) | Strong | 1486 (sym. $NH_3$ deformation) | Strong | 1490 (sym. $NH_3$ deformation) | Strong | 1588 (Aromatic C=C and/or asym $-COO^-$ stretch) | Strong |
| 1587 (Aromatic C=C and/or asym. $COO^-$ stretch) | Strong | 1585 (Aromatic C=C and/or asym. $COO^-$ stretch) | Strong | 1593 (Aromatic C=C and/or asym. $COO^-$ stretch) | Strong | 2925 ($-CH_2-$ sym. stretch) | Weak |
| 2949 ($-CH_2-$ sym. stretch) | Weak | 2944 ($-CH_2-$ sym. stretch) | Weak | 2949 ($-CH_2-$ sym. stretch) | Weak | 3376 (stretching vibration of H-bonded OH) | Broad, strong |
| 3342 (stretching vibration of H-bonded OH) | Broad, strong | 3396 (stretching vibration of H-bonded OH) | Broad, strong | 3342 (stretching vibration of H-bonded OH) | Broad, strong | | |

[†] The assignations are based on Rubinsztain et al. (1986a, b); Colthup et al. (1990) and Wang and Huang (1992).

FTIR analysis was also performed on humic acid extracted from (a) the supernatant of the glycine-catechol-birnessite system and (b) the supernatant of the glucose-glycine-catechol-birnessite system, and on (c) humic and (d) fulvic acids extracted from the supernatant of glucose-glycine-birnessite system. All systems had an initial pH of 7.00 and were heated at 45°C for 15 days. The results are shown in Figure 3.4.3. and Table 3.4.6.

Humic acid (Figure 3.4.3 a) extracted from the supernatant of the glycine-catechol-birnessite system had bands at 1206 (C-O) stretch, 1284 (aromatic C=C), 1373 (aliphatic C-H), 1437 (aromatic C=C), 1501 (sym- $NH_3$ and/or aromatic C=C), 1601 (aromatic C=C), 1706 (carbonyl of carboxyl) and 3213 $cm^{-1}$ (H-bonded OH).

Humic acid (Figure 3.4.3 b) extracted from the supernatant of the glucose-glycine-catechol-birnessite system had bands at 1276 (aromatic C=C), 1384 (aliphatic C-H or $COO^-$ overlap), 1457 (-$CH_2$ probably overlapped with aromatic C=C), 1514 and 1600 (aromatic C=C), 1717 and 3382 (H-bonded OH).

Humic acid (Figure 3.4.3 c) extracted from the supernatant of the glucose-glycine-birnessite system had bands at 1090 (-OH of polysaccharide), 1269 (aromatic C=C), 1354 (aliphatic C-H), 1523 (heterocyclic or aromatic C=C), 1623 (carbonyl), 1725 (carbonyl of carboxyl) and 3423 $cm^{-1}$(H-bonded OH).

Fulvic acid (Figure 3.4.3 d) extracted from the supernatant of the glucose-glycine-birnessite system had bands at 1044 (-C-O stretch of hydrated polyols and polysaccharides), 1210 and 1402 $cm^{-1}$ (carboxyl groups), 1649 (amide or quinone structures probably overlapped by carboxyl groups), 1722 (carbonyl of carboxyl), 2615 ($NH_3^+$ stretch), and 2930 $cm^{-1}$ (-$CH_2$- groups). There is a strong, very broad band stretching from <3200 $cm^{-1}$ to >3600 $cm^{-1}$ which is caused by H-bonded OH.

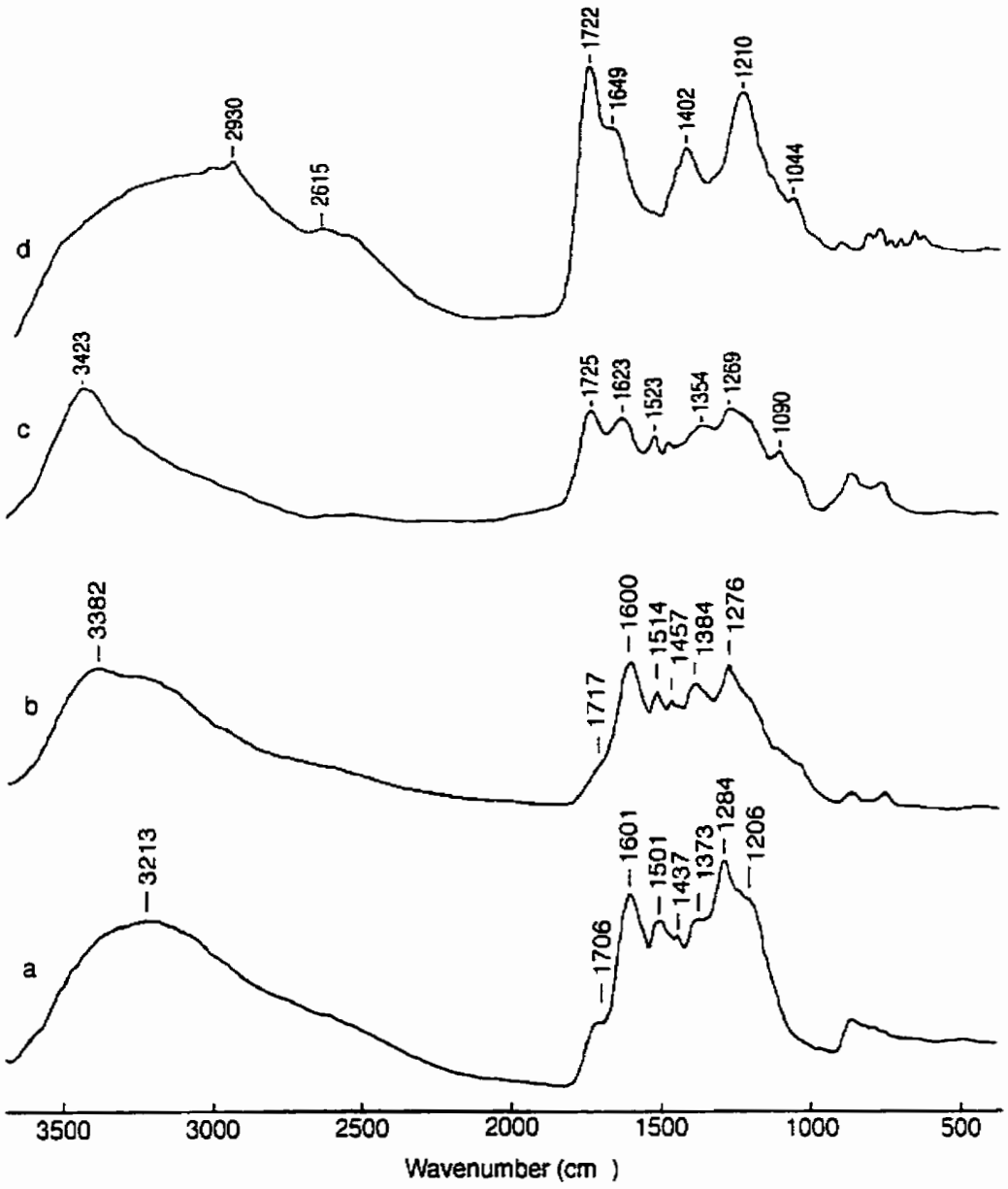


**Figure 3.4.3** FTIR spectra of humic substances: (a) glycine-catechol-birnessite humic acid, (b) glucose-glycine-catechol-birnessite humic acid, (c) glucose-glycine-birnessite humic acid, and (d) glucose-glycine-birnessite fulvic acid. All humic substances were prepared from systems with the initially adjusted pH of 7.00 which were reacted at 45°C for 15 days.

**Table 3.4.6** Assignations of FTIR absorption bands of humic substances: (a) glycine-catechol-birnessite humic acid, (b) glucose-glycine-catechol-birnessite humic acid, (c) glucose-glycine-birnessite humic acid, and (d) glucose-glycine-birnessite fulvic acid†

| (a) glycine-catechol-birnessite humic acid | | (b) glucose-glycine-catechol-birnessite humic acid | | (c) glucose-glycine-birnessite humic acid | | (d) glucose-glycine-birnessite fulvic acid | |
|---|---|---|---|---|---|---|---|
| Wavenumber ($cm^{-1}$) | Relative Intensity | Wavenumber ($cm^{-1}$) | Relative Intensity | Wavenumber ($cm^{-1}$) | Relative Intensity | Wavenumber ($cm^{-1}$) | Relative Intensity |
| 1206 (C-O stretch) | Shoulder | 1276 (aromatic C=C ring stretch) | Strong | 1090 (-OH of polysaccharide) | Moderate | 1044 (-C-O- stretch for hydrated polyols and carbohydrate) | Moderate |
| 1284 (aromatic C=C) | Strong | 1384 (aliphatic C-H or $COO^-$ sym- stretch) | Moderate | 1269 (aromatic C=C) | Strong | 1210 (C-O stretch and OH bend of COOH) | Strong |
| 1373 (aliphatic C-H) | Shoulder | 1457 (-$CH_2$ bend overlapped with C=C ring stretch) | Weak | 1354 (aliphatic C-H) | Moderate | 1402 (sym. $COO^-$ stretch or C-H) | Moderate |
| 1437 (aromatic C=C) | Weak | 1514 (aromatic C=C stretch) | Weak | 1523 (heterocyclic C=C) | Weak | 1649 (amide I or quinone, or COOH antisym- stretch) | Shoulder |
| 1501 (sym- $NH_3$ or aromatic C=C) | Moderate | 1600 (aromatic ring C=C stretch) | Strong | 1623 (C=O) | Strong | 1722 (C=O of COOH) | Strong |
| 1601 (aromatic ring C=C stretch) | Strong | 1717 (C=O of COOH) | Shoulder | 1725 (C=O of COOH) | Strong | 2615 ($NH_3^+$ stretch and carboxyl) | Broad |
| 1706 (C=O of COOH) | Shoulder | 3382 (stretching vibration of H-bonded OH) | Broad, strong | 3423 (stretching vibration of H-bonded OH) | Broad, strong | 2930 (-$CH_2$- sym stretch) | Weak |
| 3213 (stretching vibration of H-bonded OH) | Broad, strong | | | | | 3200 – 3600 (stretching vibration of H-bonded OH) | Broad, strong |

† All humic substances were prepared from systems with initial adjusted pH of 7.00 following reaction at 45°C for 15 days. The assignations are based on MacCarthy and Rice (1985), Rubinsztain et al. (1986a, b) Lobartini and Tan (1988), Colthup et al. (1990), Wang and Huang (1992), and Arfaioli et al. (1999).

### 3.4.3.5 $^{13}C$ Cross polarization magic angle spinning nuclear magnetic resonance spectroscopy

**Fulvic acid isolated from the supernatant of the glucose-glycine-birnessite system**

$^{13}C$ CPMAS NMR spectroscopic analysis was performed on FA obtained from the glucose-glycine-birnessite system. The data obtained are shown in Figure 3.4.4 and Tables 3.4.7 and 3.4.8.

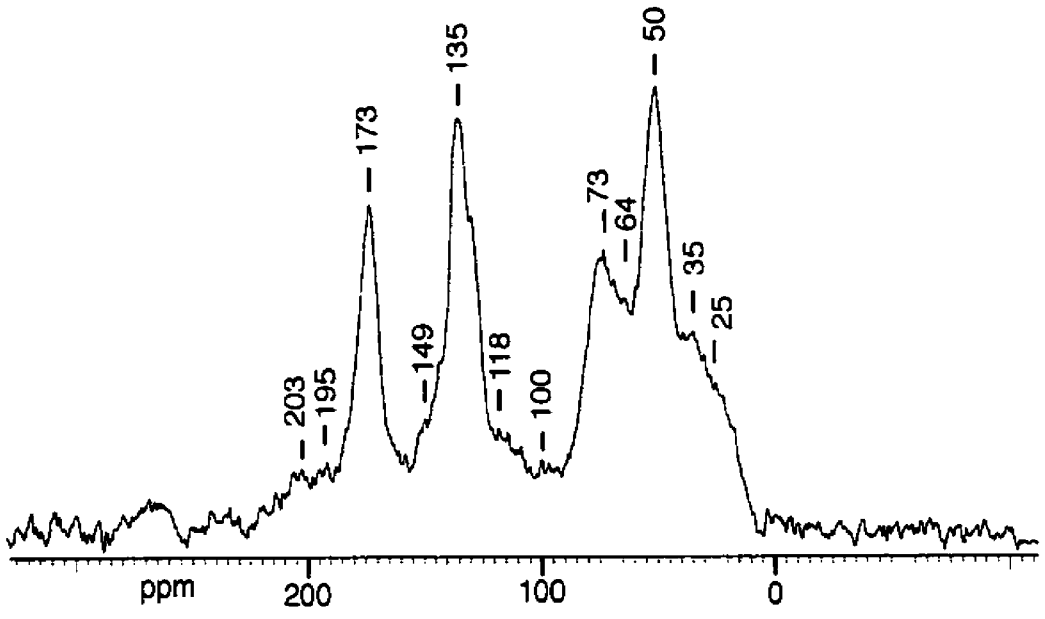


**Figure 3.4.4** $^{13}C$ CPMAS NMR spectrum of FA extracted from the supernatant of the glucose-glycine-birnessite system at an initial pH of 7.00 and at 45°C for 15 days. The peak assignations and areas are given in Tables 3.4.7 and 3.4.8.

The peak shoulders at 25 and 35 ppm (Figure 3.4.4) arise from predominantly $CH_2$ and CH carbons. Quaternary carbon may also be found in the spectral region below 50 ppm. Oxygen and nitrogen substituted carbon atoms resonate between 50 and 105 ppm (Ikan et al., 1986). In this region are found carbohydrate, ether, oxygenated heterocyclic and methoxyl and ethoxyl carbons. An intense peak with maximum at 50 ppm probably arises from aliphatic ester and methoxyl and/or ethoxyl carbon. The signals at 64 and 73 ppm are ascribed to carbohydrate structures. Acetal or ketal carbon (from carbohydrates) gives rise to the signal at 100 ppm. The total aromatic content of the glucose-glycine-birnessite FA is approximately 27% (Table 3.4.8), which is high considering that the starting materials were simple aliphatic molecules. The strong resonance signal in the aromatic region with the peak maximum at 135 ppm is attributed to polymeric carbons that form the core of the melanoidin molecule. The structures responsible for the signal have been postulated to be alkenic moieties conjugated with furanoid or aromatic rings (Benzing-Purdie et al., 1985). Alternatively, the signals in the region 110-160 ppm could arise from heterocyclic moieties known to be formed in the Maillard reaction. Under alkaline conditions, and in the presence of amino acids, sugars enolize and form active molecules such as amino reductones and methylglyoxal. (Wolfrom et al., 1947; Hodge, 1953). These compounds, together with molecules such as furfuryl alcohol and hydroxylcyclopentenones may polymerize in mildly alkaline environments (Hodge, 1953; Chuang et al., 1984). Gillam and Wilson (1985) reported that the $^{13}C$ CPMAS NMR spectra of marine coastal humic substances had the major peak in the aromatic region centred at 135-136 ppm. The FA formed in the presence of birnessite also exhibits two weak signals at 195 and 203 ppm indicating the presence of ketonic or acetal carbonyl carbon.

**Table 3.4.7** $^{13}C$ CPMAS NMR signal assignations for the FA obtained from the glucose-glycine-birnessite system†

| Assignation | ppm |
|---|---|
| Methylene and/or methine carbon in alkyl chains | 25 |
| Methylene and methine carbon in alkyl chains | 35 |
| Aliphatic esters and ethers, methoxyl and ethoxyl, carbon bonded to amino groups | 50 |
| $CH_2OH$, e.g. $C_6$ in carbohydrates; ether bonded aliphatic carbon | 64 |
| CHOH, e.g. ring carbon ($C_2$-$C_5$) of polysaccharides | 73 |
| Carbon singly bonded to two oxygen atoms e.g., acetal or ketal carbon in carbohydrates | 100 |
| Aromatic carbon ortho to oxygen substituted aromatic carbon and protonated aromatic carbon | 118 |
| Unsubstituted and alkyl substituted aromatic carbon also alkenic carbon | 135 |
| Mainly phenols also aromatic amines | 149 |
| Mostly carboxyl carbon, also some ester and amide carbon. | 173 |
| Carbonyl carbon (from aldehydes and ketones) | 195 |
| Carbonyl carbon (from aldehydes and ketones) | 203 |

†Peak assignations were based on Choudhry and Webster (1989), Malcolm (1989, 1990), and Rasyid et al. (1992).

**Table 3.4.8** Relative integrated intensity of $^{13}C$ CPMAS NMR spectral regions expressed as a percentage of the total intensity for the FA obtained from the glucose-glycine-birnessite system

| Ranges in ppm | Percentage area | Structural assignment |
|---|---|---|
| 0-47 | 18 | Aliphatic (alkyl) structures – C, CH, $CH_2$, $CH_3$ |
| 48-62 | 16 | Methoxyl, ethoxyl |
| 63-96 | 19 | Alkyl-O (carbohydrates, alcohols) |
| 97-105 | 2 | Acetal and ketal carbon (carbohydrates) |
| 106-139 | 20 | Aryl-H and aryl-C carbons |
| 140-158 | 7 | Aryl-O and aryl-N carbons including phenols and aromatic amines |
| 159-190 | 14 | Carboxyl and amide carbon |
| 191-220 | 4 | Aldehyde and ketone carbon |

The $^{13}C$ CPMAS NMR spectrum of the FA (Figure 3.4.4) is compared with a sample of melanoidin prepared by Hayase et al. (1986), from glucose and glycine alone(heating at 95°C for 26 h) (Figure 3.4.5). It can be seen that the two spectra (Figures 3.4.4 and 3.4.5) have some qualitative similarities, i.e., both have signals in the regions of approximately 10 to 50 (aliphatic C), 60 to 75 (carbohydrate C), 100 to 105 (carbohydrate C), 130 to 140 (aromatic C), 170 to 180 (carboxyl C) and 190 to 205 (carbonyl C) ppm. However the melanoidin (Figure 3.4.4) prepared from glucose and glycine (at 45°C for 15 d) in the presence of birnessite does not have a strong peak at approximately 200 ppm as is the case with melanoidin prepared (at 95°C for 26 h) by Hayase et al. (1986). The $^{13}C$ NMR spectrum of the FA prepared from glucose and glycine in the presence of birnessite (Figure 3.4.4) is basically similar to $^{13}C$ NMR spectra of naturally occurring humic substances which themselves exhibit a wide variation in spectral characteristics (Malcolm, 1989).

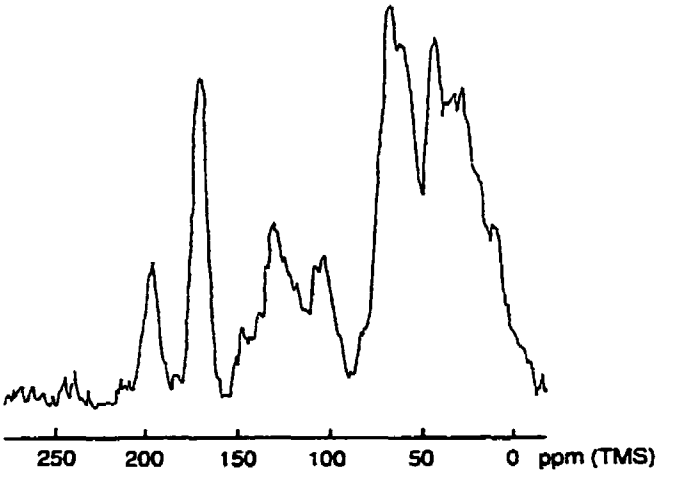


**Figure 3.4.5** $^{13}C$ CPMAS NMR spectrum of D-glucose-glycine system melanoidin prepared by heating a solution (adjusted pH 6.8) containing 1M glucose and 1M glycine at 95°C for 26 h (Hayase et al., 1986).

**Humic acid isolated from the supernatant of the glycine-catechol-birnessite system**

The spectrum is shown in Figure 3.4.6. Peak assignations are shown in Table 3.4.9. The spectrum can be divided into three parts: (1) <100 ppm, (2) 110-160 ppm, and (3) >160 ppm. The signals at 47 ppm probably arise from amino acid carbon or from aliphatic esters or methoxyl groups. The signal at 60 ppm which corresponds to the carbon in $CH_2OH$ groups, i.e., polysaccharide carbon indicates that birnessite promotes the ring cleavage of catechol and the formation of carbohydrate moieties. Signals in the region of 110-160 ppm arise from aromatic ring carbon (119 ppm) and from phenolic carbon (145 ppm) in the polycondensate (Figure 3.4.6). The signals at 166 and 173 ppm are ascribed to carboxyl groups from glycine which are incorporated into the polycondensate and also from the ring cleavage of catechol by the action of birnessite.

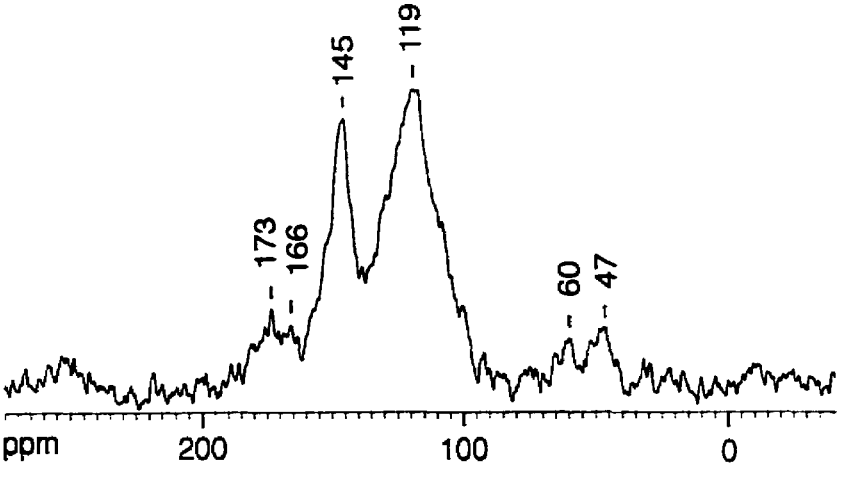


**Figure 3.4.6** $^{13}C$ CPMAS NMR spectrum of HA extracted from the supernatant of the glycine-catechol-birnessite system at an initial pH of 7.00 and heating 45°C for 15 days. The signal assignations are given in Table 3.4.9.

The data indicate that birnessite promoted the polycondensation reaction between catechol and glycine leading to the formation of high molecular weight products as postulated by Wang and Huang (1987a) and illustrated in Figure 3.4.7.

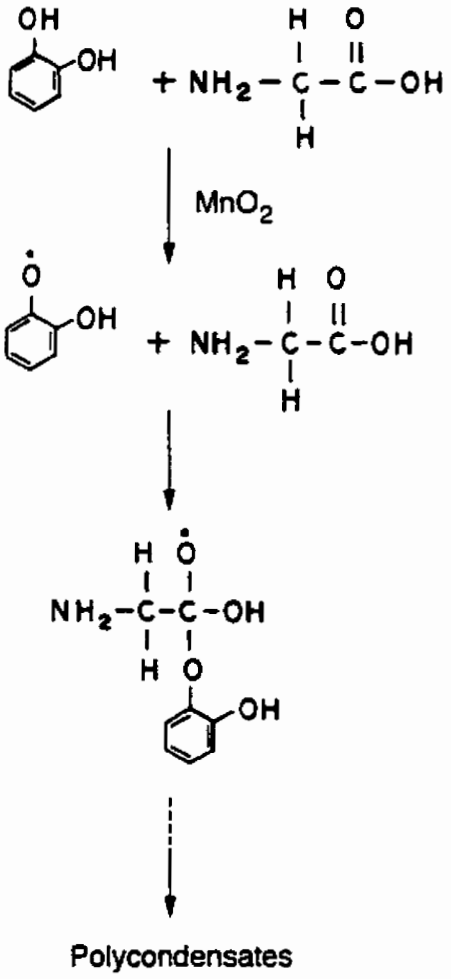


**Figure 3.4.7** Reaction of catechol-derived free radicals with glycine (adapted from Wang and Huang, 1987a).

**Table 3.4.9** $^{13}C$ CPMAS NMR signal assignations for HA obtained from the glycine-catechol-birnessite system†

| Assignation | ppm |
|---|---|
| Aliphatic esters and ethers, methoxyl and ethoxyl, amino acid carbon, α-carbon in aliphatic acids | 47 |
| $CH_2OH$, e.g. $C_6$ in carbohydrates; ether bonded aliphatic carbon | 60 |
| Aromatic carbon ortho to oxygen substituted aromatic carbon and protonated aromatic carbon | 119 |
| Mainly phenols also aromatic amines | 149 |
| Mostly carboxyl carbon, also some ester and amide carbon | 166 |
| Mostly carboxyl carbon, also some ester and amide carbon | 173 |

†Peak assignations were based on Choudhry and Webster (1989), Malcolm (1989, 1990), Rasyid et al. (1992).

### 3.4.3.6 $^{14}C$ tracer analysis

The presence of birnessite in the UL $^{14}C$-labelled glucose-glycine system markedly increased the evolution of $^{14}CO_2$ (Table 3.4.10). In the glucose-glycine system, 14.0 Bq of $^{14}CO_2$ were released whereas 28.3 Bq were released when birnessite was present. Similarly, in the glucose-glycine-catechol system 22.4 Bq of $^{14}CO_2$ was released and the addition of birnessite to the system resulted in the release of 38.8 Bq of $^{14}CO_2$. The increase in $^{14}CO_2$ release in the presence of birnessite is evidently caused by the enhanced cleavage of the $^{14}C$-UL-glucose. In addition, the birnessite may have also decarboxylated oxidation products of glucose such as gluconic and glucuronic acids. The data also show that catechol enhanced the cleavage of the $^{14}C$-UL-glucose both in the presence and absence of birnessite.

**Table 3.4.10** The release of $^{14}CO_2$ from the glucose-glycine, glucose-glycine-birnessite, glucose-glycine-catechol, and glucose-glycine-catechol-birnessite systems at 45°C for the period 15 days

| Reaction conditions | | | | $^{14}CO_2$ released |
|---|---|---|---|---|
| Glucose | Glycine | Catechol | Birnessite | Bq |
| +[†] | + | + | + | 38.8 |
| + | + | -[‡] | + | 28.3 |
| + | + | + | - | 22.4 |
| + | + | - | - | 14.0 |

[†] - Presence

[‡] - Absence

# 4. General Discussion and Conclusions

Transformations of natural and anthropogenic organic compounds by abiotic catalytic reactions are extremely significant and more common than previously believed in soil and related environments. These reactions are heterogeneously catalysed by various clay minerals and metal oxides and also by dissolved metals and include the formation of organo-mineral complexes, and nutrient and toxic substance release and retention (Wang et al., 1986; Huang, 1990, 2000). Birnessite, a tetravalent manganese oxide common in soils and sediments (McKenzie, 1989) is highly effective in promoting the oxidative polymerization of phenolic compounds (Shindo and Huang, 1982, 1984a) and the polycondensation of phenolic compounds such as hydroquinone and pyrogallol with amino acids (Shindo and Huang, 1984b; Wang and Huang, 1987a).

The Maillard reaction was initially proposed by Maillard (1912, 1913) who investigated the formation of yellow-brown to dark-brown "pigments" or melanoidins upon refluxing solutions of glucose and lysine together. Since then, evidence provided by spectroscopic (IR, UV, $^{13}$C-CPMAS NMR, ESR), chromatographic (GC and GC/MS), thermogravimetric, pyrolytic (Curie point), oxidative ($KMNO_4$) and isotopic methods, has accumulated which suggests that melanoidins synthesized in the laboratory are similar to natural humic substances (Ikan et al., 1992; Ikan et al., 1996). Evershed et al. (1997) have recently detected the presence of Maillard reaction products in decayed plant materials from an archaeological site dating from ancient Egypt. Therefore it is probable that the Maillard reaction between sugars and amino acids plays a significant

role in the formation of humic substances in soils and aquatic environments. However, there are significant gaps in knowledge since the catalytic role of minerals common in nature in the Maillard reaction and the resultant formation of humic substances in nature are little understood.

Visible absorption spectroscopy of supernatants (Tables 3.1.1, 3.1.2, Figure 3.1.1), and FTIR spectroscopy (Table 3.1.4 and Figure 3.1.8) revealed that birnessite, a mineral common in natural environments, is a powerful catalyst in the Maillard reaction between glucose and glycine at room temperature (25°C) and at 45°C, a surficial soil temperature widely encountered in tropical and subtropical regions, and even in temperate regions during the summer months. Further, visible absorption spectroscopy of supernatants, Table 3.1.1, shows that birnessite exerted a catalytic effect on transformations of glucose alone and of glycine alone. The Mn(IV) in birnessite was reduced to Mn(II) and, therefore, there must be the concomitant oxidation of the organic compounds. (EPR spectroscopy: Figures 3.1.2 - 3.1.5; XANES spectroscopy: Table 3.1.5 and Figure 3.1.10). The above effects are most pronounced in the glucose-glycine-birnessite system. The increased degree of browning in the glucose-glycine-birnessite system compared to the glucose-glycine system containing no Mn(IV) oxide is attributed to three simultaneously occurring processes:

(a) The birnessite acts as a Lewis acid which accepts electrons from glucose and probably oxidizes it to D-gluconic acid initially. Then, decarboxylation with loss of carbon dioxide occurs and/or there is further oxidation and formation of, e.g., α-dicarbonyl compounds as postulated by the scheme in Figure 4.1. The evidence from FTIR and XANES spectroscopy, Figures 3.1.8 and 3.1.10 respectively, indicates that

a complex polycondensation process involving glycine apparently proceeds on the surface of birnessite with the formation of coloured Maillard reaction products.

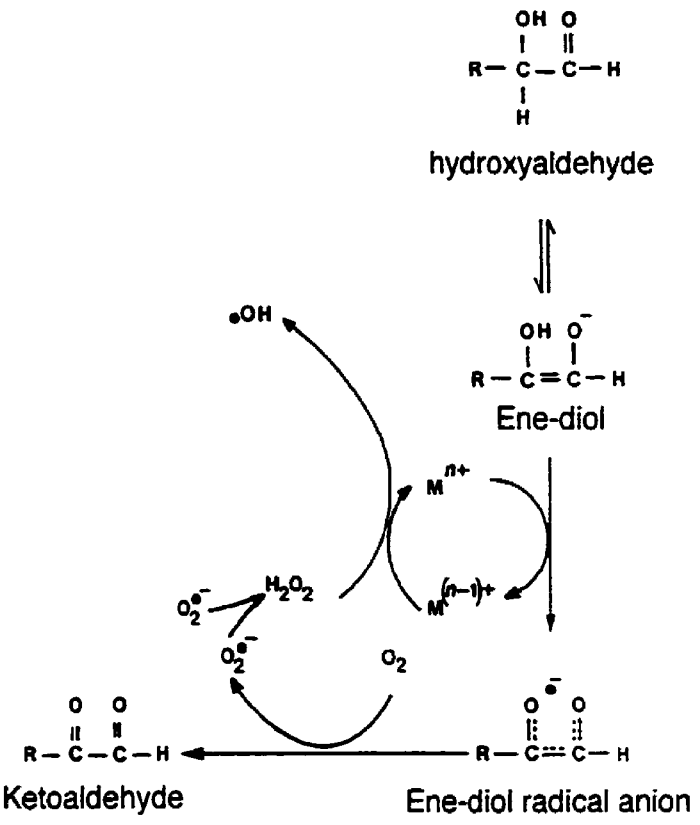


**Figure 4.1** Glucose can enolize and reduce transition metal thereby generating superoxide free radical ($O_2^{\bullet-}$), hydrogen peroxide ($H_2O_2$) and the hydroxyl radical (•OH) and forming dicarbonyl compounds (Wolff, 1996).

(b) The polycondensation is accelerated by an increase in pH as a result of the reduction of Mn(IV) to Mn(II): $MnO_2 + 4H^+ + 2e^- \leftrightarrow Mn^{2+} + 2H_2O$

Hedges (1978) found that for a range of amino acids in the Maillard reaction, the rate of polycondensate formation increased with increasing pH. He also noted that glucose polymerized with itself at an appreciable rate at pH 8 or higher, and

believed that at this pH a significant amount of the polycondensate formed could result from glucose-glucose condensations. A possible pathway (Figure 2.20. page 59) for the formation of aromatic compounds from carbohydrates was proposed by Popoff and Theander (1976).

(c) The Mn(II) that is formed may also catalyze the polycondensation reaction between glucose and glycine.

The dicarbonyl compound formed in the scheme in Figure 4.1 could then react with the amino acid present, undergoing the Strecker degradation reaction, leading to the formation of heterocyclics (Figure 4.2). These compounds could undergo further reaction and be incorporated into the core polymer structure of melanoidin. The Strecker degradation itself is an essential part of the Maillard reaction (Wong and Shibamoto, 1996).

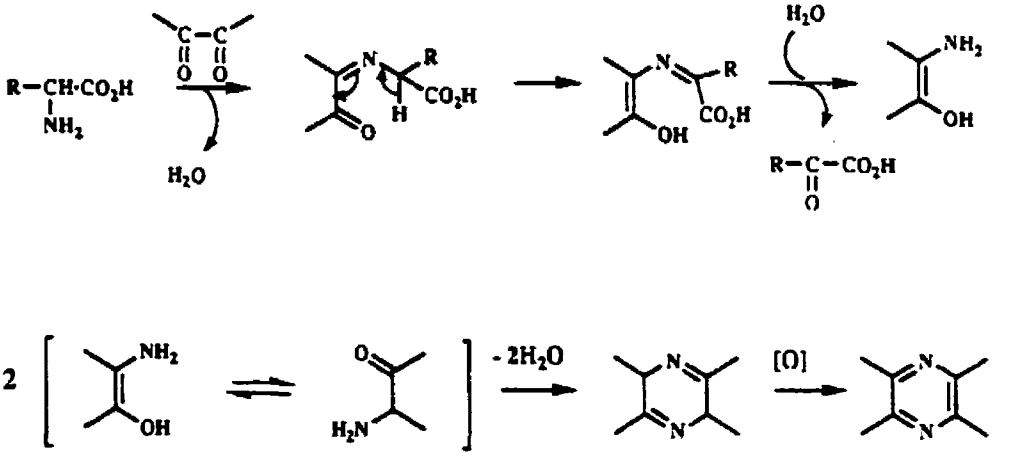


**Figure 4.2** Strecker degradation of amino acids and α-dicarbonyls to form heterocyclic compounds. For glycine, R = H (Wong and Shibamoto, 1996).

In addition to high molecular weight polycondensates, lower molecular weight polycondensation products that incorporate Mn(II) could also be formed. O'Brien and Morrisey (1997) suggested that fructosylglycine (FG) may complex zinc and probably copper and suggested a stepwise scheme for their formation. In a similar manner. Mn(II) might also form complexes with fructosylglycine and the possible structures of such complexes are shown in Figure 4.3.

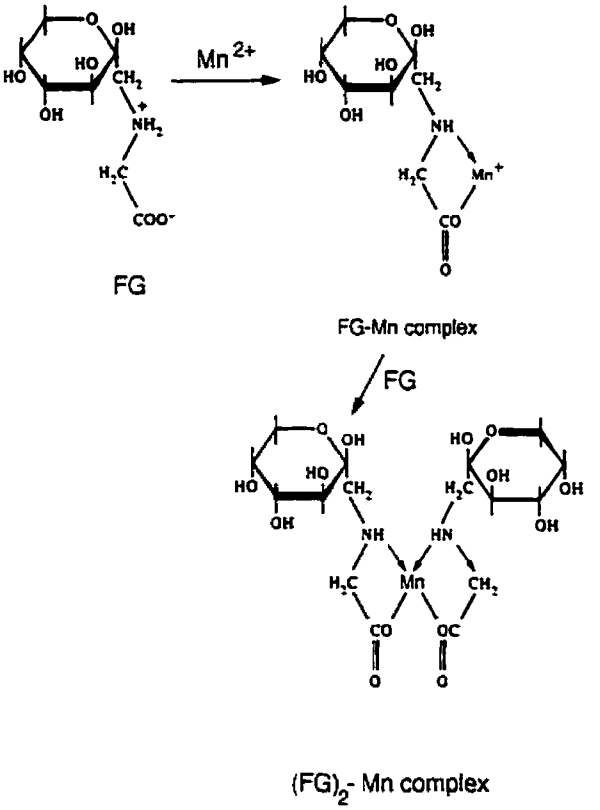


**Figure 4.3** Proposed stepwise formation of low molecular weight complexes between the Amadori compound fructosylglycine (FG) and divalent manganese. Adapted from O'Brien and Morrissey (1997) who considered divalent zinc. copper. calcium and magnesium in their model.

The data reveals that birnessite is a powerful catalyst in the Maillard reaction promoting polycondensation/browning processes between glucose and glycine at room temperature and at 45°C, which is the approximate temperature of the soil surface on a day when the ambient air temperature is 25°C (Baver, 1956), and therefore is a surficial soil temperature frequently encountered in tropical and subtropical areas, and even in temperate areas during the summer months.

Photoreduction of Mn oxides by marine fulvic acid, was first observed by Sunda et al. (1983) and Stone and Morgan (1984) noted that dissolution of Mn oxides by a marine fulvic acid increased significantly upon exposure to strong illumination. Lee and Huang (1995) studied the photochemical effect on the abiotic transformations of polyphenolics as catalyzed by Mn(IV) oxide. However, the effect of light in promoting birnessite catalysis of the Maillard reaction is unknown. In this research, light was found to significantly promote browning in the glucose-glycine-birnessite system. Evidence is provided by visible absorption spectroscopy (Tables 3.2.1, 3.2.2 and Figures 3.2.1, 3.2.2), EPR spectroscopy (Figure 3.2.3), FTIR absorption spectroscopy (Table 3.2.3 and Figure 3.2.4), and XANES spectroscopy (Figure 3.2.5). Further, the catalytic effect of birnessite on the Maillard reaction is still evident even under conditions of complete darkness and therefore, this heterogeneous catalysis may occur at any depth in soil and related environments. The catalytic role of birnessite in the Maillard reaction in soil and aquatic environments and the resultant abiotic formation of refractory humic substances from labile organic compounds in nature merits close attention.

Molecular Iso-Density Contours (MIDCO's), which are electron density contour faces where along each surface the electron density is constant, were constructed for glucose, glycine and the Amadori compound fructosylglycine (Figure 3.3.2). Molecular

topological analysis was performed using the molecular modelling program Gaussian 92 in an attempt to observe what occurred when the distance between the molecules of glucose and glycine was altered and how this change influenced the internal coordinates of the atoms in the Amadori compound and the mutual orientation of the two constituent molecules (glucose and glycine) (Figure 3.3.3). The structure of the Amadori compound was optimized at a quantum mechanical level and its ground state electron energy was calculated (Table 3.3.1 and Figure 3.3.4). The results indicate that the potential energy barrier will be high (Figure 3.3.4) and therefore the reaction between glucose and glycine alone to form FG is very slow at room temperature.

Polyphenols present in terrestrial and aquatic environments are regarded as important precursors in the formation of humic substances via processes of oxidative polymerization which take place in soils and sediments (Huang, 1990, 2000). The role of polyphenols in influencing condensation processes between sugars and amino acids and the catalytic effect of birnessite on such polyphenol-sugar-amino acid ternary systems as would apparently occur in soils and related environments is, however, not known.

The data obtained in the present study show that in the presence of catechol, the accelerating effect of birnessite on the polymerization and polycondensation in the glucose-glycine-catechol ternary system is even more dramatic. Further, glucose apparently perturbed polymerization of catechol and polycondensation of glycine-catechol by birnessite. Evidence for these statements is provided by visible absorption spectroscopy and related analyses: Tables 3.4.1 - 3.4.4; XANES spectroscopy: Figure 3.4.1; and FTIR absorption spectroscopy: Table 3.4.5 and Figure 3.4.2. Humic substances from the glucose-glycine-birnessite, glucose-glycine-catechol-birnessite and glycine-catechol-birnessite systems were extracted, separated and analyzed by FTIR absorption

spectroscopy (Table 3.4.6. and Figure 3.4.3) and $^{13}C$ CPMAS NMR spectroscopy (Tables 3.4.7 - 3.4.9 and Figures 3.4.4 and 3.4.6). The fulvic acid formed from glucose and glycine in the presence of birnessite was isolated and found to contain aromatic structures (Figure 3.4.4). The $^{13}C$ NMR spectrum of the fulvic acid (Figure 3.4.4) is basically similar to $^{13}C$ NMR spectra of naturally occurring humic substances isolated from soil and sediment environments (Malcolm. 1989). The release of $^{14}CO_2$ was greatest in the glucose-glycine and glucose-glycine-catechol systems which contained birnessite (Table 3.4.10). This is evidently due to the birnessite-induced cleavage of glucose and the resultant release of $^{14}CO_2$.

In summary. this study reveals that birnessite is a powerful catalyst in the Maillard reaction promoting polycondensation processes between glucose and glycine and therefore merits attention as an important abiotic pathway for the formation of humic substances in soil and aquatic environments. Further. the evidence that birnessite exerts a significant catalytic role in the glucose-glycine-catechol-birnessite ternary system points to a linking of the polyphenol and Maillard reaction pathways into an integrated pathway – a significant advancement in the understanding of natural humification processes in soils.

# 5. REFERENCES


Achard, F.K. 1786. Chemische untersuchungen des torfs. Crell's *Chem. Ann.* **2**:391-403.

Aiken, G.R., D.M. McKnight, R.L. Wershaw and P. MacCarthy. 1985. An introduction to humic substances in soil, sediment and water. p. 1- 9. In: G.R. Aiken, D.M. McKnight, R.L. Wershaw and P. MacCarthy (eds.) Humic Substances in Soil, Sediment and Water - Geochemistry, Isolation and Characterization. John Wiley and Sons, New York, NY.

Allison, F.E. 1973. Soil Organic Matter and Its Role in Crop Production. Elsevier Scientific Publishing, Amsterdam.

Amberger, A., and K. Vilsmeier. 1978. Anorganisch-katalytische Umsetzungen von Cyanamid und dessen Metaboliten in Quarzsand I. Mechansimus des Cyanamidabbaues unter dem Einflu$\beta$ von Eisenoxiden und Feuchtigkeit. *Z. Pflanzenernaehr. Bodenkd.* **141**:665-676.

Andreux, F., M. Schiavon, C. Munier-Lamy, M. Mansour, and I. Scheunert. 1995. Factors affecting the movements, reactions, and biotransformations of xenobiotics. p. 383-408. In: P.M. Huang, J. Berthelin, J-M. Bollag, W.B. McGill, and A.L. Page (eds.) Environmental Impact of Soil Component Interactions: Vol. 1 Natural and Anthropogenic Organics. CRC Lewis Publishers, Boca Raton, FL.

Arfaioli P., O.L. Pantani, M. Bosetto and G.G. Ristori 1999. Influence of clay minerals and exchangeable cations on the formation of humic-like substances (melanoidins) from D-glucose and L-tyrosine. *Clay Miner.* **34**:487-497.

Aue, W.P., D.J. Ruben, and R.G. Griffin. 1981. Two-dimensional rotational spin-echo NMR in solids: resolution of isotropic and anisotropic chemical shifts. *J. Magn. Reson.* **43**:472-476.

Axelson, D.E. 1987. Spinning sideband suppression and quantitative analysis in solid state $^{13}C$ NMR of fossil fuels. *Fuel* **66**:195-199.

Baes, A.U., and P.R. Bloom. 1990. Fulvic acid ultraviolet-visible spectra: Influence of solvent and pH. *Soil Sci. Soc. Am. J.* **54**: 1248-1254.

Baker, M.D., and C.I. Mayfield. 1980. Microbial and non-biological decomposition of chlorophenols and phenol in soil. *Water Air Soil Pollut.* **13**:411-424.

Bardossy, G., and G. Brindley. 1978. Rancieite associated with a karstic bauxite deposit. *Am. Mineral.* **63**:762-767.

Bartlett, J.R. 1986. Soil redox behavior. p. 179-207. In: D.L. Sparks (ed.) Soil Physical Chemistry. CRC Press, Inc., Boca Raton, FL.

Baver, L.D. 1956. Soil Physics. 3rd Edn. John Wiley & Sons, Inc. New York. NY

Becking, L.G.M.B., I.R. Kaplan, and D. Moore. 1960. Limits of the natural environment in terms of pH and oxidation-reduction potentials. *J. Geol.* **68**:243-284.

Bell, R.P. 1941. Acid-base Catalysis. Oxford University Press, Oxford, UK.

Benzing-Purdie, L., J.A. Ripmeester and C.I. Ratcliffe. 1985. Effect of temperature on Maillard reaction products. *J. Agric. Food Chem.* **33**:31-33.

Berzelius, J.J. 1836. Edinburgh New Philosophical Journal. 21:223.

Berzelius, J.J. 1839. Lehrbuch der Chemie. Arnoldische Buchhandlung, Dresden, Leipzig, FRG.

Bloom, P.R., and J.A. Lenheer. 1989. High-energy spectroscopic methods. p. 409-446. In: M.H.B. Hayes, P. MacCarthy, R.L. Malcolm and R.S. Swift (eds.) Humic Substances II. In Search of Structure. Wiley-Interscience, Chichester, UK.

Bollag, J.-M. 1992. Enzymes catalyzing oxidative coupling reactions of pollutants. p. 205-217. In: H. Siegel and A. Siegel (eds.) Metal Ions In Biological Systems. Marcel Dekker, New York, NY.

Bollag, J.-M., J. Dec, and P.M. Huang. 1998. Formation mechanisms of complex organic structures in soil habitats. *Advances in Agronomy*. **63**:237-266.

Bollag, J.-M., C. Meyers, S. Pal, and P.M. Huang. 1995. The role of abiotic and biotic catalysts in the transformation of phenolic compounds. p. 299-310. In: P.M. Huang, J. Berthelin, J-M. Bollag, W.B. McGill, and A.L. Page (eds.) Environmental Impact of Soil Component Interactions: Vol. 1 Natural and Anthropogenic Organics CRC Lewis Publishers, Boca Raton, FL.

Bosetto, M. P.Arfaioli, O.L. Pantani and G.G. Ristori. 1997. Study of the humic-like compounds formed from L-tyrosine on homoionic clays. *Clay Miner*. **32**:341-349.

Boyd, S.A., M.D. Mikesell, and J.-F. Lee. 1989. Chlorophenols in soils. p. 209-228. In: B.L. Sawhney and K. Brown (eds.) Reactions And Movement of Organic Chemicals in Soils. SSSA Spec. Publ. 22. Soil Science Society of America and American Society of Agronomy. Madison, WI.

Brown, S.B. 1980. Ultraviolet and visible spectroscopy. p. 1-15. In: S.B. Brown (ed.) An Introduction to Spectroscopy for Biochemists. Academic Press, New York. NY.

Buffle, J. 1990. The analytical challenge posed by fulvic and humic compounds. *Anal. Chim. Acta* **232:** 1-2.

Burns, R.G., and V.M. Burns. 1977. Mineralogy. p. 185-248. In: G.P. Glasby (ed.) Marine Manganese Deposits. Elsevier, Amsterdam, NL.

Burns, R.G., V.M. Burns, W. Sung, and B.A. Brown. 1974. Ferromanganese mineralogy – Suggested terminology of the principal manganese oxide phases. *Geol. Soc. Am. Ann. Meet. Miami. Abstr.* **6**:1029-1031.

Campbell, I.M. 1988. Catalysis at Surfaces. Chapman and Hall, London, UK.

Chen, C-L., and H.M. Chang, 1985, Chemistry of lignin biodegradation. p. 535-578. In: T. Higuchi (ed.) Biosynthesis and Biodegradation of Wood Components Academic Press, Orlando, FL.

Chen, Y., and T.Aviad. 1990. Effects of humic substances on plant growth. p. 161-186. In: P. MacCarthy, P.R. Bloom, C.E. Clap., and R.L. Malcolm (eds.) Humic Substances in Soil and Crop Sciences – Selected Readings. American Society of Agronomy and Soil Science Society of America. Madison, WI.

Chen, Y., N. Senesi, and M. Schnitzer. 1977. Information provided on humic substances by $E_4/E_6$ ratios. *Soil. Sci. Soc. Am. J.* **41**:352-358.

Cheshire, M.V. 1979. Nature and Origin of Carbohydrates in Soils. Academic Press, New York. NY.

Childs, C.W. 1975. Composiition of iron-manganese concretions from some New Zealand soils. *Geoderma* **13**:141-152.

Choudhry, G.G., and G.R.B. Webster. 1989. Soil organic matter chemistry. Part 1. Characterization of several humic preparations by proton and carbon-13 nuclear magnetic resonance spectroscopy. *Toxicol. Environ. Chem.* **23**:227-242.

Chuang, I.S., G. Maciel and G. Myers. 1984. $^{13}C$ NMR study of curing in furfuryl alcohol resins. *Macromol.* **17**:1087-1090.

Chukhrov F.V., and A.I. Gorshkov. 1981. Iron and manganese oxide minerals in soils. *Trans. R. Soc. Edinburgh: Earth Sci.* **72**:195-200.

Chukhrov F.V., A.I. Gorshkov, E.S. Rudnitskaya, V.V. Berevsoskaya, and A.V. Sivtsov. 1980. Manganese minerals in clays – A review. *Clays Clay Miner.* **28**:346-354.

Collins, M.J., P. Westbroek, G. Muyzer and J.W. de Leeuw. 1992. Experimental evidence for condensation reactions between sugars and proteins in carbonate skeletons. *Geochim. Cosmochim. Acta* **56**:1539-1544.

Colthup, N.B., L.H. Daly, and S.E. Wiberley. 1990. Introduction to Infrared and Raman Spectroscopy. Academic Press Inc. Harcourt Brace Jovanovich, Boston, MA.

Conte, P., and A. Piccolo. 1999. Conformational arrangement of dissolved humic substances. Influence of solution composition on association of humic molecules. *Environ. Sci. Technol.* **33**:1682-1690.

Cook, R.L., and C.H. Langford. 1999. Biogeopolymeric view of humic substances with application to $^{13}C$ NMR. p. 31- 48. In: E.A. Ghabbour and G. Davies (eds.) Understanding Humic Substances – Advanced Methods, Properties and Applications. Royal Society of Chemistry, Cambridge, UK.

Cook, R.L., C.H. Langford, R. Yamdagni and C.M. Preston. 1996. A modified cross-polarization magic angle spinning $^{13}C$ NMR procedure for the study of humic materials. *Anal. Chem.* **68**:3979-3986.

Crerar, D.A., and H.L. Barnes. 1974. Deposition of deep-sea manganese nodules. *Geochim. Cosmochim. Acta.* **38**:279-300.

Crosby, D.G. 1972. Environmental photooxidation of pesticides. 260-278. In: Degradation of Synthetic Organic Molecules in the Biosphere: Natural, Pesticidal, and Various Other Man-made Compounds. National Academy of Sciences, Washington, D.C.

Crosby, D.G. 1979. The significance of light induced pesticide transformations. p. 568-576. In: H. Geissbuhler, G.T. Brooks and P.C. Kearney (eds.) Advances in Pesticide Science. Part 3. Pergamon Press, New York, NY.

Daintith, J. 1990. A Concise Dictionary of Chemistry. New Ed. Oxford University Press. Oxford, UK.

Dandurand, L.-M.C and G.R. Knudsen. 1997. Sampling microbes from the rhizosphere and phyllosphere. p. 391-399. In: C.J. Hurst (ed.-in-chief.) Manual of Environmental Microbiology. Am. Soc. Microbiol., Washington, D.C.

De Kimpe, C.R., and M. Schnitzer. 1990. Low-temperature ashing of humic and fulvic acid. *Soil Sci. Soc. Am. J.* **54**:399-403.

Dec, J., and J.-M. Bollag. 1990. Detoxification of substituted phenols by oxidoreductive enzymes through polymerization reactions. *Arch. Environ. Contamin. Toxicol.* **19**:543-550.

Demolon, A., and G. Barbier. 1929. Conditions de formation et constitution du complexe argilo-humique des sols. *C. R. Acad. Sci. Paris.* **188**:654-662.

Dekker, R.F.H. 1985., Biodegradation of the hemicelluloses. p. 505-533. In: T. Higuchi (ed.) Biosynthesis and Biodegradation of Wood Components. Academic Press. Orlando, FL.

Dixon, W.T. 1981. Spinning-sideband-free NMR. *J. Magn. Reson.* **44**:220-227.

Dixon, W.T., J. Schaefer, M.D. Sefeik, E.O. Stejskal, and R.A. McKay. 1982. Total suppression of sidebands in CPMAS C-13 NMR. *J. Magn. Reson.* **49**:341-345.

Dragunov, C.C., H.H. Zhelokhovtseva, and E.J. Strelkova. 1948. A comparative study of soil and peat humic acids. *Pochvovedenie* **7**: 409-420.

Drits, V.A., E. Silvester, A.I. Gorshkov, and A. Manceau. 1997. Structure of synthetic monoclinic Na-rich birnessite and hexagonal birnessite: I. Results from X-ray diffraction and selected-area electron diffraction. *Am. Mineral.* **82**:946-961.

Engelhardt, G., P.R. Wallnofer, W. Mucke, and G. Renner. 1986. Transformations of pentachlorophenol. *Toxicol. Environ. Chem.* **11**:233-252.

Eriksson, K-E., and T.M. Wood. 1985. Biodegradation of cellulose. p. 469-503. In: T. Higuchi (ed.) Biosynthesis and Biodegradation of Wood Components. Academic Press. Orlando, FL.

Evershed, R.P., H.A. Bland, P.F. van Bergen, J.F. Carter. M.C. Horton, and P.A. Rowley-Conwy. 1997. Volatile compounds in archaeological plant remains and the Maillard reaction during decay of organic matter. *Science* **278**: 432-433.

Filip, Z., and J.J. Alberts. 1993. Formation of humic like substances by fungi epiphytic on *Spartina alterniflora Estuaries* **16**:385-390.

Filip, Z., W. Flaig, and E. Ritz. 1977. Oxidation of some phenolic substances as influenced by clay minerals. *Isot. Radiat. Soil Org. Matter Stud.*, **II**:91-96. *IAEA Bull.* Vienna,.

Flaig, W., 1966. The chemistry of humic substances. p. 103-127. In: The Use of Isotopes in Soil Organic Matter Studies. Pergamon Press. Oxford, UK.

Flaig, W., 1988. Generation of model chemical precursors. p. 75-92. In: F.H. Frimmel and R.F. Christman (eds.) Humic Substances and Their Role in the Environment. John Wiley and Sons Ltd., Chichester. UK.

Flaig, W., H. Beutelspacher, and E. Rietz. 1975. Chemical Composition and Physical Properties of Humic Substances. p. 1-212. In: J.E. Gieseking (ed.) Soil Components vol 1: Organic Components. Springer-Verlag. Berlin. FRG.

Foresman, J.B., and Æ. Frisch. 1996. Exploring Chemistry with Electronic Structure Methods. Gaussian Inc. Pittsburgh. PA.

Ghiorse, W.C. 1985. Biology of iron- and manganese-depositing bacteria. *Ann. Rev. Microbiol.* 38:515-550.

Ghosh, K., and M. Schnitzer. 1979. UV and visible absorption spectroscopic investigations in relation to macromolecular characterizations in humic substances. *J. Soil Sci.* **30:** 735-745.

Gillam, A.H., and M.A. Wilson. 1985. Pyrolysis-GC-MS and NMR studies of dissolved sea water humic substances and isolates of a marine diatom. *Org. Geochem.* **8**:15-25.

Giovanoli, R. 1969. A simplified scheme for polymorphism in the manganese dioxides. *Chimia* **23**:470-472.

Giovanoli, R. 1970a. Vernadite is random-stacked birnessite. *Miner. Deposita* **15**:251-253.

Giovanoli, R. 1970b. On natural and synthetic manganese nodules. p. 159-202. In: I.M. Varentsov and G. Grasselly (eds.) Geology and Geochemistry of Manganese. Vol. 1. Publ. House, Hung. Acad. Sci., Budapest.

Giovanoli, R., and B. Balmer. 1981. A new synthesis of hollandite. A possibility for immobilization of nuclear waste. *Chimia* **35**:53-55.

Giovanoli, R., and R. Brutsch. 1979. Über Oxidhydoxide des Mn(IV) mit Schichtengitter. 5. Mitteilung: Stoichiometrie, Austauschverhalten und die Rolle bei der Bildung von Tiefsee-Mangankonkretionen. *Chimia* **33**:372-376.

Gonzalez-Vila, F.J., H. Lentz, and H.D. Ludeman. 1976. FT-C13 nuclear magnetic resonance spectra of natural humic substances. *Biochem. Biophys. Res. Commun.* **72**:1063-1070.

Haider, K. 1976. Microbial synthesis of humic materials. p. 244-257. In: D.D. Kaufmann, G-G. Still, G.D. Paulson and S.K. Bandal (eds.) Bound and Conjugated Pesticide Residues. American Chemical Society Symposium Series No. 29, Washington, D.C.

Haider, K. 1994. Advances in the basic research of the biochemistry of humic substances. p. 91-107. In: N. Senesi and T. Miano (eds.) Humic Substances in the Global Environment and Implications on Human Health. Elsevier Science, B.V. NL.

Haider, K., and J.P. Martin, 1967, Synthesis and transformation of phenolic compounds by *Epicoccum nigrum* in relation to humic acid formation. *Soil Sci. Soc. Am. Proc.* **31**:766-774.

Haider, K., and J.P. Martin. 1970. Humic acid type phenolic polymers from *Aspergillus sydowi* culture medium, *Stachybotrys* sp. cells and autooxidized phenol mixtures. *Soil Biol. Biochem.* **2**:145-156.

Haider, K., J.P. Martin, Z. Filip and E. Fustec-Mathon. 1972. Contribution of soil microbes to the formation of humic compounds. Proceedings p. 71-85. International Meeting on Humic Substances,. Nieuwersluis Pudoc. Wageningen, NL.

Harada, H., and W.A. Côté Jr. 1985. Structure of wood. p. 1-42. In: T. Higuchi (ed.) Biosynthesis and Biodegradation of Wood Components Academic Press. Orlando. FL.

Harvey, H.W. 1969. The Chemistry And Fertility Of Sea-Water. Cambridge University Press. Cambridge. UK.

Hatcher, P.G., I.A. Breger, and M.A. Mattingly. 1980. Structural characteristics of fulvic acids from continental shelf sediments. *Nature* (London) **285**:560-562.

Hatcher, P.G., G.E. Maciel, and L.W. Dennis, 1981. Aliphatic structure of humic acids; a clue to their origin. *Org. Geochem.* **3**:43-48.

Hayase, F., S.B. Kim and H. Kato. 1986. Analyses of the chemical structures of melanoidins by $^{13}C$ NMR. $^{13}C$ and $^{15}N$ CP-MAS NMR spectrometry. *Agric. Biol. Chem.* **50**:1951-1957.

Hayes, M.H.B. 1985. Extraction of humic substances from soils. p. 329-362 In: G.R. Aiken, D.M. McKnight, R.L. Wershaw and P. MacCarthy (eds.) Humic Substances in Soil. Sediment and Water - Geochemistry. Isolation and Characterization. John Wiley and Sons, New York. NY.

Hayes, M.H.B. 1991. Concepts of the origins, composition, and structure of humic substances. p. 3-22. In: W.S. Wilson (ed.) Advances in Soil Organic Matter Research: The Impact on Agriculture and the Environment. Royal Soc. Chem. Cambridge, UK.

Hayes, M.H.B., and R.S. Swift. 1978. The chemistry of soil organic colloids. p. 179-230. In: M.H.B. Hayes and R.S. Swift (eds.) The Chemistry of Soil Constituents, Wiley-Interscience, New York, NY.

Hayes, M.H.B., P. MacCarthy, R.L. Malcolm, and R.S. Swift. 1989. The search for structure: Setting the scene. p. 3-30. In: M.H.B. Hayes, P. MacCarthy, R.L. Malcolm and R.S. Swift (eds.) Humic Substances II. In Search of Structure. Wiley-Interscience. Chichester. UK.

Hedges, J.I. 1978. The formation and clay mineral reactions of melanoidins. *Geochim. Cosmochim. Acta* **42**:69-76.

Hedges, J.I., 1988. Polymerization of humic substances in natural environments. p. 45-58. In: F.H. Frimmel and R.F Christman (eds.) Humic substances and Their Role in the Environment. John Wiley and Sons, Chichester, UK.

Hedges, J.I., and P.L. Parker. 1976. Land-derived organic matter in surface sediments from the Gulf of Mexico. *Geochim. Cosmochim. Acta* **40**:1019-1029.

Hemings, M.A., and P.A. Dejaeger. 1983. Suppression of spinning sidebands in magic-angle-spinning NMR spectroscopy. *J. Magn. Reson.* **51**:339-348.

Herzfeld, J., and A.E.J. Berger. 1980. Sideband intensities in NMR spectra of samples spinning at the magic angle. *J. Chem. Phys.* **73**:6021-6030.

Hidaka, H., K. Nohara, J. Zhao, E. Pelizzetti, N. Serpone, C. Guillard, and P. Pichat. 1996. Photodegradation of surfactants XVII Photo-oxidation processes in amphoteric surfactants catalyzed by irradiated $TiO_2$ suspensions. Abstract. *Journal Adv. Oxid. Tech.* Vol.1. No.1. via Internet http://info.london.on.ca/~sti.ekabi/research.html.

Hilgendorff, M. M. Hilgendorff and D. W. Bahneman. 1996. Mechanisms of photocatalysis: The reductive degradation of tetrachloromethane in aqueous titanium dioxide suspensions. Abstract. *Journal Adv. Oxid. Tech.* Vol.1. No.1. via Internet http://info.london.on.ca/~sti.ekabi/research.html.

Hodge. J.E. 1953. Chemistry of browning reactions in model systems. *Agric. Food Chem.* **1**:928-943.

Hoppe-Seyler, F. 1889. Uber Huminsubstanzen, ihre Enstehung und ihre Eigenschafte. *Z. Physiol. Chem.* **13:** 66-122.

Huang, P.M. 1990. Role of soil minerals in transformations of natural organics and xenobiotics. *Soil Biochem.* **6**: 29-115.

Huang, P.M. 1995. The role of short-range ordered mineral colloids in abiotic transformations of organic components in the environment. p. 135-167. In: P.M. Huang, J. Berthelin, J-M. Bollag, W.B. McGill. and A.L. Page (eds.) Environmental Impact of Soil Component Interactions: Vol. 1 Natural and Anthropogenic Organics CRC Lewis Publishers, Boca Raton. FL.

Huang, P.M. 2000. Abiotic catalysis. p. B303-B332. In: M.E. Sumner (ed. in chief) Handbook of Soil Science. CRC Press. Boca Raton. FL.

Ikan, R., Y. Rubinsztain, Z. Aizenshtat, R. Pugmire, L.L. Anderson. and W.R. Woolfenden. 1986. Carbon-13 cross polarized magic-angle samples spinning nuclear magnetic resonance of melanoidins. *Org. Geochem.* **9**:199-212.

Ikan. R., T. Dorsey and I.R. Kaplan. 1990. Characterization of natural and synthetic humic substances (melanoidins) by stable carbon and nitrogen isotope measurements and elemental compositions. *Anal. Chim. Acta* **232**:11-18.

Ikan, R., P. Ioselis, Y. Rubinsztain, Z. Aizenshtat, I. Miloslavsky, S. Yariv, R. Pugmire, L.L. Anderson, W.R. Woolfenden, I.R. Kaplan, T. Dorsey, K.E. Peters, J.J. Boon, J.W. de Leeuw, R. Ishawatari, S. Morinaga, S. Yamamoto, T. Macihara, M. Muller-Vonmoos and A. Rub. 1992. Chemical, isotopic, spectroscopic, and geochemical aspects of natural and synthetic humic substances. *Sci. Tot. Environ.* **117/118**:1-12.

Ikan, R. Y. Rubinsztain, A. Nissenbaum, and I.R. Kaplan. 1996. Geochemical aspects of the Maillard Reaction. p. 1-25. In: R. Ikan (ed.) The Maillard Reaction: Consequences for the Chemical and Life Sciences. John Wiley and Sons, Chichester, UK.

Ioselis, P., Y. Rubinsztain, R. Ikan, and K.E. Peters. 1981. Pyrolysis of natural and synthetic humic substances. *Adv. Org. Geochem.* 824-827.

Izumi, Y., K. Urabe, and M. Onaka. 1992. Zeolite, Clay, and Heteropolyacid in organic reactions. VCH, Weinheim, FRG.

Joergensen, R.G., and B. Meyer. 1990. Chemical change in organic matter decomposing in and on a forest Rendzina under beech (*Fagus sylvatica* L.). *J. Soil Sci.***41**:17-27.

Kalinowski, H.-O., S. Berger, and S. Braun. 1988. Carbon-13 NMR Spectroscopy. John Wiley and Sons, Chichester, UK.

Kasatochkin, V.I. 1951. The structure of carbonized substances. *Izv. Akad. Nauk. SSSR. Otd. Tekh. Nauk.* **9**. Op. cit. W. Ziechmann. 1988. p. 113-132. In: F.H. Frimmel and R.F. Christman (eds.) Humic Substances and their Role in the Environment. Wiley-Interscience, Chichester, UK.

Kepkay, P.E. 1985. Kinetics of microbial manganese oxidation and trace metal binding in sediments: Results from an in situ dialysis technique. *Limnol. Oceanogr.* **30**:713-726.

Khan, S.U., and F.J. Sowden. 1971. Distribution of nitrogen in the black solonetzic and chernozemic soils of Alberta. *Can. J. Soil Sci.* **51**:185-193.

Kirk, T.K., and M. Shimada. 1985. Lignin biodegradation - the microorganisms involved and the physiology and biochemistry of degradation by white-rot fungi. p. 579-605. In: T. Higuchi (ed.) Biosynthesis and Biodegradation of Wood Components. Academic Press, Orlando, FL.

Kirk, T.K., and R.L. Farrell. 1987. Enzymatic "combustion" - The microbial degradation of lignin. *Ann. Rev. Microbiol.* **41**: 465-505.

Kleinhempel, D. 1970. Ein Betrag zur Theorie des Huminstoffzustandes. *Albrecht Thear Archives.* **14:** 3-14. Op. cit. W. Ziechmann, 1988. p. 113-132. In: F.H. Frimmel and R.F. Christman (eds.) Humic Substances and their Role in the Environment. Wiley-Interscience, Chichester, UK.

Kögel-Knaber, I. 1993. Biodegradation and humification processes in forest soils. *Soil Biochem.* **8**: 101-135.

Kolattudukudy, P.E., and K.E. Espelie. 1985. Biosynthesis of cutin, suberin and associated waxes. p. 161-207. In: T. Higuchi (ed.) Biosynythesis and Biodegradation of Wood Components. Academic Press, Orlando, FL.

Kononova, M.M. 1966. Soil Organic Matter. Its Nature, Its Role in Soil Formation and in Soil Fertility. 2nd edn. Pergamon Press, Oxford.

Koshijima, T., T. Watanabe, and F. Yaku. 1989. Structure and properties of the lignin-carbohydrate complex polymer as an amphiphathic substance. p. 11-28. In: W.G. Glasser and S. Sarkanen (eds.) Lignin Properties and Materials. American Chemical Society Symposium Series 397. Washington DC.

Kumada, M., and H. Kato. 1970. Browning of pyrogallol as affected by clay minerals. *Soil Sci. Plant Nutr.* **16**:195-200.

Kuwahara, M., J.K. Glenn, M.A. Morgan and M.H. Gold. 1984. Separation and characterization of two extracellular $H_2O_2$-dependent oxidases from lignolytic cultures of *Phanaerochaete chrysosporium*. *FEBS Letters* **169**:247-250

Larson, R.A., and J.M. Hufnal Jr. 1980. Oxidative polymerization of dissolved phenols by soluble and insoluble inorganic species. *Limnol. Oceanogr.* **25**:505-512.

Lee, J.S.K, and P.M. Huang. 1995. Photochemical effect on the abiotic transformations of polyphenolics as catalysed by Mn(IV) oxide: p. 177-189. In: P.M. Huang, J. Berthelin, J-M. Bollag, W.B. McGill, and A.L. Page (eds.) Environmental Impact of Soil Component Interactions - Natural and Anthropogenic Organics. CRC Lewis Publishers, Boca Raton, FL.

Lehmann, R.G., H.H. Cheng, and J.B. Harsh. 1987. Oxidation of phenolic acids by soil iron and manganese oxides. *Soil Sci. Soc. Am. J.* **51**:352-356.

Levy, G.C., R.L. Lichter, and G.L. Nelson. 1980. Carbon-13 Nuclear Magnetic Resonance Spectroscopy. Wiley-Interscience, John Wiley and Sons, New York, NY.

Lindqvist, I. 1972. Charge-transfer interaction of humic acids with donor molecules in aqueous solutions. *Swed. J. Agric. Res.* **12**:105-109. Op. cit. P.R. Bloom and J.A. Lenheer 1989. p. 409-446. In: M.H.B. Hayes, P. MacCarthy, R.L. Malcolm and R.S. Swift (eds.) Humic Substances II. In Search of Structure. Wiley-Interscience, Chichester, UK.

Lindqvist, I. 1973. Partial reduction of a humic acid. *Swed. J. Agric. Res.* **13**:69-73. Op. cit. P.R. Bloom and J.A. Lenheer 1989. p. 409-446. In: M.H.B. Hayes, P. MacCarthy, R.L. Malcolm and R.S. Swift (eds.) Humic Substances II. In Search of Structure. Wiley-Interscience, Chichester, UK.

Lindsay, W.L. 1979. Chemical Equilibria in Soils. John Wiley and Sons, New York, NY.

Lipard, S.J., and J.M. Berg. 1994. Principles of Bioinorganic Chemistry. University Science Books, San Diego, CA.

Lobartini, J.C., and K.H. Tan. 1988. Differences in humic acid characteristics as determined by carbon-13 nuclear magnetic resonance, scanning electron microscopy and infrared analysis. *Soil Sci. Soc. Am. J.* **52**:125-130.

Lowe, L.E. 1978. Carbohydrates in soils. p. 65-94. In: M.Schnitzer and S.U. Khan (eds.) Soil Organic Matter. Elsevier, Amsterdam,NL.

MacCarthy, P., and J.A. Rice. 1985. Spectroscopic methods (other than NMR) for determining functionality in humic substances. p. 527-559. In: G.R. Aiken, D.M. McKnight, R.L. Wershaw and P. MacCarthy. (eds.) Humic Substances in Soil, Sediment and Water - Geochemistry, Isolation and Characterization. John Wiley and Sons, New York, NY.

MacCarthy, P., P.R. Bloom, C.E. Clapp, and R.L. Malcolm. 1990. Humic substances in soil and crop sciences – An overview. p. 261-271. In: P. MacCarthy, P.R. Bloom, C.E. Clapp, and R.L. Malcolm (eds.) Humic Substances in Soil and Crop Sciences – Selected Readings. American Society of Agronomy and Soil Science Society of America, Madison, WI.

Maillard, L.C. 1912. Action des acides amines sur les sucres: formation des melanoidines par voie methodologique. *C.R. Acad. Sci.* **154**:66-68.

Maillard, L.C. 1913. Formation de matieres humiques par action de polypeptides sur sucres. *C.R. Acad. Sci.* **156**:148-149.

Malcolm, R.L. 1989. Applications of solid-state $^{13}C$ NMR spectroscopy to geochemical studies of humic substances. p. 339-372. In: M.H.B. Hayes, P. MacCarthy, R.L. Malcolm, and R.S. Swift (eds.) Humic Substances II. In Search of Structure. Wiley-Interscience, John Wiley and Sons, Chichester, UK.

Malcolm, R.L. 1990. The uniqueness of humic substances in each of soil, stream and marine environments. *Anal. Chem. Acta* **232**:19-30.

Manceau, A., and J.M. Combes. 1988. Structure of Mn and Fe oxides and oxyhydroxides. A topological approach by EXAFS. *Phys. Chem. Min.* **15**:283-295.

Manceau, A., A.I. Gorshkov, and V.A. Drits. 1992a. Structural chemistry of Mn, Fe, Co, and Ni in manganese hydrous oxides: Part I. Information from XANES spectroscopy. *Am. Mineral.* **77**:1133-1143.

Manceau, A., A.I. Gorshkov, and V.A. Drits. 1992b. Structural chemistry of Mn, Fe, Co, and Ni in manganese hydrous oxides: Part II. Information from EXAFS spectroscopy and electron and X-ray diffraction. *Am. Mineral.* **77**:1144-1157.

Maricq, M.M., and J.S. Waugh. 1979. NMR in rotating solids. *J. Chem. Phys.* **70**:3300-3316.

Martin, J.P., and K. Haider. 1969. Phenolic polymers of *Stachybotrys atra*, *Stachybotrys chartarum* and *Epicoccum nigrum* in relation to humic acid formation. *Soil Sci.* **107**:260-270.

Martin, J.P., and K. Haider. 1971. Microbial activity in relation to soil humus formation *Soil Sci.* **111**: 54-63.

Mattson, S. 1932. The laws of soil colloidal behaviour. VII. Proteins and proteinated complexes. *Soil Sci.* **23**:41-72.

Mayer, L.M. 1994. Relationships between mineral surfaces and organic carbon concentrations in soils and sediments. *Chem. Geol.* **114**:347-383.

McBride, M.B. 1987. Adsorption and oxidation of phenolic compounds by iron and manganese oxides. *Soil Sci. Soc. Am. J.* **51**:1466-1472.

McBride, M.B. 1989a. Surface chemistry of soil minerals. p. 35-88. In: J.B. Dixon and S.B. Weed (eds.) Minerals in Soil Environments. 2nd edn. SSSA. Madison, WI.

McBride, M.B. 1989b. Oxidation of dihydroxybenzenes in aerated aqueous suspensions of birnessite. *Clays Clay Miner.* **37**:341-347.

McBride, M.B. 1989c. Oxidation of 1,2- and 1,4-dihydroxybenzenes by birnessite in acidic aqueous suspension. *Clays Clay Miner.* **37**:479-486.

McBride, M.B. 1994. Environmental Chemistry of Soils. Oxford University Press, Oxford.

McKenzie, R.M. 1971. The synthesis of birnessite, cryptomelane, and some other oxides and hydroxides of manganese. *Mineral Mag.* **38**:493-502.

McKenzie, R.M. 1989. Manganese oxides and hydroxides. p. 439-465. In: J.B. Dixon and S.B. Weed (eds.) Minerals in Soil Environments. 2nd ed. SSSA. Madison, WI.

McKenzie, R.M., A.W.H. Damman, and P.K. Harringa. 1968. Iron-Manganese and other pans in some soils of Newfoundland. *Can. J. Soil Sci.* **48**:243-253.

McKeague, J.A., M.V. Cheshire, F. Andreux, and J. Berthelin. 1986. Organo-mineral complexes in relation to pedogenesis. p. 549-592. In: P.M. Huang and M. Schnitzer (eds.) Interactions of Soil Minerals with Natural Organics and Microbes. SSSA Spec. Publ. 17.SSSA. Madison, WI.

Mezey, P.G. 1986. Group theory of electrostatic potentials : A tool for quantum chemical drug design. *Int. J. Quantum Chem. Quantum Biol. Symp.* **12**:113-122.

Mezey, P.G. 1987. The shape of molecular charge distributions: Group theory without symmetry. *J. Comput. Chem.* **8**:462-469.

Mezey, P.G. 1988. Shape groups of molecular similarity: Shape groups and shape graphs of molecular contour surfaces. *J. Math. Chem.* **2**:299-323.

Mezey, P.G. 1993. Shape in Chemistry: Introduction to Molecular Shape and Topology. VCH, New York, NY.

Mezey, P.G. 1998. Molecular structure-reactivity-toxicity relationships. In: P.M. Huang (ed). Soil Chemistry and Ecosystem Health. Soil Science Society of America, Pittsburgh, PA.

Mezey, P.G., Z. Zimpel, P. Warburton, P.D. Walker, D.G. Irvine, D.G. Dixon, and B.M. Greenberg. 1996. A high-resolution shape-fragment MEDLA database for toxicological shape analysis of PAH's. *J. Chem. Inf. Comput. Sci.* **36**:602-611.

Mezey, P.G., Z. Zimpel, P. Warburton, P.D. Walker, D.G. Irvine, X.-D. Huang, D.G. Dixon, and B.M. Greenberg. 1998. Use of quantitative shape-activity relationships to model the photoinduced toxicity of polycyclic aromatic hydrocarbons: electron density shape features accurately predict toxicity. *Env. Toxicol. Chem.* **17**: 1207-1215.

Miknis, F.P., V.J. Bartuska, and G.E. Maciel. 1979. Cross-polarization magic-angle spinning 13C NMR spectra of oil shales. *Org. Geochem.* **1**:169-176.

Moore, J.W., and R.G. Pearson. 1981. Kinetics and Mechanism. 3rd edn. John Wiley and Sons, New York, NY.

Mossine, V.V., G.V. Glinsky and M.S. Feather. 1994. The preparation and characterization of some Amadori compounds (1-amino-1-deoxy-D-fructose derivatives) derived from a series of aliphtic ω-amino acids. *Carbohydr. Res.* **262**:257-270.

Mortland, M.M. 1986. Mechanisms of adsorption of nonhumic organic species by clays. p. 59-76. In: P.M. Huang and M. Schnitzer (eds.) Interactions of Soil Minerals with Natural Organics and Microbes. Soil Science Society of America. Madison, WI.

Naidja, A., P.M. Huang, and J.-M. Bollag. 1997. Activity of tyrosinase immobilized on hydroxy-aluminum-montmorillonite complexes. *J. Mol. Catal.* **A115**:305-316.

Naidja, A., P.M. Huang, J. Dec, and J.-M. Bollag. 1999. Kinetics of catechol oxidation catalyzed by tyrosinase or δ-$MnO_2$. p. 181- 188. In: J. Berthelin (ed.) Effect of Mineral-Organic-Microorganism Interactions on Soil and Freshwater Environments. Kluwer Academic/Plenum Publishers. New York, NY.

Newman, R.H., K.R. Tate, P.F. Barron and M.A. Wilson. 1980. Towards a direct non-destructive method of characterizing soil humic substances using $^{13}C$ NMR. *J. Soil Sci.* **31**:623-631.

Nesbitt, H.W., and D. Banerjee. 1998. Interpretation of XPS Mn(2p) spectra of Mn oxyhydroxides and constraints on the mechanism of $MnO_2$ precipitation. *Am. Mineral.* **83**:305-315.

Nissenbaum, A., and J.R. Kaplan. 1972. Chemical and isotopic evidence for the *in situ* origin of marine humic substances. *Limnol. Oceanogr.* **17**:570-582.

O'Brien, J., and P.A. Morrissey. 1997. Metal ion complexation by products of the Maillard reaction. *Food Chem.* **58**:17-27.

Pal, S., J-M. Bollag and P.M. Huang. 1994. Role of abiotic and biotic catalysts in the transformation of phenolic compounds through oxidative coupling reactions. *Soil Biol. Biochem.* **26**: 7. 813-820.

Paul, E.A., and F.E. Clark. 1989. Soil Microbiology and Biochemistry. Academic Press Inc., San Diego, CA.

Paul, E.A., and P.M. Huang. 1980. Chemical aspects of soil. p. 69-86. In: O. Hutzinger (ed.) The Handbook of Environmental Chemistry. Vol. 1, pt. A. Springer-Verlag, Berlin.

Pauli, F.W. 1967. Soil Fertility. Adam Hilger, London, UK.

Perseil, F.A., and R. Giovanoli. 1979. La "rancieite" du gisement ferromanganisifere de Rancie (Pyrenees Ariegeoises). In: C. Lalou (ed.) La Genese des Nodules de Manganese. Colloques Int. Du Centre National de la Reserche Scientifique. 1978. **289**:369-377.

Pinnavaia, T.J., P.L. Hall, S.S. Kady, and M.M. Mortland. 1974. Aromatic radical cation formation on the intercrystal surfaces of transition metal layer lattice silicates. *J. Phys. Chem.* **78**:994-999.

Pizzigallo, M.D.R., P. Ruggiero, C. Crecchio, and R. Mininni. 1995. Manganese and iron oxides as reactants for oxidation of chlorophenols. *Soil Sci. Soc. Am. J.* **59**:444-452.

Popoff, T., and O. Theander. 1976. Formation of aromatic compounds from carbohydrates. IV. Chromones from reaction of hexuronic acids in slightly acidic, aqueous solution. *Acta Chem. Scan.* **B30** 705-709.

Post, J.E., R.B. Von Dreele and P.R. Buseck. 1982. Symmetry and cation displacements in hollandites. Structure refinements of hollandite, cryptomelane, and priderite. *Acta Cryst.* **B38**:1056-1065.

Potter, R.M., and G.R. Rossman. 1979. The tetra-valent manganese oxides: identification, hydration, and structural relationships by infrared spectroscopy. *Am. Mineral.* **64**:1199-1218.

Pulgarin, C.O., J.-P. Schwitzguebel, P.A. Peringer, G.M. Pajonk, J.S. Bandara, and J.T. Kiwi. 1996. Abiotic oxidative degradation of atrazine on zero-valent iron activated by visible light. Abstract. *Journal Adv. Oxid. Tech.* Vol.1, No.1. via Internet http://info.london.on.ca/~sti.ekabi/research.html.

Rashid, M.A., and L.H. King. 1970. Major oxygen containing functional groups present in humic and fulvic acid functions isolated from contrasting marine environments. *Geochim. Cosmochim. Acta* **34**:193-201.

Rasyid, U., W.D. Johnson, M.A. Wilson, and J.V. Hanna. 1992. Changes in organic structural group compositions of humic and fulvic acids with depth in sediments from similar geographical but different depositional environments. *Org. Geochem.* **18**:521-529.

Risser, J.A., and G.W. Bailey. 1992. Spectroscopic study of surface redox reactions with manganese oxides. *Soil. Sci. Soc. Am. J.* **56**:82-88.

Rubinsztain, Y., P. Ioselis, R. Ikan, and Z. Aizenshtat. 1984. Investigations on the structural units of melanoidins. *Org. Geochem.* **6**:91-804.

Rubinsztain, Y. S. Yariv, P. Ioselis, Z. Aisenshtat and R. Ikan. 1986a. Characterization of melanoidins by IR spectroscopy – I. Galactose-glycine melanoidins. *Org. Geochem.* **9**:117-125.

Rubinsztain, Y. S. Yariv, P. Ioselis, Z. Aisenshtat and R. Ikan. 1986b. Characterization of melanoidins by IR spectroscopy – II. Melanoidins of galactose with arginine, isoleucine, lysine and valine. *Org. Geochem.* **9**:371-374.

Scheffer, F., B. Meyer, and E.A. Niederbudde. 1959. Huminstoffbildung unter katalyischer Einwirkung naturlich vorkommender Eisenverbindungen im Modellversuch. *Z. Pflanzenernaehr. Bodenkd.* **87**:26-44.

Schoemaker, H.E., E.M. Meijer, M.S.A. Leisola, S.D. Haemmerli, R. Waldner, D. Sangland and H.W. Schmidt. 1989. Oxidation and reduction in lignin biodegradation. p. 454-471. In: M.G. Paice and N.G. Leevis (eds.) Plant Cell Wall Polymers Biogenesis and Biodegradation. American Chemical Society, Washington D.C.

Schnitzer, M. 1972. Humic Substances In The Environment. Marcel Dekker, New York, NY.

Schnitzer, M. 1978. Humic substances: Chemistry and reactions. p. 1-64. In: M. Schnitzer and S.U. Khan (eds.) Soil Organic Matter, Vol. 8. Elsevier, Amsterdam, NL.

Schnitzer, M. 1982. Quo vadis soil organic matter research? p. 67-78. Panel discussion papers. Publ. 5. Whither Soil Research? Trans. 12th Int. Congr. Soil Sci.

Schnitzer, M. 1985. Nature of nitrogen in humic substances. p. 303-325. In: G.R. Aiken, D.M. McKnight, R.L. Wershaw, and P. MacCarthy (eds.) Humic Substances in Soil, Sediment and Water - Geochemistry, Isolation, and Characterization. John Wiley, New York, NY.

Schnitzer, M. 1991. Soil organic matter: The next 75 years. *Soil Sci.* **151**:41-58.

Schnitzer, M., and Barton, D.H.R. 1963. A new experimental approach to the humic acid problem. *Nature* (London) **198:** 217-219.

Schnitzer, M., and H.-R. Schulten. 1998. New ideas on the chemical make-up of soil humic and fulvic acids. p. 153-177. In: P.M. Huang, D.L. Sparks and S.A. Boyd (eds.) Future Prospects for Soil Chemistry. SSSA Special Publication no. 55. Soil Science Society of America, Madison, WI.

Schulten, H.-R., and M. Schnitzer. 1991. A chemical structure for humic substances. *Naturwissenschaften* **78**:311-312.

Schulten, H.-R., and M. Schnitzer. 1993. A state of the art structural concept for humic substances. *Naturwissenschaften* **80**:29-30.

Schwertmann, U., H. Kodama, and W.R. Fischer. 1986. Mutual interactions between organics and iron oxides. p. 223-250. In: P.M. Huang, and M. Schnitzer (eds.) SSSA Special Publication Number 17. Soil Science Society of America, Inc. Madison, WI.

Scott, A.I. 1964. Interpretation of Ultraviolet Spectra of Natural Products. Pergamon Press, New York, NY.

Senesi, N., T.M. Miano, M.R. Provenzano, and G. Brunneti. 1989. Spectroscopic and compositional characterization of I.H.S.S. reference and standard fulvic and humic acids of various origin. *Sci. Tot. Env.* **81/82:**143-156.

Shindo, H., and T. Higashi. 1986. Polymerization of hydroquinone as influenced by selected inorganic soil components. *Soil Sci. Plant. Nutr.* **32**:305-309.

Shindo, H., and P.M. Huang. 1982. Role of Mn (IV) oxide in abiotic formation of humic substances in the environment. *Nature* (London) **298**:363-365.

Shindo, H., and P.M. Huang. 1984a. Catalytic effects of manganese (IV), iron (III), aluminium and silicon oxides on the formation of phenolic polymers. *Soil Sci. Soc. Am. J.* **48**:927-934.

Shindo, H., and P.M. Huang. 1984b. Significance of Mn(IV) oxide in abiotic formation of organic nitrogen complexes in natural environments. *Nature* (London) **308**:57-58.

Shindo, H., and P.M. Huang. 1985a. The catalytic power of inorganic components in the abiotic synthesis of hydroquinone-derived humic polymers. *Appl. Clay. Sci.* **1**:71-81.

Shindo, H., and P.M. Huang. 1985b. Catalytic polymerization of hydroquinone by primary minerals. *Soil Sci.* **139**:505-511.

Shindo, H., and P.M. Huang. 1992. Comparison of the influence of Mn(IV) oxide and tyrosinase on the formation of humic substances in the environment. *Sci. Tot. Environ.* **117/118**:103-110.

Sidhu, P.S., J.L. Seghal, M.K. Sinha, and N.S. Randhawa. 1977. Composition and mineralogy of iron-manganese concretions from some soils of the Indo-Gangetic plain in northwest India. *Geoderma* **18**:241-249.

Siegel, H. 1976. Metal Ions in Biological Systems. Marcel Dekker, New York, NY.

Sihombing, R., W.D. Johnson, M.A. Wilson, M. Johnson, A.M. Vassallo, and D. Alderice 1991. Origins of Humus Variation. *Org. Geochem.* **17**: 85-91.

Silvester E., A. Manceau, and V.A. Drits. 1997. Structure of synthetic monoclinic Na-rich birnessite and hexagonal birnessite: II. Results from chemical studies and EXAFS spectroscopy. *Am. Mineral.* **82**:962-978.

Sjoblad, R.D., and J.-M. Bollag. 1981. Oxidative coupling of aromatic compounds by enzymes from soil microorganisms. *Soil Biochem.* **5**:113-152.

Smolen, J.M., and A.T. Stone. 1998. Organophosphorus ester hydrolysis catalyzed by dissolved metals and metal-containing surfaces. p. 157-171. In: P.M. Huang (ed.) Soil Chemistry and Ecosystem Health. Soil Science Society of America, Special Publication 52, Madison, WI.

Sparks, D.L. 1995. Environmental Soil Chemistry. Academic Press. San Diego, CA.

Stevenson, F.J. 1986. Cycles of Soil. – Carbon, Nitrogen, Phosphorus, Sulfur, Micronutrients. John Wiley, New York, NY.

Stevenson, F.J. 1994. Humus Chemistry – Genesis, Composition, Reactions. 2nd edn. John Wiley and Sons. New York, NY.

Stone, A.T. 1986. Adsorption of organic reductants and subsequent electron transfer on metal oxide surfaces. *ACS Symp. Ser.* **323**:446-461.

Stone, A.T. 1987. Reductive dissolution of manganese (III/IV) oxides by substituted phenols. *Environ. Sci. Technol.* **21**:979-986.

Stone, A.T., and J.J. Morgan. 1984. Reduction and dissolution of manganese (III) and manganese (IV) by organics. 1. Reaction with hydroquinone. *Environ. Sci. Technol.* **18**:450-456.

Stone, A.T., and A. Torrents. 1995. The role of dissolved metals and metal-containing surfaces in catalyzing the hydrolysis of organic pollutants. p. 275-298. In: P.M. Huang, J. Berthelin, J-M. Bollag, W.B. McGill, and A.L. Page (eds.) Environmental Impact of Soil Component Interactions: Vol. I Natural and Anthropogenic Organics CRC Lewis Publishers, Boca Raton, FL.

Stuermer, D.H., and G.R. Harvey. 1974. Humic substances from seawater. *Nature* (London) **250**:480-481.

Stuermer, D.H., and J.R. Payne. 1976. Investigations of seawater and terrestrial humic substances with carbon-13 and proton nuclear magnetic resonance. *Geochim. Cosmochim. Acta.* **40**:1109-1114.

Sunda, W.G, S.A. Huntsman, and G.R. Harvey. 1983. Photoreduction of manganese oxides in seawater and its geochemical and biological implications. *Nature* (London) **301**:234-236.

Sunda, W.G., and D.J. Kieber 1994. Oxidation of humic substances by manganese oxides yields low-molecular weight organic substances. *Nature* (London) **367**:62-64.

Taguchi, K., and Y. Sampei. 1986. The formation and clay mineral and $CaCO_3$ association reactions of melanoidins. *Org. Geochem.* **10**:1081-1089.

Tebo, B.M., and S. Emerson. 1985. Effect of oxygen tension, Mn(II) concentration and temperature on the microbially catalyzed Mn(II) oxidation rate in a marine fjord. *Appl. Environ. Microbiol.* **50**:1268-1273.

Teppen, B.J. 1998. Computational chemistry in the future of soil chemistry. p. 39-67. In: P.M. Huang, D.L. Sparks and S.A. Boyd (eds.) Future Prospects for Soil Chemistry. SSSA Special Publication no. 55. Soil Science Society of America, Madison, WI.

Thiele, H., and Kettner, H. 1953. Uber Huminsauren. *Kolloid-Z.* **130:** 131-160. Op. cit. W. Ziechmann, 1988. p. 113-132. In: F.H. Frimmel and R.F. Christman (eds.) Humic Substances and their Role in the Environment, Wiley-Interscience, Chichester, UK.

Thomas, J.M., and W.J. Thomas. 1967. Introduction to the Principles of Heterogeneous Catalysis. Academic Press, New York, NY.

Thurman, E.M. 1985. Organic geochemistry of Natural Waters. Niyhoff/Junk Publishers, Boston, MA.

Thurman, E.M., and R.L Malcolm, 1983. Structural study of humic substances: New approaches and methods. p. 1-25. In: R.F. Christman and E.T. Gjessing (eds.) Aquatic and Terrestrial Humic Materials. Ann Arbor Science, Ann Arbor, MI.

Tien, M., and T.K. Kirk. 1984. Lignin degrading enzyme from *Phanaerochaete chrysosporium*: Purification, characterization and catalytic properties of a unique $H_2O_2$-requiring oxygenase. *Proceedings Nat. Acad. Sci. USA* **81**:2280-2284.

Trigo, C., and A.S. Ball. 1994. Is the solubilized product from the degradation of lignocellulose by actinomycetes a precursor of humic substances? *Microbiology* **140**:3145-3152.

Tsutsuki, K., and S. Kuwatsuka. 1979. Chemical studies on soil humic acids: VII. pH dependent nature of the ultraviolet and visible absorption spectra of humic acids. *Soil Sci. Plant Nutr.* **25**:373-384.

Twigg, M.V. 1989. Catalyst Handbook. 2nd edn. Wolfe Publishing Ltd., London, UK.

Ulrich, J.-J., and A.T. Stone. 1989. Oxidation of chlorophenols adsorbed to manganese oxide surfaces. *Environ. Sci. Technol.* **23**:421-428.

Vilsmeier K., and A Amberger 1978. Anorganisch-katalytische Umsetzungen von Cyanamid und dessen Metaboliten in Quarzsand. II. Cyanamidabbau unter dem Einflu$\beta$ von Metaloxiden und Temperatur. *Z. Pflanzenernaehr. Bodenkd.* **141**:677-685.

Waksman, S.A. 1932. Humus. Williams and Wilkins, Baltimore, Md.

Waksman, S.A., and K.R.N. Iyer. 1933. Contribution to our knowledge of the chemical nature and origin of humus. IV. Fixation of proteins by lignins and formation of complexes resistant to microbial decomposition. *Soil Sci.* **36**:69-79.

Wang, M.C., and P.M. Huang. 1986. Humic macromolecule interlayering in nontronite through interaction with phenol monomers. *Nature* (London) **323**:529-531.

Wang, M.C., and P.M. Huang. 1987a. Polycondensation of pyrogallol and glycine and the associated reactions as catalysed by birnessite. *Sci. Tot. Environ.* **62**: 435-442.

Wang, M.C., and P.M. Huang. 1987b. Catalytic polymerization of hydroquinone by nontronite. *Can. J. Soil Sci.* **67**:867-875.

Wang, M.C., and P.M. Huang. 1989. Pyrogallol transformations as catalyzed by nontronite, bentonite, and kaolinite. *Clays Clay Miner.* **37**:525-530.

Wang, M.C., and P.M. Huang. 1991. Nontronite catalysis in polycondensation of pyrogallol and glycine and the associated reactions. *Soil Sci. Soc. Am. J.* **55**:1156-1161.

Wang, M.C., and P.M. Huang. 1992. Significance of Mn(IV) oxide in the abiotic ring cleavage of pyrogallol in natural environments. *Sci. Tot. Environ.* **113**: 147-157.

Wang, M.C., and P.M. Huang 1994. Structural role of polyphenols in influencing the ring cleavage and related chemical reactions as catalysed by nontronite. p. 173-180. In: N. Senesi and T.M. Miano. (eds.) Humic Substances in the Global Environment and Implications on Human Health. Elsevier Science, Amsterdam.

Wang, M.C., and P.M. Huang. 1997. Catalytic power of birnessite in abiotic formation of humic polycondensates from glycine and pyrogallol. p. 59-65. In: J. Drozd, S.S. Gonet, N.Senesi and T.M. Miano (eds.) Proc. 8th Int. Conf. Int. Humic Substances Society, Wroclaw, Poland.

Wang, T.S.C., and S.W. Li. 1977. Clay minerals as heterogeneous catalysts in preparation of model humic substances. *Z. Pflanzenernaehr. Bodenkd.* **140**:669-676.

Wang, T.S.C., J.-H. Chen, and W.-M. Hsiang. 1985. Catalytic synthesis of humic acids containing various amino acids and dipeptides. *Soil Sci.* **140**:3-10.

Wang, T.S.C., M-M. Kao, and S.W. Li, 1978a. A new proposed mechanism of formation of soil humic substances. p. 357-372. In: Studies and Essays in Commemoration of the Golden Jubilee of Academica Sinica. Academica Sinica. Taipei, Taiwan.

Wang, T.S.C., M.-M. Kao, and P.M. Huang. 1980 The effect of pH on the catalytic synthesis of humic substances by illite. *Soil Sci.* **129**:333-338.

Wang, T.S.C., S.W. Li, and Y.L. Ferng. 1978b. Catalytic polymerization of phenolic compounds by clay minerals. *Soil Sci.* **126**:15-21.

Wang, T.S.C., M.C. Wang, Y.L. Ferng and P.M. Huang. 1983. Catalytic synthesis of humic substances by natural clays, silts and soils. *Soil Sci.* **135**:350-360.

Wang, T.S.C, P.M. Huang, C-H. Chou, and J-H. Chen. 1986. The role of soil minerals in the abiotic polymerization of phenolic compounds and formation of humic substances. p. 251-281. In: P.M. Huang and M. Schnitzer (eds.) Interactions of Soil Minerals with Natural Organics and Microbes. SSSA Special Publication No. 17. Soil Science Society of America, Madison, WI.

Warren, S.W. 1994. The Physical Basis Of Chemistry. Academic Press Inc., San Diego, CA.

Wershaw, R.L. 1994. Membrane-Micelle Model for Humus in Soils and Sediments and Its Relation to Humification. U.S. Geological Survey Water-Supply Paper 2410. United States Government Printing Office.

Wilkie, K.C.B. 1983. Hemicelluloses. *Chemtech* **13**:306-319.

Wilson, M.A., and K.M. Goh. 1977a. Proton-decoupled pulse Fourier-Transform magnetic resonance of soil organic matter. *J. Soil Sci.* **28:** 645-652.

Wilson, M.A., and K.M. Goh. 1977b. C-13 nuclear magnetic resonance of humic substances. *Plant Soil* **46:** 287-289.

Wolff, S.P. 1996. Free radicals and glycation theory. p. 73-88. In: R.Ikan (ed.) The Maillard Reaction. Consequences for the Chemical and Life Sciences. John Wiley and Sons, Chichester, UK.

Wolfrom, M.L. L.F. Cavalieri and D.K. Cavalieri. 1947. Chemical interaction of amino compounds and sugars. II Methylation experiments. *J. Am. Chem. Soc.* **69**:2411-2413.

Wong, J.W., and T. Shibamoto. 1996. Genotoxicity of Maillard reaction products. p. 129-159. In: R.Ikan (ed.) The Maillard Reaction. Consequences for the Chemical and Life Sciences. John Wiley and Sons, Chichester, UK.

Wood, T.M. 1988. Cellulose mechanisms. p. 333-346. In: D.R. Houghton, R.N. Smith, H.O.W. Eggins (eds.) Biodeterioration 7 Elsevier Applied Science, London, UK.

Wood, T.M. 1989. Mechanisms of cellulose degradation by enzymes from aerobic and anaerobic fungi. p. 17-35. In: M.P. Coughlan (ed.) Enzyme Systems For Lignocellulose Degradation. Elsevier Applied Science, London, UK.

Xing, B., J. Mao, W.-G. Hu, K.Schmidt-Rohr, G. Davies, and E.A. Ghabbour. 1999. Evaluation of different solid-state $^{13}C$ NMR techniques for characterizing humic acids. p. 49-61. In: E.A. Ghabbour and G. Davies (eds.) Understanding Humic Substances – Advanced Methods, Properties and Applications. Royal Society of Chemistry, Cambridge.

Xyla, A.G., B. Sulzberger, G.W. Luther III, J.G. Hering, P.V. Cappellen, and W. Stumm. 1992. Reductive dissolution of manganese (III,IV) (hydr)oxides by oxalate: The effect of pH and light. *Langmuir* **8**:95-103.

Ziechmann, W. 1972. Uber die Elektronen-Donator und Acceptor Eigenschaften von Huminstoffen. *Geoderma* **8:**111-131.

Ziechmann, W. 1988 Evolution of Structural Models from Consideration of Physical and Chemical Properties. p. 113-132. In: F.H. Frimmel and R.F. Christman (eds.) Humic Substances and their Role in the Environment. Wiley-Interscience, Chichester, UK.

Ziechmann, W., and M. Mittel. 1976. Naturliche Huminstoffe als E-Donator-Acceptor Komplexe. *Erdol Kohle Ergas* **29**:279-302. Op. cit. P.R Bloom and J.A. Lenheer. 1989. p. 409-446. In: M.H.B. Hayes, P. MacCarthy, R.L. Malcolm and R.S. Swift (eds.) Humic Substances II In Search of Structure. Wiley-Interscience, Chichester. UK.

# APPENDIX

A study was conducted on the interference posed on $^{13}C$ CPMAS NMR by paramagnetic materials. A sample of glycine was spiked with increasing amounts of manganese (II) sulphate and the results on spectral quality are shown below (Figure A1). These results indicate that moderate amounts of paramagnetic material can cause serious interference and the creation of spurious signals.

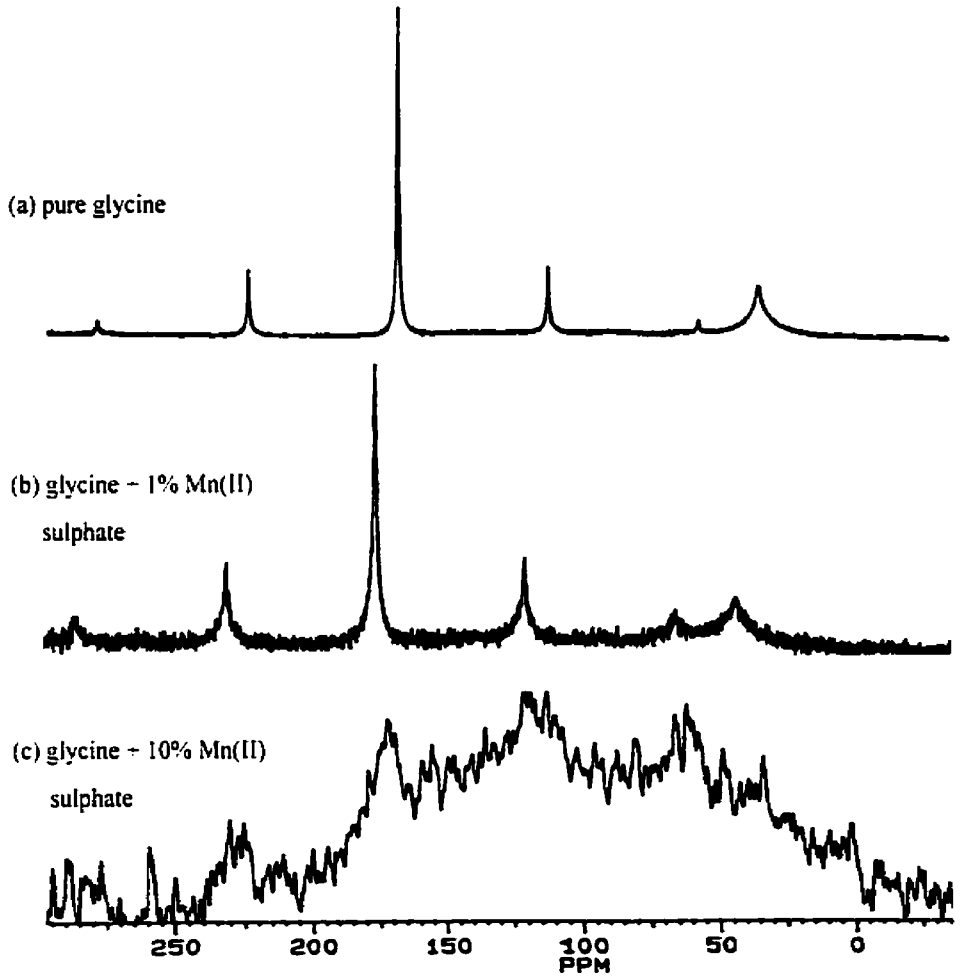


**Figure A1** $^{13}C$ CPMAS NMR spectrum of (a) pure glycine, (b) pure glycine + 1% w/w Mn (II) sulphate, and (c) pure glycine + 10% w/w Mn (II) sulphate.

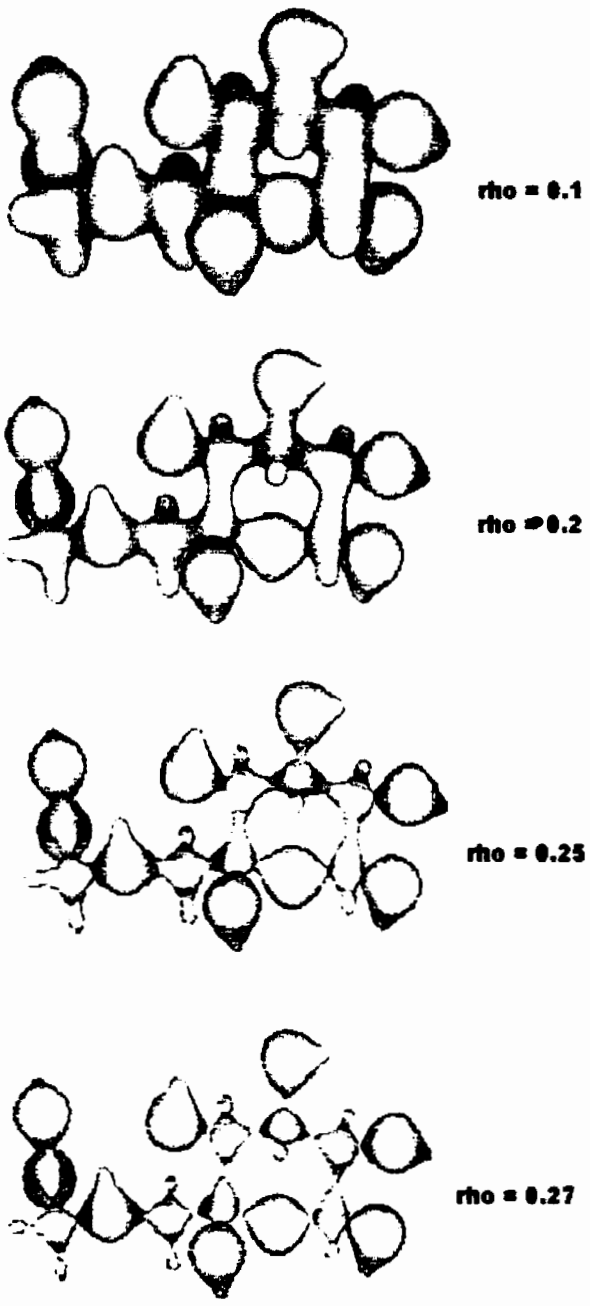


**Figure A2** MIDCO's of fructosylglycine at $\rho = 0.1, 0.2, 0.25, 0.27$.